



## AN ABSTRACT OF THE THESIS OF

Emma L. Ehret for the degree of Master of Science in Environmental Engineering presented on November 16, 2017.

Title: Inhibition of Organohalide-Respiring Bacteria by Carbon Tetrachloride and Chloroform

Abstract approved:

---

Lewis Semprini

Despite decades of cleanup efforts, chlorinated solvents are some of the most common groundwater and subsurface contaminants of the industrialized world. These compounds include chlorinated ethenes (CEs) such as trichloroethene (TCE) and chlorinated methanes (CMs) such as carbon tetrachloride (CT). *Dehalococcoides mccartyi* belongs to a class of microorganisms called organohalide-respiring bacteria (OHRB) and is the only organism known to completely transform TCE, a chlorinated ethene, to harmless ethene via reductive dehalogenation, a process commonly exploited in bioremediation schemes. However, this process has been shown to be inhibited by the presence of chlorinated methanes. In order to gain strategic insight for sites co-contaminated with CEs and CMs, we explored the dynamics further to gain a better understanding of how CMs affect microbially-facilitated CE transformation.

The impact of CT and chloroform (CF), a CT transformation product, on microbial performance was assessed and compared by evaluating CE transformation rates. Transformation rates served as a proxy for microbial health and viability and were compared across experiments to establish trends in CM inhibition. Hydrogen production and consumption behavior was also monitored. Kinetic transformation experiments were conducted in triplicate batch reactors containing anaerobic TCE-dehalogenating cultures harvested from chemostats. Day 0 of each experiment began with the addition of TCE, formate, and either CT (“CT-exposed”) or CF (“CF exposed”). Further additions of TCE

and formate were delivered on days 1, 2, or 14 to establish the short and long term effects of CM exposure on CE transformation. Every addition of TCE was transformed to ethene, and the mass profile was analyzed to obtain zero-order transformation rates for each CE. Relative to controls, VC rates were decreased in reactors that were exposed to CT on day 0, and significant reductions in TCE, cDCE, and VC rates were achieved after 1 and 2 days of exposure, indicating an early time CT-related inhibition of OHRB. After CT transformation was complete, rates did not recover, and day 14 exposure rates were similar to those obtained after 2 days of exposure. Rates obtained from reactors exposed to CF without CT were slowed but not as dramatically, indicating the CF as a product of CT transformation was not primarily responsible for the CT toxicity. Increasing the CT concentration and adjusting the CT delivery scheme indicated a dependence of CE transformation inhibition on both concentration and the amount of CT mass transformed. Amendment of vitamin B12 to cultures prior to CT and TCE addition resulted in a faster VC transformation rate than in a control without B12 amendment and improved H<sub>2</sub> consumption, indicating B12 as a key player in the CT mechanism of inhibition. Recovery potential of both CT-exposed and CF-exposed was assessed in select reactors sparged after 7 weeks of CT or CF addition. Reactors did not recover rates under either condition, indicating a permanent toxicity exerted by CT and CF for the time frame tested. The series of tests ultimately demonstrate that CT toxicity on OHRB is not explained by presence of the CF product alone, and that other mechanisms of toxicity contribute to the inhibition of CE transformation observed.

©Copyright by Emma L. Ehret  
November 16, 2017  
All Rights Reserved

Inhibition of Organohalide-Respiring Bacteria by Carbon Tetrachloride and Chloroform  
by  
Emma L. Ehret

A THESIS

submitted to

Oregon State University

in partial fulfillment of  
the requirements for the  
degree of

Master of Science

Presented November 16, 2017  
Commencement June 2018

Master of Science thesis of Emma L. Ehret presented on November 16, 2017.

APPROVED:

---

Major Professor, representing Environmental Engineering

---

Head of the School of Chemical, Biological & Environmental Engineering

---

Dean of the Graduate School

I understand that my thesis will become part of the permanent collection of Oregon State University libraries. My signature below authorizes release of my thesis to any reader upon request.

---

Emma L. Ehret, Author

## ACKNOWLEDGEMENTS

This project was funded by the National Science Foundation, grant 1330832. I greatly appreciate the opportunity that this funding has provided.

So much support, patience, and wisdom of others has been woven into this thesis project, and I have so many to thank for their guidance along my journey.

To my advisor, Dr. Lewis Semprini: I cannot summon the right words to thank you for the opportunity you gave me by accepting me into your research lab. Despite what doubts you might have had, you let me flounder a little and never reprimanded the parts of my learning process that I found most embarrassing and difficult. You gave me the ideas that turned into work I enjoyed and care about, offering wisdom to help me shape the research into a story that I couldn't have dreamed of when I walked into your office for the first time. I'm not exactly sure what keeps that twinkle in your eye, but you are such a joy to work for, so you must enjoy your work too. Thank you for sharing it with me and all of your students.

I want to especially thank Dr. Mohammad Azizian for being an incredible beacon of hope and expertise in the laboratory. Your magic touch with analytical instruments has saved countless experiments and prevented untold heart attacks. Your enduring calm and kindness make the lab a great place to be, and I am grateful to your assistance on this project, particularly in regards to media preparation, chemostat maintenance, and the gas chromatographs.

Next, a big thank you to my committee members: Drs. Tyler Radniecki, Mark Dolan, and Jack Istok and also to Dr. Jeff Nason. Thank you for taking my unannounced visits and inspiring me to think. Thank you for the words I needed to hear and for your dedication to your students.

I have made some wonderful friends along the way. Hannah Rolston, the most graceful graduate student I know – equal parts feisty and patient – thanks for being such an awesome role model. Marina Cameron, always ready to laugh, I owe you some credit for rough times when I needed a study buddy. Thanks for Christmas music in Merryfield and truffle-making. Kyle Vickstrom, thank you for your constant support during my process and for setting such a great example for the caliber of work this project deserves.

So many other CBEE graduate students who kept me laughing and reassured me I wasn't going crazy: Alyssa, Mark, Rich, Robby, Rebecca, Thaddeus, Kristin, Doug, Sassan, Ehsan, Corey, Brit, Genevieve, Mitchell, Riley, and more... Huge thank yous and hugs.

I want to thank my fitness family at CrossFit Ubiquity for all the laughs, sweat, blood, and tears shared over the last two years. Having that separate world has been a saving grace, and I will miss you all dearly: Jake, Pam, Althea, Austin, Sharon, Clayton, Grant, Elliott, Tausha, Robert, Angi, and more.

Thank you to my family, especially my mom, Bailey, who taught me to enjoy the journey, and my dad, Jeff, who taught me to finish what I started.

And of course, this would have gone so differently without the unwavering love and support from my partner, Tyrell Jackson, who selflessly served as therapist, cook, housekeeper, dog daddy, and cheerleader throughout my entire grad school journey. Thank you, darling.

# TABLE OF CONTENTS

	<u>Page</u>
CHAPTER 1 – INTRODUCTION .....	1
CHAPTER 2 – LITERATURE REVIEW .....	4
1. Subsurface Contamination by Chlorinated Solvents .....	4
2. Bioremediation as a Solution .....	10
3. Anaerobic CE and CM Transformation Pathways and Associated Microorganisms .....	11
i. CE OHR and OHRB Communities .....	11
ii. Abiotic and Biotic Anaerobic Transformation of CT .....	15
4. Inhibition and Toxicity of Chlorinated Methanes on Microbial Systems.....	21
i. Vocabulary and Introduction.....	21
ii. Methanogenic systems .....	27
iii. OHRB Systems .....	30
iv. Other Microbial Systems.....	32
5. CE/CM Co-contamination: Examples of Simultaneous Transformation .....	35
CHAPTER 3 – METHODS .....	39
1. Chemicals.....	39
2. OHRB Cultures .....	39
3. Design of Kinetic Transformation Experiments .....	40
4. Analytical methods .....	44
5. Data Analysis .....	44
CHAPTER 4 – RESULTS AND DISCUSSION .....	47
1. Overview.....	47
2. Performance of the Evanite Culture with Carbon Tetrachloride Addition .....	47

TABLE OF CONTENTS (Continued)

	<u>Page</u>
3. Performance of the Evanite Culture with Chloroform Addition .....	70
4. Comparison of Evanite Performance in Reactors Exposed to CT or CF.....	77
5. Probing the Mechanism of Carbon Tetrachloride Inhibition .....	85
i. High level CT (HiCT) tests .....	86
ii. Multiple CT Additions .....	94
6. Vitamin B12 Amendment .....	102
7. Post-Exposure Recovery Potential.....	108
CHAPTER 5 – CONCLUSIONS .....	121
CHAPTER 6 – FUTURE WORK .....	124
BIBLIOGRAPHY .....	126
APPENDIX.....	136
1. Log-linearization of CT and CF transformation data to obtain first order transformation rate constants .....	136
2. Day 0 CT Exposure – Experiment 5 .....	139
3. Comprehensive Transformation Rate Tables for All Experiments.....	140
4. Process for obtaining the Maximum Observed Rate from Sum of Products with Example Data Set from Experiment 1 .....	142
5. Additional CF exposed Experiments .....	143
6. CT Rate Analysis for Multiple Delivery Experiment .....	144

LIST OF FIGURES

<u>Figure</u>	<u>Page</u>
Figure 1. Anaerobic Reductive Dehalogenation Pathway for Chlorinated Ethenes. ....	12
Figure 2. Proposed pathways of CT transformation in reduced environments affected by vitamin B12.....	20
Figure 3. Simplified schematic of the design for Experiments 1-6. ....	42
Figure 4. CM transformation profile for Experiment 1 (2.3µM CT addition), including production and consumption of H <sub>2</sub> .. ....	49
Figure 5. Day 0 CE transformation profile for a representative CT-free control (Panel A) and CT-exposed reactor (Panel B) after a 2.3µM CT addition (Experiment 1). ....	51
Figure 6. Modeled transformation rates for Day 0 control (CT-free) and CT-exposed (2.3µM CT) reactors of Experiment 1. ....	52
Figure 7. Day 14 CE transformation profile for a representative CT-free control (Panel A) and CT-exposed reactor (Panels B and C) with a 2.3 µM CT addition (Experiment 1). ....	55
Figure 8. Modeled transformation rates for Day 14 control and CT-exposed reactors of Experiment 1 (2.3µM CT).. ....	57
Figure 9. CM transformation profile for Experiment 2 (2.4µM CT addition).....	59
Figure 10. Day 0 CE Transformation Profile for a representative CT-exposed reactor after 2.4 µM CT addition (Experiment 2).. ....	60
Figure 11. Day 2 CE transformation for a representative CT-free control (Panel A) and CT-exposed reactor (Panel B) with a 2.4 µM CT addition (Experiment 2).....	62
Figure 12. Modeled transformation rates for Day 2 control and CT-exposed reactors after addition of 2.4 µM CT (Experiment 2).....	63
Figure 13. Day 1 CE transformation profile for a representative CT-exposed reactor after 2.9 µM CT addition (Experiment 3). ....	65
Figure 14. Zero order transformation rates determined by the Multi-Fit Monod model (Panels A and B) and SOP linearization (Panel C) for Experiments 1-3.....	67
Figure 15. CF transformation profile for Experiment 4 (5.8 µM CF addition), including production and consumption of H <sub>2</sub> until completion of the second CE transformation on day 14 .....	71
Figure 16. Representative CE Transformation profiles for Experiments 4 and 5 with CF exposed on day 0 (Panel A), day 2 (Panel B), and day 14 (Panel C), all with 1-day time scales beginning at the time of TCE addition. ....	73

LIST OF FIGURES (continued)

<u>Figure</u>	<u>Page</u>
Figure 17. Zero order transformation rates determined by the Multi-Fit Monod model (Panels A,B) and SOP linearization (Panel C) for Experiments 4 and 5 .....	75
Figure 18. A side-by-side comparison of modeled CE transformation rates for each exposure time under CT and CF additions.....	78
Figure 19. CT exposure log transformed average CE rates from Experiments 1 and 2. ...	81
Figure 20. Natural log transformation of CE rates with exposure time to CF.....	82
Figure 21. H <sub>2</sub> production and subsequent consumption in reactors exposed to CT addition, CF addition, or TCE only.....	83
Figure 22. CM transformation profile for Experiment 6 with production and consumption of H <sub>2</sub> .....	87
Figure 23. Day 0 CE transformation profile for a representative CT-free control (Panel A) and CT-exposed reactor (Panel B) after a 7.2 μM CT addition (HiCT, Experiment 6).....	88
Figure 24. Modeled transformation rates for Day 0 control (CT-free), low, and high CT-exposed reactors of Experiments 1 and 6.....	90
Figure 25. Day 14 CE transformation profile for a representative CT-free control (Panel A) and CT-exposed reactor (Panels B and C) 14 days after 7.2 μM CT addition (Experiment 6) .....	92
Figure 26. Modeled transformation rates for Day 14 control (CT-free), low, and high CT-exposed reactors of Experiments 1 and 6.....	93
Figure 27. CM transformation and addition profile (Panel A) and H <sub>2</sub> production and consumption (Panel B) for Experiment 8 beginning 4/25/17. ....	96
Figure 28. Day 0 CE transformation profile for a CT-free control (Panel A) and representative CT-exposed reactor (Panel B) subject to CT addition at 0, 0.5, and 1 days (Experiment 8) .....	98
Figure 29. Modeled transformation rates for day 0 control and CT-exposed reactors of Experiment 8 (multiple CT addition).....	99
Figure 30. Day 2 CE transformation profile for a CT-free control (Panel A) and representative CT-exposed reactor (Panel B) following 3 separate additions of CT (Experiment 8). ....	100
Figure 31. Modeled CE transformation rates for Day 2 control (CT-free), single CT addition, and multiple CT addition reactors (Experiment 8). ....	101
Figure 32. Color observations in B12 amendment tests (Experiment 9).....	104
Figure 33. H <sub>2</sub> profiles for B12 amendment (Experiment 9) .....	105

LIST OF FIGURES (continued)

<u>Figure</u>	<u>Page</u>
Figure 34. Day 5 CE Transformation Profiles for Various Reactor Conditions of the Vitamin B12 Amendment (Experiment 9).....	106
Figure 35. Day 5 CE Transformation Rates for Reactors in the B12 Amendment Experiment (9) .....	107
Figure 36. Day 49 CE transformation profile for a representative control batch reactor.....	110
Figure 37. Control batch reactor CE transformation performance with time after sampling from the chemostat reactors demonstrate the culture robustness despite periods without feeding or cell wastage.....	110
Figure 38. Day 50 CE transformation profile for a representative CT-exposed batch reactor.....	112
Figure 39. Modeled CE transformation rates occurring in CT-exposed reactors at various times before and after sparging .....	113
Figure 40. H <sub>2</sub> production and consumption profile for recovery test (Experiment 10) with reactors from Experiment 1 during the transformation of TCE and products to ethene. ....	114
Figure 41. CF recovery days 50, 56,60 TCE spikes and profiles. ....	116
Figure 42. Modeled CE transformation rates occurring in CF exposed reactors at various times before and after sparging .....	117
Figure 43. Same time scale H <sub>2</sub> profiles during recovery tests for Experiment 4 (Panel A, CF exposed) and Experiment 1 (Panel B, CT exposure) .....	119

LIST OF TABLES

<u>Table</u>	<u>Page</u>
Table 1. Prevalence, Select Properties, and Regulatory Information for Select CEs and CMs .....	8
Table 2. Select Experiments Testing Inhibition of Methanogenesis by CT or CF .....	24
Table 3. Results from Representative Studies with Inhibition of OHRB by CT or CF .....	25
Table 4. Results from Representative Studies with Inhibition of Other Microbial Systems by CT or CF .....	26
Table 5. Experiments of this Project .....	43
Table 6. Points of Comparison for Chlorinated Methane Transformation Profiles of Experiments 1 and 2 .....	59
Table 7. Modeled and Linear SOP Transformation Rates ( $\mu\text{mol/L-d}$ ) for various exposure times following addition of 2.3-2.9 $\mu\text{M}$ CT .....	68
Table 8. Modeled and Linear SOP Transformation Rates ( $\mu\text{mol/L-d}$ ) for various exposure times following addition of 5.8-6 $\mu\text{M}$ CF .....	76
Table 9. A Comparison of CE Transformation Rates for Evanite cultures with CT and CF Exposures .....	78
Table 10. T-test Analyses Comparing CE Day 0 Transformation Rates Between CT Exposures and Between Associated Controls .....	90
Table 11. A Comparison of CE Transformation Rates in Low Level CT and HiCT Exposures .....	94
Table 12. CT Mass Introduced to Reactors in Single and Multiple Addition Experiments .....	96
Table 13. Comparison of CE Transformation Rates in Single Addition and Multiple Addition CT Exposures .....	101
Table 14. Comparison of CE Transformation Rates in Various Reactors of the B12 Amendment Experiment .....	106
Table 15. Transformation Rates and Comparisons for Recovery Test of CF-Exposed Reactors from Experiment 4. ....	117

## LIST OF APPENDIX FIGURES

<u>Figure</u>	<u>Page</u>
Figure A1. CT mass data long linearization for Experiment 1. ....	136
Figure A2. Log linearization of CF mass data from Experiment 1. ....	136
Figure A3. Log-linearization of CF mass data from Experiment 4. ....	137
Figure A4. Day 0 CE transformation profile for Experiment 3. ....	139
Figure A6. Stepwise process to obtain maximum observed transformation rates. ....	142
Figure A7. Control (Panel A) and Experimental (Panel B) transformation rates from an additional CF exposed experiment with 5 separate TCE additions. ....	143
Figure A8. First order CT transformation rate analysis for each addition (“spike”) of a multiple addition delivery experiment. ....	144

LIST OF APPENDIX TABLES

<u>Table</u>	<u>Page</u>
Table A1. First Order Transformation Constants for CT and CF in Experiment 1 Reactors.....	137
Table A2. First Order Transformation Rate Constants for CF in Experiment 4 Reactors.....	137
Table A3. Control Rates .....	140
Table A4. CE Transformation Rates for all 2.3-2.9 $\mu\text{M}$ CT Exposures Tested .....	141
Table A5. CE Transformation Rates for all 5.8-6 $\mu\text{M}$ CF Exposures Tested.....	141

## CHAPTER 1 – INTRODUCTION

Organohalide-respiring bacteria (OHRB) are a specialized group of microorganisms (microbes) that biodegrade compounds such as chlorinated solvents to harvest energy for growth via anaerobic reductive dehalogenation <sup>1</sup>. Chlorinated solvents, such as trichloroethene (TCE) and carbon tetrachloride (CT), are common subsurface and groundwater contaminants of the industrialized world <sup>2</sup>. TCE is a chlorinated ethene (CE), and CT is a chlorinated methane (CM) <sup>3</sup>. CEs and CMs are contaminants of concern because of toxicity risks they pose to environmental and human health <sup>4</sup>.

*Dehalococcoides mccartyi* is the only known organism to completely transform tetrachloroethene (TCE), to non-toxic ethene product via organohalide respiration (OHR) <sup>5</sup>. This metabolic capability is commonly exploited for remediation of contaminated sites in a strategy called *in situ* bioremediation <sup>6</sup>. CT is not biodegraded via energy-yielding pathways for microbial life, however its transformation can be facilitated in a number of abiotic or biotic systems depending on reductants and catalysts present, often resulting in various products from multiple parallel pathways <sup>7-13</sup>. Incomplete transformations of either TCE or CT yields toxic intermediate compounds, such as vinyl chloride (VC) or chloroform (CF) <sup>3,14,15</sup>. Thus, complete transformation of organohalides to nontoxic products is critical to successful bioremediation at contaminated sites.

However, such pathways can be complicated at sites co-contaminated with more than one class of chlorinated solvents, as in the case of CEs and CMs. CT and CF have been shown to inhibit, or block, growth and/or vital metabolic pathways of various microorganism classes, including OHRB that transform TCE <sup>16-18</sup>. Methanogenesis, nitrification, iron, nitrate, and sulfate reduction <sup>19-21</sup>, acetogenesis <sup>21,22</sup>, and fermentation <sup>20,23</sup> are other microbial processes reported to be inhibited by CT and/or CF. In cases where inhibition prevents a vital cell function, it can lead to toxicity, or permanent damage resulting in cell death. Other studies have shown successful simultaneous transformation of CEs and CMs, although the combined factors that allow this is often unclear <sup>7,24-26</sup>.

Despite evidence to support inhibition by CT and CF, few studies specify the mechanism of toxicity. A few proposed pathways include an interaction between essential microbial corrinoids and CT and/or its transformation intermediate, the trichloromethyl radical<sup>22,25,27</sup>. However, these mechanisms have not been verified, and limited work has attempted to clarify the mechanisms of CT toxicity. Most studies commonly cited for CT and CF inhibition or toxicity focus on CF as the primary inhibitor, and the specific response of OHRB to CM exposures is not clear. The relative inhibitory potential of CT and CF, a CT transformation product, remain unresolved, and until recently, the presence of CF was thought to serve as the primary inhibitor of TCE transformation in studies with CT addition to the microbial cultures used for the present study<sup>26</sup>. To resolve complications encountered in the remediation of CE/CM co-contaminated sites, it is necessary to better understand the dynamics of these mixed systems in laboratory settings.

To address uncertainties surrounding the impact of CT and CF upon OHRB activity, kinetic transformation tests were designed with batch reactors containing established TCE-respiring microbial culture. CE transformation rates were analyzed under various CM exposure conditions, and inhibition was indicated by decreases in these rates. The experiments were performed to achieve the following research goals:

1. Establish time-dependence of the CT and CF inhibition of CE transformation rates
2. Identify differences in CE transformation and hydrogen (H<sub>2</sub>) consumption, if any, between exposure to CT and its transformation and exposure to CF added directly
3. Evaluate the nature of the CT-related inhibition or toxicity by adjusting CT concentration and delivery schemes
4. Test vitamin B12 as a potential protectant against CT-related inhibition or toxicity of OHRB
5. Determine recovery potential of long term batch reactor cultures after CT and CF exposures to propose inhibition or toxicity response.

This document will begin with the Literature Review to establish the foundation for this research and examine relevant observations of the field. Next, the Results and Discussion will outline findings according to the research objectives stated above, followed by Conclusions, Future Work, Bibliography, and Appendices.

## CHAPTER 2 – LITERATURE REVIEW

### 1. Subsurface Contamination by Chlorinated Solvents

Humans and natural ecosystems rely on underground sources of water (groundwater) for water supply and surface water recharge. More than 20% of the 355,000 million gallons of water used per day in the United States in 2010 was withdrawn from groundwater supplies<sup>28</sup>. In the Earth's subsurface, groundwater and associated sediments make up aquifers, which are susceptible to contamination by surface chemicals if they are allowed to escape underground. Chlorinated solvents are toxic compounds that contaminate aquifers across the globe<sup>2</sup>. Chlorinated ethenes (CEs) and methanes (CMs), two classes of these solvents, are known as legacy contaminants due to their recalcitrant qualities that have challenged remediation engineers and scientists for decades. This section will discuss their history of use, prevalence, and relevant chemical and toxic properties.

Chlorinated solvent use and production in the United States surged in the early 20<sup>th</sup> century when World War I halted European imports to the U.S.<sup>29</sup>. The popularity of chlorinated solvents arose from their low flammability, low odor, and potential for reuse. Carbon tetrachloride (CT) was the first chlorinated compound to be widely used. It had applications in cleaning (household and dry), fire extinguishing, grain fumigation, and later in production of chlorofluorocarbons (CFCs). Commonly used in dry cleaning throughout the 1920s, it was largely replaced in the 1930s by tetrachloroethene (PCE), which was apparently less toxic and became the dry cleaning chemical of choice in the following decades. World War II military operation demanded high amounts of chlorinated solvents for metal cleaning and vapor degreasing. Trichloroethene (TCE) was primarily used as a degreaser but like other chlorinated solvents had applications in textiles, food processing, pharmaceuticals, consumer products, paints, and more, along with other chlorinated solvents. CT, PCE, and TCE production peaked during the 1970s and 1980s, reaching annual levels of over 1100 million, 800 million, and 600 million pounds, respectively<sup>29,30</sup>.

The 1960s and 1970s brought an increase in both public and scientific awareness concerning the toxicity and disposal of chlorinated solvents and other chemicals, eventually leading to the drastic reduction in their production and use<sup>29</sup>. The Environmental Protection Agency was founded in 1970, which gave rise to the Clean Air Act (1970), Clean Water Act (1977), Resource Conservation and Recovery Act (RCRA), and their amendments established regulations concerning the air emissions, solid waste handling, and drinking water exposures. The 1980 Comprehensive Environmental Response, Compensation & Liability Act (CERCLA) established the Superfund for the most highly contaminated sites that were created from the decades of inadequate contaminant disposal, many of which contain CT, PCE, and TCE. Chloroform (CF), originally used as an anesthetic, was prohibited from consumer products in 1976<sup>31</sup>. In 1977, TCE was banned in food products and in the decaffeination process for coffee. The 1992 amendments to the Montreal Protocol established the complete ban of CT production by 2000<sup>29</sup>.

PCE and TCE are still used, primarily as a dry cleaning solvent and TCA substitute, respectively<sup>29,30</sup>. CF is currently used to manufacture refrigerants and polymers, also appearing in products such as pesticides, rubber, and resins. Estimated global emissions from anthropogenic sources, such as pulp and paper manufacture, were 150 million pounds per year in the late nineties, a figure dwarfed by estimated natural emission source contribution, however global production was estimated to be about 1150 million pounds per year<sup>31</sup>.

Only after CERCLA and RCRA legislation was established did the magnitude of subsurface contamination become evident, and nearly 40 years later, contaminated groundwater and soil remains a significant challenge. Chlorinated solvents are widely reported to be the most common subsurface contaminants, with PCE and TCE as the most frequently detected<sup>32-36</sup>. In a survey of contaminated sites managed by RCRA, CERCLA, Underground Storage Tank (UST), Department of Defense (DoD), Department of Energy (DOE), other Federal programs, the National Research Council (NRC) estimated that at least 126,000 sites in the United States contained groundwater contamination at levels preventing closure in 2013<sup>34</sup>. Examples of major DOE sites

requiring cleanup of TCE, PCE, CT, and other metals and mixed wastes include the Savannah River Site and the Hanford site, which were estimated to have contaminated  $3.1 \times 10^8$  and  $2.0 \times 10^7$  m<sup>3</sup> of groundwater, respectively, in addition to soil and sediment volumes on the order of  $10^6$  and  $10^7$  m<sup>3</sup> <sup>37</sup>. Contaminated groundwater at the Anniston Army Depot in Alabama may contain as much as 27 million pounds of TCE <sup>34</sup>. Many other sites harboring chlorinated solvent contamination are also current or former military bases <sup>6,34,38</sup>.

The NRC reports, “while there have been success stories over the past 30 years, the majority of hazardous waste sites that have been closed were relatively simple compared to the remaining caseload.” This is devastating in light of the decades of time and financial investments that have already been made, such as by the DoD (more than \$30 billion) <sup>34</sup> or by private parties deemed responsible by the Superfund program (\$35.1 billion) <sup>39</sup>. Further, the EPA recently estimated that costs for the mitigation of groundwater contamination would exceed \$200 billion by 2033 <sup>34</sup>.

The problem of chlorinated solvent contamination began with decades of inadequate handling, storage, and disposal methods. Incidences of contamination include leaks, such as in underground or above-ground storage tanks and distribution pipelines, or spillage, such as in loading and off-loading facilities or highway accidents and train derailments. Solvents were also released intentionally to poorly contained receptacles such as landfills (domestic, municipal, and chemical) and settling ponds. Destinations with no containment included land application in sludge and disposal via injection well <sup>40</sup>. However, other factors complicate the issue further.

The characteristic hydrogeology at sites of contamination combines with the unique properties of chlorinated solvents to send them deeper into the subsurface. Chlorinated solvents form a dense non-aqueous phase liquid (DNAPL), which is transported through the vadose zone to the water table by gravity. Soil and sediment properties dictate the travel path of the compound, diverting it away from areas of low hydraulic conductivity, such as clays. Contaminants travel faster in areas of fractured bedrock than in unfractured areas where movement is limited by diffusion through the

rock matrix. Following this path of least resistance can result in spreading of the contaminant throughout the soil<sup>32</sup>. DNAPL not held by capillary forces in the vadose zone continues to travel below the water table because chlorinated solvents are denser than water. Thus, DNAPL becomes a source of contamination to passing groundwater, or source zone, which can contaminate an aquifer for decades<sup>40,41</sup>. Geological formations, groundwater dissolution and flow, and high compound density effectively distribute contaminants in three dimensions. This distribution can create plumes of contamination with dimensions on the order of miles<sup>6</sup> with contaminant concentrations on the order of  $\mu\text{g/L}$  or  $\text{mg/L}$  in areas away from the source zone. Thus, remediation efforts must target concentrations across multiple orders of magnitude<sup>40</sup>. To further complicate matters, original DNAPL compounds such as PCE transform abiotically and biotically in the subsurface, often producing other toxic chemicals, such as vinyl chloride<sup>3,42</sup>.

As an indication of relative abundances at contaminated sites, Table 1 shows the prevalence of CEs and CMs at National Priority List (NPL) contaminated sites, which represent the locations of highest priority for cleanup as determined by the EPA. The NPL is a management tool used in the Superfund cleanup process to guide in the determination of possible remedial actions and risks posed by the site. As of September 2017, there were 1342 current NPL sites, with 49 proposed and 394 that have been deleted<sup>4</sup>. PCE and TCE occur at more than half of current and former NPL sites, consistent with the trend for other hazardous waste sites across the nation.

TOXMAP® is a GIS program offered by the U.S. National Library of Medicine that allows users to view data from the Toxics Release Inventory (TRI) and Superfund Programs. Koenig et al.<sup>43</sup> recently used TOXMAP® to report the number of NPL sites containing various chlorinated solvents with similar results. NPL site counts containing respective compounds were reported as follows: 807 (PCE), 634 (TCE), 151 (cDCE), 529 (VC), 244 (CT), 474 (CF), 389 (DCM), with the latter three compounds at much lower frequency than reported by the ATSDR (see Table 1). Discrepancies reflect changes in the total number of declared NPL sites as sites are closed or added.

CM and CE anaerobic transformation products are also shown in Table 1 and will be discussed in Section 3. While a specific breakdown of chlorinated solvent combinations found at each contaminated site in the nation is not available, individual prevalence at a representative group of sites (such as for NPLs) indicates overlap in the prevalence of CEs and CMs. This co-contamination of multiple chlorinated solvent classes has implications for removal efficiency, especially considering CMs are widely reported to inhibit removal of CEs.

Table 1. Prevalence, Select Properties, and Regulatory Information for Select CEs and CMs

Compound	Chlorinated Class	H <sub>cc</sub> (L/L/G) <sup>a</sup>	Water Solubility (20°C, mg/L) <sup>b</sup>	SPL Rank <sup>c</sup>	MCL (mg/L) <sup>d</sup>	Toxicity to Humans <sup>e</sup>	NPL Prevalence <sup>e</sup>
PCE	Ethene	0.533	400	33	0.005	Likely carcinogen	55% (945 of 1699)
TCE	Ethene	0.2964	1000	16	0.005	Carcinogen	62% (1045 of 1699)
cDCE	Ethene	0.1224	3500	220	0.07	Not classifiable	10% (146 of 1430)
VC	Ethene	0.903	90	4	0.002	Carcinogen	37% (616 of 1662)
CT	Methane	0.949	800	50	0.005	Probable carcinogen	26% (425 of 1662)
CF	Methane	0.126	8000	11	0.07	Anticipated carcinogen	50% (717 of 1430)
DCM	Methane	0.0904	13,000	88	0.005	Probable carcinogen	56% (882 of 1569)

<sup>a</sup>Dimensionless Henry's Constants at 20°C for PCE, CT, CF, DCM from Staudinger and Roberts, 2001<sup>44</sup>; TCE, cDCE, VC from Gossett, 1987<sup>45</sup>

<sup>b</sup>Obtained from Schnoor 1996<sup>46</sup>

<sup>c</sup>ATSDR, 2017<sup>47</sup>

<sup>d</sup>US EPA, 2015<sup>48</sup>

<sup>e</sup>ATSDR<sup>14,15,49-53</sup>

CEs and CMs have a similar history of use and contamination, but they differ in molecular structure. While both are organic molecules made up of carbon, hydrogen (H<sub>2</sub>), and chlorine atoms, CEs contain two double-bonded carbon atoms, whereas CMs have a single, central carbon atom. While other classes of chlorinated solvents exist, these two will be the focus of the present work. The variation in quantity of chlorine atoms surrounding the central carbon(s) allows for a family of similarly structured compounds.

By degree of chlorination, CEs include perchloroethene (PCE), trichloroethene (TCE), dichloroethenes (cis-DCE, 1,1-DCE, trans-DCE), and vinyl chloride (VC), where PCE contains 4 chlorines and VC has only 1. CMs include carbon tetrachloride (CT), chloroform (CF), dichloromethane or methylene chloride (DCM), and chloromethane (CM) <sup>3</sup>.

All of these compounds are volatile and can easily evaporate from contaminated water to air. Shown in Table 1 for each CE and CM, the dimensionless Henry's constant ( $H_{cc}$ ) indicates the relative amount of a molecule in a gas-liquid system that partitions into each phase at a particular temperature.  $H_{cc}$  values greater than 0.1 indicates that a chemical is liquid-film controlled, and more mass of a compound will partition into the gaseous phase than in the liquid phase at equilibrium conditions.  $H_{cc}$  values less than 0.1 occur for chemicals that are gas-film controlled, where proportionally more mass partitions into the liquid phase <sup>46</sup>. CT is thus the most volatile of the chlorinated compounds shown, with a Henry's constant of 0.949. Because of the volatility of chlorinated compounds, humans exposed to contaminated water while bathing or showering are at risk of consumption in liquid or vapor forms <sup>52</sup>.

Other properties of chlorinated solvents that made them desirable for use in various industries are the very same ones that complicate their cleanup. These properties include low liquid viscosities, low interfacial tensions with water, low absolute solubilities, high solubilities relative to drinking water limits, low soil partitioning, and low degradability <sup>40</sup>.

All CEs and CMs appear on the Substance Priority List (SPL) put forth by the Agency for Toxic Substances and Disease Registry (ATSDR) and the U.S. Environmental Protection Agency (USEPA) <sup>47</sup>. This list is updated every two years and ranks 275 environmental contaminants of National Priority List (NPL) sites according to their frequency, toxicity, and potential for human exposure. Vinyl chloride, a human carcinogen, ranks 4<sup>th</sup> on the Substance Priority List. The other CEs and CMs span between 11<sup>th</sup> (chloroform) and 220<sup>th</sup> (cis-DCE) as shown in Table 1. Most of these compounds are suspected or known carcinogens and cause both acute and chronic health

effects to humans and animals. In particular, TCE can cause headaches, dizziness, coma, and skin rash as well as liver and kidney damage<sup>53</sup>. Carbon tetrachloride is a notorious hepatotoxin and cause damage to the kidneys and central nervous system<sup>51</sup>.

The EPA regulates contaminants according to the Safe Drinking Water Act (SDWA), which requires publication of contaminant lists and a defined decision making process for harmful chemicals that could be present in drinking water supplies<sup>54</sup>. The National Primary Drinking Water Regulations (NPDWR) enforced by the EPA include values of maximum contaminant levels (MCLs) for each regulated compound. Water treatment facilities that supply public drinking water must adhere to these MCLs, shown for CEs and CMs in Table 1.

The combination of poor practices, site characteristics, and chemical properties make clean up of subsurface chlorinated solvent contamination an immense endeavor. Some professionals have declared the removal of DNAPLs to be “the greatest technical challenge in the field of groundwater engineering”<sup>41</sup>. However, remediation efforts have been employed with varying degrees of success, with bioremediation emerging as an advantageous alternative to pump-and-treat.

## 2. Bioremediation as a Solution

Early cleanup efforts to mitigate subsurface chlorinated solvent contamination began in the 1980s, just after the establishment of CERCLA. Remediation typically involved pumping contaminated water to the ground surface for *ex situ* treatment before return back into the subsurface. Commonly called pump-and-treat, this was a common approach for chlorinated solvent remediation, however it did little to actually remediate DNAPL-contaminated sites, and this problem was only realized after years of mere hydraulic containment<sup>40,41,55</sup>.

Over the last 20 years, a variety of remediation technologies for chlorinated solvent plumes have emerged from attempts to find alternatives to pump-and-treat<sup>55</sup>. This transition has seen the decrease in pump-and-treat installations coupled with the increase in *in situ* technologies, which are generally less expensive and less demanding to

operate. *In situ* chemical and physical categories include approaches such as chemical oxidation, injection of zero-valent iron for chemical reduction, and air sparging, among others. Biological *in situ* treatment, or bioremediation, is relatively easy, flexible, and inexpensive to apply where appropriate, and is now one of the most commonly employed technologies for site cleanup<sup>55</sup>.

Bioremediation is an approach in which environmental conditions are manipulated to capitalize on the biodegradation ability of microorganisms for the removal or detoxification of contaminants. Biodegradation is the natural process of microbial activity that results in transformations of compounds in a system containing the appropriate geochemical characteristics and microbial ecology for that particular metabolic pathway<sup>32,56</sup>. Sufficient intrinsic biodegradation at a contaminated site can warrant a non-engineered *in situ* approach called Monitored Natural Attenuation (MNA), which will not be discussed here.

Bioremediation can be applied above ground, or *ex situ*, such as in the case of land farms and biopiles, or *in situ*, below ground in the soil and groundwater of a contaminated site<sup>56</sup>. *In situ* strategies include biostimulation, which is the amendment of native microbial populations with nutrients, electron donor, or electron acceptor to enhance performance, or bioaugmentation, which is the addition of non-indigenous microorganisms to boost metabolic capabilities of the environment. These may act to facilitate a variety of microbial pathways, such as those for aerobic, cometabolic, and anaerobic oxidative transformations. However, since its successful implementation in the early 2000s, the most common application for chlorinated solvent remediation capitalizes on the anaerobic reductive dehalogenation pathway<sup>55,56</sup>.

### **3. Anaerobic CE and CM Transformation Pathways and Associated Microorganisms**

#### *i. CE OHR and OHRB Communities*

Biodegradation of CEs is well-established in anaerobic environments, and was originally demonstrated in laboratory in mixed methanogenic cultures<sup>57</sup>. The

organohalide respiration (OHR) pathway shown in Figure 1, features a step-wise reduction of a chlorinated ethene (the electron acceptor), where a chlorine atom is replaced by a hydrogen atom (the electron donor) in each reduction reaction. Each step is facilitated by a reductive dehalogenase (RDase) enzyme <sup>58</sup>.

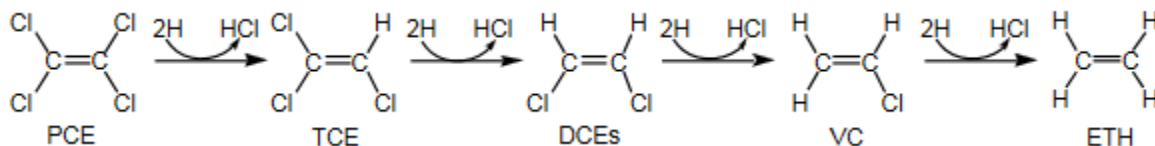


Figure 1. Anaerobic Reductive Dehalogenation Pathway for Chlorinated Ethenes. Stepwise reduction of each chlorinated ethene electron acceptor involves the replacement of a chlorine atom with a hydrogen atom. Complete conversion results in non-toxic ethene. Diagram courtesy of Maymó-Gatell et al. 1997.

An effective bioremediation scheme would facilitate the complete conversion of chlorinated contaminant mass to non-toxic ethene, shown at the far right of Figure 1. The OHR pathway is especially critical in the bioremediation of higher chlorinated compounds such as PCE, which is resistant to aerobic transformations. However, VC is more receptive to oxidation, thus increasing interest in sequential anaerobic-aerobic strategies, which is not discussed here further <sup>59-61</sup>.

Microorganisms that directly obtain energy from reduction of halogenated compounds (organohalides) in anoxic environments are called organohalide-respiring bacteria (OHRB). Since 1990, a myriad of OHRB have been isolated, all from bacterial phyla *Firmicutes*, *Chloroflexi*, and *Proteobacteria* <sup>62</sup>. OHRB are found in a variety of subsurface environments and have RDase enzymes that allow them to use an array of organohalides as terminal electron acceptors. OHRB that facilitate one or more steps of the CE OHR pathway shown above include members of *Dehalobacter* <sup>63</sup>, *Desulfitobacterium* <sup>64</sup>, *Sulfurospirillum* <sup>65</sup>, *Geobacter*, *Desulfuromonas* <sup>66</sup>, and *Dehalococcoides* <sup>67</sup> genera.

The obligate OHRB *Dehalococcoides mccartyi* is the only known organism to accomplish transformation of PCE to ethene, and only a few strains are able to complete

the final step of VC transformation via halo-respiration. In 1989, Freedman and Gossett first reported the complete CE biotransformation to ethene by a mixed methanogenic enrichment culture sourced from a sewage treatment plant<sup>57</sup>. This discovery caused a revival in the interest for using reductive dehalogenation as a remediation strategy for complete detoxification of PCE and TCE, which, until then, had only been biologically transformed to toxic intermediates cDCE and VC<sup>68</sup>. Shortly thereafter, it was established that methanogenesis was not required for this process to occur<sup>69</sup>, and the first isolation of an organism responsible for complete CE reduction occurred in 1997, and it was originally named *Dehalococcoides ethenogenes* 195<sup>70</sup>. Since its discovery, 16 other strains of *D. mccartyi* have been isolated in pure culture, and most perform CE OHR. Unlike 195, several strains, such as Victoria<sup>71</sup> and BAV1<sup>72</sup>, grow on the VC to ethene step as well as earlier steps in the pathway. Enrichment cultures have also been developed by various research laboratories, some of which are produced for commercial use in bioremediation<sup>67,73</sup>.

*D. mccartyi* is a unique organism, highly specialized to fit a particular niche. Among the smallest bacteria known, it harbors a streamlined yet elaborate genome encoding 11-36 RDase genes responsible for its metabolism<sup>67</sup>. However, this specialization is also what makes *D. mccartyi* dependent on neighboring microorganisms. Thus, it survives best in consortium, mixed with other microbial population<sup>67</sup>. As an obligate OHRB, *D. mccartyi* requires H<sub>2</sub> electron donor, an organohalide electron acceptor, and cyanocobalamin (vitamin B12) for growth and survival<sup>5</sup> and depends on the metabolic capabilities of organisms to obtain these and other nutrients in the phenomenon of cross-feeding<sup>74</sup>. Common members of an OHRB community include *Desulfovibrio*, *Desulfuromonas*, gammaproteobacteria (*Citrobacter*), methanogenic euryarchaeota (various), *Clostridiales* (including *Clostridium*, *Sedimentibacter*, *Eubacterium*, *Syntrophomonas*, *Acetobacterium*), *Selenomonadales* (*Sporomusa* and *Pelosinus*), *Bacteroidetes*, *Spirochaeta*, *Chloroflexi*, *Geobacter*, and *Nitrospira*. Most of these are methanogens, homoacetogens, or fermenters that can produce H<sub>2</sub> from fermentable organic substrates<sup>75</sup>.

RDase enzymes are critical to the successful CE OHR pathway, and their function requires organometallic cofactors called corrinoids<sup>58</sup>. Complete corrinoids are called cobamides and contain a cobalt (Co) atom hexacoordinated by four nitrogen atoms of a corrin ring (tetrapyrrole), an upper ligand, and a lower ligand<sup>76</sup>. These cofactors are proposed to function at the active site within the RDase protein, where the Co(I) is involved in the reductive dehalogenation of the CE<sup>58</sup>. Cobalamin is a cobamide with a 5,6-dimethylbenzimidazole (DMB) lower ligand base. If the upper ligand is a cyano-group, the cofactor is called cyanocobalamin, or vitamin B12<sup>77</sup>. The identity of the cobamide cofactor in most RDases is unknown<sup>78</sup>, but it has been established that *D. mccartyi* requires vitamin B12 for growth and CE OHR<sup>5</sup>. Thus, it is likely that RDase function is critically dependent upon vitamin B12 supply.

Many organisms require cobamides for growth, but only some Bacteria and Archaea can synthesize them *de novo*. Examples include members of *Geobacter*<sup>79,80</sup>, *Acetobacterium*<sup>81,82</sup>, and *Clostridium*<sup>83,84</sup>, but *D. mccartyi* cannot synthesize corrinoids. However, genes involved in corrinoid transport, harvesting, and remodeling have been identified in the genome of *D. mccartyi*<sup>85</sup>, and corrinoid remodeling by *D. mccartyi* has been implicated experiments for which DMB was supplied to co-cultures without vitamin B12<sup>80,86</sup>. Research is ongoing to learn more about environmental sources of cobamides and how OHRB communities share and remodel them<sup>78</sup>.

In addition to cross-feeding relationships, competition for resources occurs in dynamic food webs<sup>74</sup>. Some microbial populations that supply *D. mccartyi* with cofactors may also compete with *D. mccartyi* for H<sub>2</sub>, such as in the case of homoacetogens and methanogens<sup>87,88</sup>. Facultative OHRB such as *Geobacter*, *Desulfuromonas*, and *Desulfovibrio* can also compete for H<sub>2</sub> when they switch to alternate non-organohalide electron acceptors<sup>75</sup>. Methanogens are sometimes present in OHRB communities and are potential competitors for H<sub>2</sub>, however they are less of a threat against OHRB at low H<sub>2</sub> thresholds<sup>89,90</sup>.

Successful field application of CE bioremediation is influenced by a myriad of environmental, geological, and microbial factors such as aquifer temperature and pH, the

presence of OHRB and their necessary nutrients, and co-contaminants<sup>75,91</sup>. A stable OHRB community involves a healthy cross-feeding network across various microbial populations. Thus, favorable conditions must extend to non-OHRB in remediation schemes, and impacts of co-contamination must be considered across this food web. As discussed in Section 1, chlorinated methanes are potential co-contaminants of CEs, and thus, CM transformations will be discussed presently.

*ii. Abiotic and Biotic Anaerobic Transformation of CT*

In contrast to the linear CE OHR transformation pathway shown in Figure 1, anaerobic transformations of CT are more complex and usually involve multiple parallel pathways. As included in the synthesis by Criddle and McCarty<sup>9</sup>, abiotic and biotic transformations of CT most likely begin with a single-electron reduction to yield the trichloromethyl radical (TCMR). From here, the TCMR can bind to cell material, further reduce to produce CF and DCM, dimerize with itself to form hexachloroethane, or form a carbenoid or chloromethyl complex depending on system conditions. Abiotic and biotic transformation studies have revealed that reaction pathway(s) vary depending on system conditions, and improving the predictability of these mechanisms is valuable for subsurface remediation design that seeks to avoid the production of toxic chemical intermediates such as CF.

Chiu and Reinhard<sup>8,92</sup> reported reductant-dependent product distributions in the transformation of CT by vitamin B12 in aqueous solutions with titanium(III) citrate or cysteine as reducing agents. CT reduction was mediated by vitamin B12 which had been reduced by either reductant. However, the extent to which each reductant reduced B12 influenced the interaction of B12 with CT. Titanium(III) citrate reduced B12 so that the cobalt atom achieved the Co(I) oxidation state, which in turn was a stronger reductant for CT. Under these strong reducing conditions, the major product of CT transformation was 58% CF at pH 7.3<sup>92</sup>. In contrast, cysteine reduced B12 to the Co(II) oxidation state, which resulted in 18% CF product at pH 8.3, where most products were soluble<sup>92</sup>.

A similar reductant-dependence was observed in another abiotic study by Lewis et al.<sup>93</sup> comparing titanium(III) citrate and thiol reductants for corrinoid-mediated CT

transformation. Titanium(III) was reported to reduce the cobalt in vitamin B12 to the Co(I) state, ultimately producing methane and chloromethane as primary CT products. In contrast, sodium sulfide ( $\text{Na}_2\text{S}$ ) and cysteine at 50 mM each allowed for the formation of CF, carbon disulfide ( $\text{CS}_2$ ), and organic acids. A different thiol reductant, dithiothreitol, was reported to yield products DCM, CO, and formate, thus indicating that not all thiols provide the same reduction mechanism to the corrinoid they reduce.

In an anaerobic, abiotic culture media with a  $\text{Na}_2\text{S}$  reductant, CT transformation was reported to be highly dependent upon sulfide, vitamin B12,  $\text{H}_2\text{PO}_4^-$ , and ammonium levels, where optimal degradation occurred with 1-2 mM  $\text{Na}_2\text{S}$  <sup>94</sup>. In contrast to Lewis et al. who supplied  $\text{Na}_2\text{S}$  at 50 mM, for transformation of 99 nmol CT produced very little CF, and vitamin B12 concentration of about 10  $\mu\text{M}$  yield no CF. DCM, chloromethane, and methane were not detected for any condition. High levels of chloride ions measured led researchers to conclude that the primary transformation reaction was the hydrolysis of CT to produce  $\text{CO}_2$  (not measured), protons, and chloride ions.

To date, no organisms are known to couple energy and carbon assimilation with the transformation of CT <sup>43</sup>, however, various microorganisms have been shown to mediate CT transformation cometabolically, usually via corrinoids they produce or are amended with. Examples include *Pseudomonas* <sup>95,96</sup>, *Acetobacterium woodii* <sup>10,97</sup>, a methanogenic culture <sup>98</sup>, and *Shewanella alga* <sup>13</sup>. As with abiotic conditions, microbially-mediated CT transformation yields different products depending on factors such as the specific microbe, electron donor supply (reductant), and corrinoid supply.

In a study with the iron-reducing bacteria *Shewanella alga* strain BrY, CT transformation was mediated by B12 that was reduced to the Co(I) oxidation state by soluble cell components <sup>13</sup>. Vitamin B12 supplied at 45-55  $\mu\text{M}$  was identified with UV-VIS spectrophotometry to evaluate the oxidation state of Co. With  $\text{H}_2$  as the electron donor, less than 20 days were required for B12 reduction to Co(II) in cells and media. This microbially-reduced B12 then transformed CT at 1 ppm (150 nmol) almost completely in about 20 days. Product distributions were assessed with additions of 2  $\mu\text{mol}$  CT and lactate as an electron donor/reductant, and only conditions with BrY,

electron donor, and B12 yielded significant CT transformation (8.62% remaining) and low CF levels (1.43% of initial CT mass). The major product at 91.9% of initial mass was reported to be CO, closing the product mass balance.

Another iron-reducing bacteria, *Geobacter metallireducens*, has been shown to facilitate CT transformation via production of magnetite ( $\text{Fe}_3\text{O}_4$ ) particles that act as reductants<sup>99</sup>. Unlike, BrY discussed above, cell components were not involved in this process, so it is technically an abiotic mechanism with a biotically-generated reductant. In transformation studies to determine CT reaction pathways, 13  $\mu\text{M}$  CT was added to suspensions of biogenic magnetite and analyzed for products periodically<sup>12</sup>. Radical traps were also used to confirm the presence of the trichloromethyl radical and dichlorocarbene with mass spectrometry, and the researchers concluded that three simultaneous pathways are likely underway in the system: hydrogenolysis to create 50% CF, carbene hydrolysis to yield 38% CO, and carbene reduction to yield 8-10% methane product. These pathways are consistent with those reported by Criddle and McCarty above but yield vastly different values of CF product.

CT removal under sulfate-reducing conditions in a packed-bed reactor was dependent on the type of electron donor and active microbial population, with no corrinoid additions tested<sup>100</sup>. With acetate electron donor, CT influent concentrations up to 30  $\mu\text{M}$  CT were completely transformed, with CF as the primary product (39-46%), which is consistent with other reports for sulfate-reducing bacteria<sup>101</sup>. After complete reduction of sulfate, remaining acetate stimulated methanogenic activity, which altered the CT product distribution so that no CF or DCM was detected. This was assumed to signify complete mineralization to  $\text{CO}_2$  but was not measured. Further addition of sulfate restored the production of CF and DCM products, and in comparing electron donors, ethanol allowed for the fastest CT transformation rate, while methanol yielded the lowest CF product formation (<0.1%).

Cobalamin-mediated CT transformation has also been reported in methanogenic cultures. Hashsham et al.<sup>11</sup> reported that 20  $\mu\text{M}$  vitamin B12 was sufficient to alter product distributions of 1.5 mg/L initial CT concentration in DCM-degrading cultures.

CO<sub>2</sub> production in B12-amended reactors tripled compared to those without, accounting for 59% of the CT mass. CS<sub>2</sub> production was cut in half (11%), and virtually no CF was measured under B12 amendment. Soluble products formate, acetate, butyrate, methanol and nonstrippable residues accounted for between 3.2 and 6.1% each. In addition to altering the product distribution vitamin B12 increased the rate of CT consumption by a factor of 10 and sustained transformations of multiple CT additions during 200 days, during which less than 1% of CT mass accumulated as CF. Similar enhancement of CT transformation these cultures was observed with addition of hydroxocobalamin, methylcobalamin, and adenosylcobalamin. The same authors also reported similar product distribution shifts in an *Acetobacterium woodii* culture with addition of hydroxocobalamin in a sulfide-reduced basal medium, where CT transformation was enhanced by a factor of 30<sup>10</sup>.

Microcosm studies have also gleaned insights regarding product distributions and their influential factors. Koenig et al.<sup>25</sup> discovered that vitamin B12 essentially eliminated the CF intermediate in CT/PCE co-contaminated microcosms inoculated with *Desulfovibrio vulgaris*, allowing for rapid CM removal prior to inoculation of a PCE-degrading enrichment culture (see “Simultaneous Transformations”). Similarly, in microcosm studies with carbon-14 labeled CT, CF, CFC-11, and 1,1-DCE, “catalytic levels” of cyanocobalamin added at “catalytic levels” shifted the CT product distribution away from reductive dechlorination products, CF and DCM and toward CO, CO<sub>2</sub>, and organic acids<sup>102</sup>. After CT and CF were transformed, 1,1-DCE transformation carried out.

Enrichment cultures (Evanite) and of *D. mccartyi* and associated sulfide-reduced medium (supernatant) were recently confirmed to transform CT to CF, DCM, and CS<sub>2</sub> in batch reactors, with CF as the major product<sup>26</sup>. These cultures have been reported to also maintain *Geobacter*, *Desulfitobacterium*, and homoacetogenic populations<sup>73,103,104</sup> but do not contain methanogens<sup>105</sup>. CO and chloromethane were not detected in these experiments, and CT transformation was confirmed to be primarily abiotic. CO<sub>2</sub> was not successfully measured but was incorporated into a first-order degradation model with multiple parallel pathways for CT transformation, which accurately predicted collected

transformation data and fit the curves proposed for CO<sub>2</sub> production that completed the CT mass balance. Response of CT transformation rates and product distribution to vitamin B12 amendment was not evaluated for this culture. However, product distributions generally agreed with studies discussed above, where CT transformations in sulfide-reduced and iron-reducing media yield greater proportions of CF and CS<sub>2</sub> products under both abiotic and biotic conditions <sup>12,93,100</sup>.

Figure 2 shows proposed pathways of CT transformation in sulfide-reduced anaerobic environments from Koenig et al. 2012 <sup>25</sup>. This diagram illustrates possible interactions between the cobalt atom of cobalamins and CT or the trichloromethyl radical. As suggested above, presence of the sulfide reductant likely reduces the cobalt to the Co(II) oxidation state, at which point the cobalt then abiotically reduces either CT or its radical, returning to its Co(III) state.

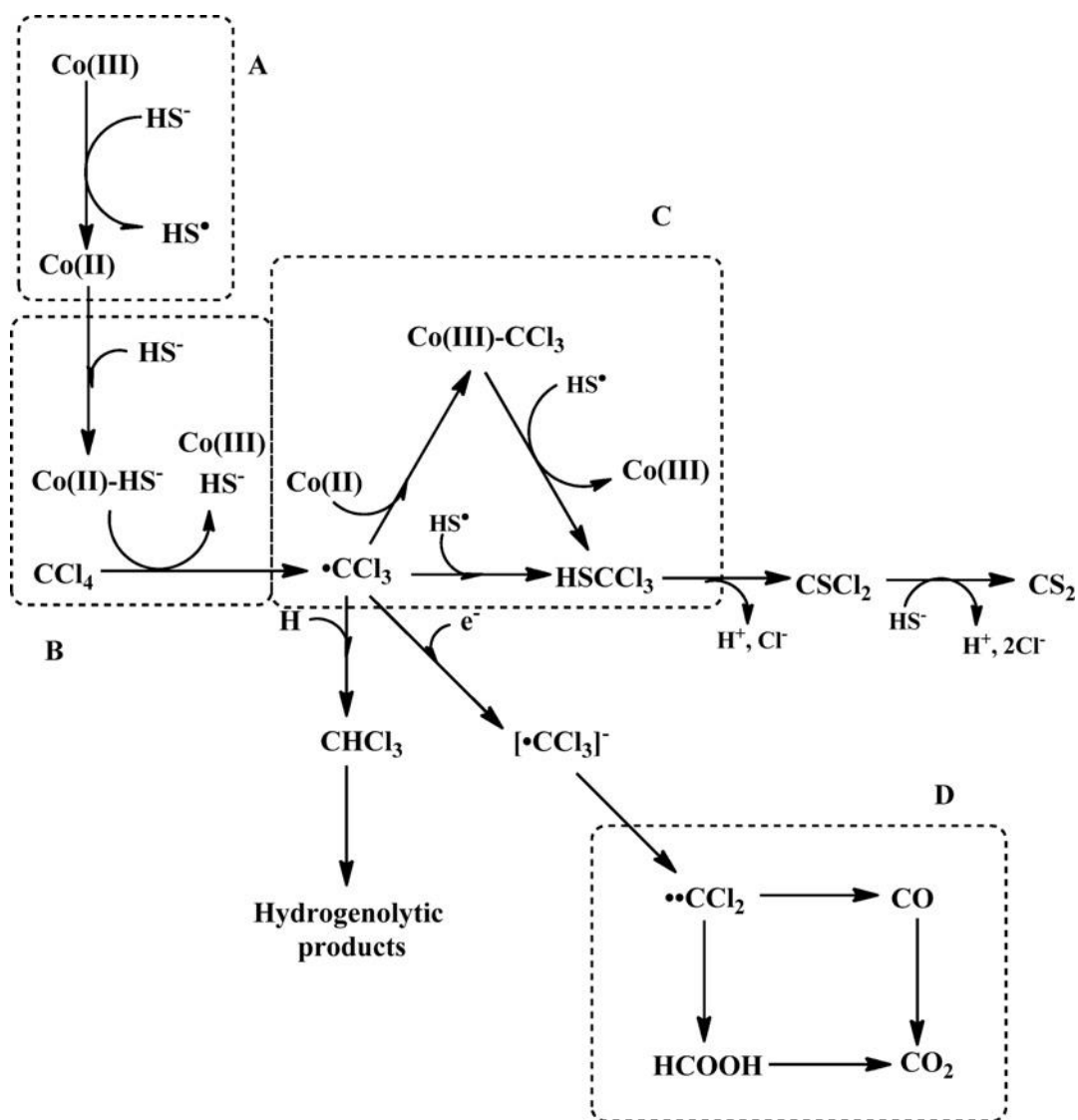


Figure 2. Proposed pathways of CT transformation in reduced environments affected by vitamin B12. Prepared by Koenig et al. 2012 after references: <sup>8,93,106,107</sup>

As evident from the work discussed here, there are many contributing factors to the fate of CT in anaerobic systems, and discrepancies in findings reflect that. However, research to understand how factors like type of organism, electron donor, quantity of cobalamin, cheaper sources of cobalamin impact feasibility and efficacy of such design. Recent work has moved beyond product analysis and consumption rates to employ techniques such as compound specific isotope analysis (CSIA) and dual element isotope

plots in evaluating proposed to better assess and product distributions based on various corrinoid/pollutant ratios as described by a recent article <sup>108</sup>.

Understanding these relationships can inform remediation strategies that seek to prevent buildup of intermediates such as CF, DCM, and CS<sub>2</sub>. Furthermore, in CE/CM co-contaminated sites, the catalysis of CT transformation with vitamin B12 may lower cobalamin supplies vital to RDase function in the CE OHR pathway. It has been proposed that CT interferes with metabolism of various microorganisms via bonding with their corrinoids and corrinoid enzymes, likely a bond between the TCM radical and the Co atom <sup>8,22,27,93,106,109</sup>. As suggested by Yu and Smith <sup>27</sup>, it is possible that the corrinoids are both catalysts to CT and CF dechlorination as well as targets of its inhibitory potential. This mechanism has not been studied in combined CE/CM systems but could have drastic implications for the success of CE OHR in CE/CM co-contaminated sites. While the mechanism(s) are not yet clearly established, a significant body of research has demonstrated the inhibition or toxicity to various microbial populations by CT and CF and will be presented in the following section.

#### 4. **Inhibition and Toxicity of Chlorinated Methanes on Microbial Systems**

##### *i. Vocabulary and Introduction*

The terms inhibition and toxicity are used inconsistently in the literature. For the following section, terms are kept consistent with the usage of respective authors. However, elsewhere in this document, the terms inhibition and toxicity are treated differently, according to the definitions below:

*Inhibition* – A blockage to some extent of a specific cellular process, regardless of whether survival is dependent upon that process, regardless of whether the blockage is reversible. This can refer to enzyme kinetics and/or general trends.

*Toxicity* – A long-lasting effect to a cell that results in permanent, irreversible damage, killing a cell.

Thus, the terms are not mutually exclusive. Inhibition can be caused by toxicity, and toxicity can be measured by an inhibition response.

Rozzi and Remigi<sup>110</sup> define inhibition as something measurable based on a reference activity, where activity is defined as “the inherent ability of a microbial population to undertake the degradation of the test material.” This baseline activity is measured at optimum conditions and then compared to inhibitor-exposed conditions, and inhibition is often reported as a percentage reduction (commonly IC<sub>50</sub> or EC<sub>50</sub>) of that activity. In the present context, the activity might be methane production or reduction of chlorinated ethenes, while the inhibitor is CT or CF. If the activity being inhibited can result in cell death, then toxicity is implicated, according to the definition above. This is consistent with the use of terms by Weathers and Parkin, who reported inhibition of methanogenesis by CF biotransformation and thus concluded that CF biotransformation was toxic to the microbes<sup>111</sup>.

The author recognizes that in the book, *Anaerobic Biotechnology for Industrial Wastewaters*,<sup>112</sup> R.E. Speece defines the terms as follows:

*Inhibition* – impairment of bacterial function

*Toxicity* – an adverse effect (not necessarily lethal) on bacterial metabolism

However, these definitions will not be used here.

Effects of carbon tetrachloride (CT) and chloroform (CF) on microbial systems have been widely studied. Most commonly reported is the inhibition of methanogenesis, but in recent decades, studies have expanded to include effects upon other microbial processes, such as sulfate reduction and acetogenesis. The broadly accepted conclusion is that chlorinated methanes (CMs) are inhibitory or perhaps even toxic to the microbial world, however only a few researchers have ventured to propose specific mechanisms of action. Furthermore, while there is general agreement regarding the detriment that CMs offer, only a handful of studies are able to illustrate how OHRB specifically are effected and even fewer that offer solutions or suggestions for microbial recovery, which is relevant to CM/CE co-contaminated. Select studies from the following three sections are

summarized in Tables 2, 3, and 4, representing the order in which the microbial systems are discussed.

Table 2. Select Experiments Testing Inhibition of Methanogenesis by CT or CF

Culture Origin	Microbial Community	Reactor Type	Inhibitor ( $\mu\text{M}$ )		Substrate	Observation(s)	Ref.
			[CT]	[CF]			
bovine rumen contents	consortium	stoppered roll tubes	1.4	7.8	formate	50% inhibition of methane production; H <sub>2</sub> accumulation	a
rumen contents of fistulated ewe	consortium	continuous N/A: in vivo	13 $1.3 \times 10^5$	NT	alfalfa hay	100% inhibition of methane production; H <sub>2</sub> accumulation; VFA product distribution shift 50% inhibition of methane production; H <sub>2</sub> accumulation	b
anaerobic digester	consortium	batch (flask)	14.5	8	ethanol	50% inhibition of methane production	c
whole rumen fluid	2 isolated strains of <i>Methanobacterium</i>	batch	32	8	formate, H <sub>2</sub>	100% inhibition of methane production; H <sub>2</sub> , CO <sub>2</sub> accumulation; inhibition of acetate utilization	d
sewage treatment plant digester sludge	consortium	batch fill-and-draw	104	NT	varied	Gas production declined in all, halted in 16 $\mu\text{M}$ , then recovered; Acclimation achieved to 1300 $\mu\text{M}$ in batch; CF = bacteriostatic	e
Not specified	enrichment	batch semi-continuous	NT	3.3 to 1300	acetate	50% inhibition of total gas production	f
Not specified	10-yr enrichment	continuous	42	7.5	acetate	Steady state achieved with each CF step; % removal of CF improved with each step (acclimation)	g
EPA Facility methanogenic reactor	consortium	continuous	NT	0.84 to 16.74 steps	acetate	Higher [CF] caused slower acetate utilization rates; Acclimated source culture concentration impacts CF rate	h
EPA Facility methanogenic reactor	consortium	batch	NT	0.17 to 5.4	acetate	Delayed methane production corresponds with mass of CF; Mass of CF biotransformed correlates best with inhibition	i
methanogenic cell suspension	consortium	batch	NT	1.7 to 8.49	acetate		j

a. Bauchop, 1967, b. Rufener and Wolin, 1968, c. Thiel, 1969, d. Prins, 1972, e. Sykes and Kirsch, 1972, f. Yang and Speece, 1986, g. Blum and Speece 1991, h,i. Gupta et al, 1996, j. Weathers and Parkin, 2000

Table 3. Results from Representative Studies with Inhibition of OHRB by CT or CF

Microbial System(s)	Microbial Community Type/Composition	Reactor Type for Inhibition Test	Inhibitor ( $\mu\text{M}$ ) CT      CF		Substrate(s)	Observation(s)	Ref.
reductive dechlorination, methanogenesis, acetogenesis	mixed culture enriched from anaerobic digester	batch	10.6 and 15.9	NT	lactate, PCE	PCE to TCE and VC to ETH steps were slowed but still completed; inhibition of methanogenesis and hydrogen utilization while present	a
reductive dechlorination	anaerobic digester sludge enrichment	microcosm	19	3.9	ethanol, PCE	Complete inhibition of PCE degradation; In column, PCE degradation did not occur with 43 $\mu\text{M}$ CT influent	b
reductive dechlorination	<i>Dehalococcoides ethenogenes</i> , strain 195	batch	NT	1.6	PCE, cDCE	Complete inhibition of biogenic cDCE degradation; Synthetic cDCE contained 0.4% CF & inhibited cDCE degradation	c
reductive dechlorination	KB-1 enrichment culture from contaminated soil and groundwater	batch vials	NT	0.4, 2.5, 6.7	CEs, methanol	Complete TCE and VC inhibition at 6.7 and 2.5 $\mu\text{M}$ ; cDCE was slightly inhibited	d
reductive dechlorination	KB-1 enrichment culture - cell-free extract and whole cell suspension	batch vials	NT	0-60	TCE, cDCE, or VC & H <sub>2</sub> or methyl viologen	Enzyme level inhibition of TCE and VC according to different models; Transformation of cDCE is less inhibited than TCE or VC	e
reductive dechlorination	KB-1 enrichment culture from contaminated soil and groundwater	batch	NT	230-250	TCE, cDCE, or VC & methanol/ethanol/lactate	20 days of CF exposure yielded no CE transformation; Removal of CF via purging allowed for CE transformation at 8x time frame of unexposed culture	f

- a. Adamson and Parkin, 2000  
b. Bagley et al., 2000  
c. Maymó-Gatell et al., 2001  
d. Duhamel, et al., 2002  
e,f. Wei, 2012

Table 4. Results from Representative Studies with Inhibition of Other Microbial Systems by CT or CF

Metabolic System(s)	Microbial Community Type/Composition	Reactor Type for Inhibition Test	Inhibitor ( $\mu\text{M}$ )		Substrate(s)	Observation(s)	Ref.
			[CT]	[CF]			
Aerobic heterotrophy	consortium, seeded by WWTP A/S liquor	batch	845	5361	infant formula	Oxygen uptake inhibited by 50%	a
Aerobic methanotrophy	methanotrophic consortium	batch	NT	142	methane, formate	Methane consumption rate decreased by 93%; CF transformation products were toxic	b
Aerobic nitrification	<i>Nitrosomonas</i> , seed from meat-packing WWTP A/S liquor	batch	332	4.02	ammonia-N	Ammonia consumption inhibited by 50%	c
sulfate, nitrate, and iron reduction, fermentation	Pure: 4 fermenters, 2 iron-reducers, 1 nitrate-reducer, 1 sulfate-reducer	batch tubes	30-80	200	multiple	No growth of sulfate reducer. No growth of iron-reducers at specified CT; Other bacteria EC50: 0.5-2.4mM CT; 3.5+mM CF	d
sulfate reduction, methanogenesis, acetogenesis	Pure: 4 methanogens, 2 acetogens, 4 sulfate-reducers	batch	NT	20 and 50	varied	Rate of product formation <1% of CF-free controls except for SRB w/o Acetyl-CoA pathway	e
DCM fermentation	sediment consortium	microcosm	NT	41.9	DCM	DCM transformation inhibited; methanogens are not involved in DCM transformation	f
fermentation, acetogenesis	pure, <i>Clostridium thermoaceticum</i>	flask/tube with gas flow	$1.7 \times 10^5$	$2.07 \times 10^5$	glucose	Near complete inhibition of CO <sub>2</sub> fixation to acetate; 10 and 25 $\mu\text{M}$ CT yielded 10 and 90% inhibitions of fixation	g
sulfate reduction	consortium, likely <i>Desulfovibrio</i> -containing	continuous and batch	NT	0.84-16.74 continuous; 0.1-29.3 batch	acetic acid	Acclimation to CF with gradual increase is possible; Batch CF transformation rate increased until 22.6 $\mu\text{M}$ slug added	h

a. Blum and Speece, 1991, b. Alvarez-Cohen and McCarty, 1991, c. Blum and Speece, 1991, d. Koenig et al., 2014, e. Scholten et al., 2000, f. Justicial-Leon et al., 2012, g. Ghambeer et al., 1971, h. Gupta et al., 1991

ii. *Methanogenic systems*

Anaerobic digestion exploits microbial methanogenesis in reactors designed for organic waste treatment often used at wastewater treatment sites and was an established process long before OHRB were discovered<sup>113</sup>. The effect of chlorinated methanes (CMs) on methanogenic systems is relevant to the study of OHRB because methanogens are often members of these communities. Also, considering that the first *Dehalococcoides*-containing culture found to fully transform PCE to ethene via reductive dehalogenation originated from a methanogenic anaerobic digester at a wastewater treatment plant, it is possible that these early studies accidentally evaluated OHRB<sup>57</sup>.

Originally studied in the 1960s, CT and CF inhibited the production of methane by methanogenic cultures in both rumen and anaerobic digester cultures, which was accompanied by the accumulation of H<sub>2</sub> gas<sup>114-117</sup>. Despite the use of mixed microbial communities of unknown composition and a range of CT concentrations, these batch culture studies agree on the inhibition of methanogenesis. As shown in Table 2, CF concentrations of 7.8-8 μM were found to inhibit methane production by either 50 or 100% in these early studies, where CT concentrations span several orders of magnitude to achieve the same inhibition. A comparison across studies demonstrates that the CT concentrations required to achieve 50% inhibition of methane production (1.4 vs 14.5 or 42 μM) and 100% inhibition (13 vs 104 μM) are lower for rumen microbes than those from anaerobic digesters<sup>114-118</sup>. This may suggest that in general anaerobic digester cultures are more robust than those in rumen fluid but could also be explained by cell density differences.

From the 1980s onward, focus shifted away from CT and studied primarily CF as an inhibitor. Yang and Speece<sup>119</sup> evaluated the impact of several different isolated operational parameters for their work with CF and acetate-fed methanogenic cultures. In semi-continuous reactors operated with a 50-day solids retention time (SRT), CF doses of 4.2-21 μM were evaluated for impact on gas production, a proxy for methanogenesis. Only the highest CF dose halted gas production; however, cultures later continued gas production to uninhibited levels. This suggested either an acclimation of viable cells to

the presence of CF or a detoxification process during the time of zero production. This recovery was seen again in tests where CF was removed after a 1 or 24-hour of exposure via supernatant replacement. The longer exposure time resulted in a greater lag time prior to gas production; however, the full recovery of gas production further indicated that CF was merely a bacteriostatic to these cultures and did not cause permanent damage. When CF was added gradually to reactors allowing for acclimation to its presence, cultures were able to maintain gas production to 126  $\mu\text{M}$  CF concentration, where unacclimated cultures' performance was severely inhibited at 21  $\mu\text{M}$  <sup>119</sup>.

Gupta et al. <sup>120</sup> reported a similar phenomenon of recovery 10 years later for a continuously operated reactor. Since acetic acid is fermented to methane, acetic acid utilization was monitored as an indicator of methanogenesis. Between each stepwise CF concentration increase to the chemostat feed, the reactor was allowed to achieve state state, which was determined by effluent VFAs, COD, ORP, and VSS. At two of these acclimation CF levels, the chemostat was sampled for batch reactor tests where CF was added as a slug dose and acetic acid utilization was evaluated in batch. The studies discovered that if the chemostat was fed 8.37  $\mu\text{M}$  prior to sampling, a CF slug concentration of 2.7  $\mu\text{M}$  resulted no acetic acid utilization within the batch bottles. In contrast, once the chemostat was achieved steady state with at constant feed of 16.37  $\mu\text{M}$ , batch bottles could withstand a slug dose of 4.2  $\mu\text{M}$  CF without a complete loss of acetic acid utilization. Stepwise increases of CF in the continuous reactor feed thus allowed for either acclimation of the cultures or proliferation of different microbial strains due to a selective pressure exerted by the presence of CF <sup>120</sup>. A reversible CF inhibition of methanogenesis was also reported for an anaerobic digester culture by Yu and Smith <sup>27</sup> at concentrations of 0.09, 0.87, and 4.35 mg/L.

While Yang and Speece concluded that it was CF exposure time that contributed to a lag in gas production as discussed above, years later Weathers and Parkin <sup>111</sup> reported that it was the biotransformation of CF that caused toxicity in their cultures. During phase 1 of their experiments, CF addition was found to strongly inhibit methanogenesis in the ranges of 1.7-8.5  $\mu\text{M}$ . After batch reactors were purged free of CF, acetic acid was added in phase 2 and subsequent methane production was monitored to identify the effect of

phase 1 CF exposure. Since the removal of CF by sparging did not recover methane production rates, the authors concluded that the inhibition was caused by a nonvolatile CF biotransformation product. This was contradictory to the finding of Yang and Speece, who had determined via the use carbon-14 labeled CF that most of the loss of CF throughout experiments was due to the semi-continuous nature of the reactors (i.e., loss through the removed gas phase volumes).

The concentrations tested and determined inhibitory by Weathers and Parkin are on the low end of the range tested by Yang and Speece, so it is unlikely that inadequate ranges tested are responsible for the different findings between the research groups. However, other differences in the cultures' biomass concentrations and non-methanogenic microbial community could explain the discrepancy. First, Yang and Speece determined that greater biomass was correlated with faster recovery from reduced gas production due to CF. Yang and Speece tested VSS concentrations of 925, 780, and 515 mg/L, where the last did not recover gas production after a 21  $\mu\text{M}$  slug CF input. In comparison, Weathers and Parkin's culture with 245 mg/L VSS exposed to 8.5  $\mu\text{M}$  CF suffered a 73% reduction in methane production rate. It is likely that Yang and Speece would achieve a similar inhibition to Weathers and Parkin at a more comparable biomass. In light of this, the cultures compare rather well, but this does not explain why the Weathers and Parkin cultures could not recover without CF present.

Second, neither study discusses the potential presence of OHRB within the methanogenic culture. It is possible that activity of OHRB such as *Dehalobacter* could have been responsible for the CF biotransformation in Weathers and Parkin cultures, inadvertently exposing methanogens to nonvolatile, toxic intermediates. Further, CF degradation in the Weathers and Parkin culture was enhanced by acetate, an electron donor used by some OHRB. If OHRB were present and responsible for CF degradation, then the inhibition due to presence of CF found in Yang and Speece would have to be explained by an alternate mechanism of inhibition/toxicity since biotransformation was reported not to have occurred there.

iii. *OHRB Systems*

Table 3 summarizes the few studies available that specifically evaluate the effects of CT or CF on OHRB. Perhaps most commonly referred to is the work by Bagley et al., wherein reductive dechlorination of about 8  $\mu\text{M}$  PCE in microcosms anaerobic digester enrichment cultures was completely inhibited by CT (19  $\mu\text{M}$ ) and CF (3.9  $\mu\text{M}$ ), tested separately<sup>17</sup>. A packed column was unable to facilitate PCE transformation during 125 days while the influent CT concentration of 43  $\mu\text{M}$  was fed with PCE, TCE, ethanol, and yeast extract. After removing CMs, rinsing, repacking, and re-inoculation, the column was able to successfully transform PCE to VC and ethene. This may suggest success of a remediation scheme aimed at eliminating CMs prior to CE removal mechanisms.

Adamson and Parkin studied CT effects on another anaerobic digester enrichment culture at similar concentrations<sup>121</sup>. CT slug inputs of 10.6 and 15.9  $\mu\text{M}$  both resulted in a dramatic slowing of 200  $\mu\text{M}$  PCE transformation. This was accompanied by inhibition of methanogenesis and  $\text{H}_2$  utilization while CT was present, indicating negative impacts upon methanogens and acetogens likely present. However, complete CE transformation was achieved, albeit it 11 days later than in PCE-only controls<sup>121</sup>.

The inhibition of CF upon a pure culture was inadvertently discovered by Maymó-Gatell et al. due to the contamination of synthetic cDCE used for enrichment. *Dehalococcoides ethenogenes* strain 195 is unique to *Dhc* in that it can transform PCE completely to ethene without other strains present<sup>70</sup>. However, when grown on synthetic cDCE, ability to degrade the latter declined with each addition (slower rate of transformation), and PCE was not immediately utilized. When biogenic cDCE was supplied as a growth substrate for strain 195 via a *Desulfitobacterium*, PCE utilization was maintained. Synthetic cDCE was found to contain 0.4% mol/mol CF and was concluded to be responsible for the poor performance of strain 195 when fed cDCE. A 1.6  $\mu\text{M}$  addition of CF was found to completely inhibit biogenic cDCE transformation<sup>122</sup>.

In contrast, TCE-fed KB-1 cultures containing *Dhc* that did not belong to strain 195 were not significantly inhibited by 6.7  $\mu\text{M}$  CF in their transformation of 21  $\mu\text{M}$

cDCE. Three concentrations of CF were tested for effects on transformation of each CE substrate in a 30-day period. TCE biotransformation was completely inhibited at 6.7  $\mu\text{M}$  CF, while VC transformation only required 2.5  $\mu\text{M}$  for the same effect. At, cDCE transformation experienced only minor inhibition <sup>123</sup>.

Ten years later, research with the same culture resolved kinetic parameterization and recovery potential with CF exposures. From cell-free extract (CFE) and whole cell suspension (WCS) assays, Wei <sup>124</sup> determined with CF concentrations between 0 and 60  $\mu\text{M}$  that inhibition of TCE and VC transformations occurred primarily at the enzyme level via uncompetitive and competitive models for TCE and VC, respectively. This was supported by the fact that inhibition constants obtained from modeling the CFE assay data were much lower than those obtained from WCS assays, indicating a greater inhibition potential exerted on the RDase enzymes of the CFE assays. Consistent with the earlier work, cDCE transformation was much less inhibited than TCE or VC <sup>123,124</sup>. Recovery potential was evaluated for the enrichment culture after 20-day exposure CF concentrations of 230-250  $\mu\text{M}$ , during TCE, cDCE, and VC transformation were each stalled in separate reactors. Reactors were purged with  $\text{H}_2$  and carbon dioxide and re-amended with CE substrate. Transformation of each CE completely to ethene then occurred within 80 days, which corresponded to a factor of 8 or more longer than unexposed controls. Further substrate additions to evaluate the potential for shortening this time were not performed, but this is the only known study to evaluate recovery potential or reversibility of CF effects on OHRB <sup>124</sup>.

The majority of research with CMs and reductive dechlorination has been performed at CF concentrations less than 20  $\mu\text{M}$ , as shown by Table 3. KB-1 is the only OHRB culture known to be tested for both kinetic parameters to describe CM inhibition and recovery potential following CM exposure <sup>124</sup>. No studies except for the two listed in Table 3 are known to evaluate the effects of CT inhibition of reductive dechlorination, and neither of these explore recovery potential. Considering the large amount of co-contaminated groundwater sites, there is relatively little substantive research to guide regulators and remediation engineers in their efforts to tackle the challenges that these sites pose.

iv. *Other Microbial Systems*

In addition to methanogenesis and reductive dechlorination, chlorinated methanes affect other microbial processes. As displayed in Table 4, the following metabolic processes have been shown to be disrupted by CT, CF or both: aerobic heterotrophy<sup>118,125</sup>, nitrification<sup>118</sup>, iron, nitrate, and sulfate reduction<sup>20,21,126</sup>, acetogenesis<sup>21,22</sup>, and fermentation<sup>20,23</sup>. Because the most successful OHRB operate in mixed microbial community, the effects of CMs on neighboring populations is relevant for this discussion<sup>75</sup>. Nutrients and cofactors that OHRB rely on may become unavailable if their microbial source is compromised by an inhibitor. Table 4 briefly summarizes findings from representative studies on CT or CF inhibition towards a variety of microbial communities and is further discussed below.

CM effects on aerobic metabolism is noted in Table 4 by several studies from the early nineties. Oxygen uptake by aerobic heterotrophs was inhibited by 50% at CT and CF concentrations much higher than those that devastated anaerobic systems discussed previously<sup>118</sup>. In this experiment, CF at more than six times the amount of CT achieved the same inhibition for a heterotrophic consortium, suggesting that CT was more toxic to the WWTP culture. In contrast, the nitrifier *Nitrosomonas* only required 4  $\mu\text{M}$  CF compared to 332  $\mu\text{M}$  to achieve the same percent inhibition, indicating that CF was more toxic to this organism<sup>118</sup>. Alvarez-Cohen and McCarty<sup>125</sup> concluded that methanotrophy was inhibited in their consortium due to nonvolatile transformation products of CF such as phosgene, an intermediate in the aerobic degradation pathway. Due to the anaerobic nature of the present study, this mechanism of toxicity was not anticipated, and the rest of this review will return to anaerobic systems.

Unlike the other studies included, Koenig et al.<sup>20</sup> measured the effects of CT and CF by analyzing differences in growth rates for the following eight pure cultures: *Escherichia coli*, *Klebsiella* sp., *Clostridium* sp., *Paenibacillus* sp., *Pseudomonas aeruginosa*, *Geobacter sulfurreducens*, *Shewanella oneidensis*, and *Desulfovibrio vulgaris*. Inhibitor concentrations reducing growth to 50% are reported as effective concentration, or EC<sub>50</sub>, values, with ranges 500-2400  $\mu\text{M}$  for CT and 3500-6000  $\mu\text{M}$  for

CF, although some cultures exhibited no growth under the lowest concentration exposures. The lower range for CT indicates a greater toxicity of this compound over CF, which is contrary to most of the work done with methanogens or OHRB. Effective concentrations were higher for fermenting bacteria and lower or not applicable for sulfate and iron reducing bacteria (SRB and IRB, respectively). For example, *Shewanella oneidensis*, *Desulfovibrio vulgaris*, and *Geobacter sulfurreducens* could not grow at the minimum CT exposure concentrations of 80, 80, and 30  $\mu\text{M}$ , respectively. Under CF exposure, *D. vulgaris* was the only culture tested that was completely inhibited, even at the lowest exposure of 200  $\mu\text{M}$ ; however, *G. sulfurreducens* was severely impeded with an  $\text{EC}_{50}$  far below the range listed above <sup>20</sup>.

Another study involving a suspected *Desulfovibrio* culture demonstrated that acclimation to the effect of CF can occur, similar to findings discussed in “Methanogenic Systems” <sup>126</sup>. This acclimation was demonstrated with small step increases of CF into chemostat feed after each previous condition reached steady state. VSS, ORP, effluent acetic acid, sulfate, and COD were monitored to establish steady state. When the chemostat achieved steady state conditions with an influent of 16.74  $\mu\text{M}$  CF, batch reactors were established with a range of slug CF inputs. Additions of CF up to 22.6  $\mu\text{M}$  achieved increasing CF degradation rates in the bottles, indicating an improvement in the culture’s ability to degrade CF, but at higher concentrations performance dropped. The SRB culture acclimated to and transformed CF at much higher concentrations than the methanogens studied by the same research group, although some of the difference can be explained by differing VSS concentrations <sup>120,126</sup>.

In a pure study with three SRB including *D. vulgaris*, 20 and 50  $\mu\text{M}$  CF was found to inhibit rates of metabolic product formation only in cultures containing the acetyl-CoA cleavage pathway. Inhibition was defined as the point at which rate of sulfide formation was less than 1% of that performed by cultures without CF exposure <sup>21</sup>. The researchers reported that the SRB *Desulfotomaculum acetoxidans* experienced inhibition, whereas *D. vulgaris* and *Desulfobacter postgatei* were not inhibited. Initially these results suggest that the acetyl-CoA metabolic pathway could be a primary indication of susceptibility to CMs for SRB. However, as presented above, Koenig et al. <sup>20</sup> reported

that 200  $\mu\text{M}$  CF inhibited *D. vulgaris* growth completely, therefore a lack of the acetyl-CoA pathway may not be the only protection against CF inhibition.

Scholten et al.<sup>21</sup> also demonstrated the inhibition of acetogens *Acetobacterium woodii* and *Sporomusa acidovorans*, where 20 and 50  $\mu\text{M}$  inhibited rates of acetate production to less than 1% of control rates. Both of these organisms also have the acetyl-CoA pathway. Another homoacetogen was evaluated for inhibition by CT and CF as early as 1971<sup>22</sup>. Both CT and CF were shown to inhibit the conversion of labeled carbon dioxide to acetate by *Clostridium thermoaceticum* during its fermentation of glucose<sup>22</sup>. A concentration of  $1.7 \times 10^5$   $\mu\text{M}$  CT almost completely prevented any acetate formation, and its effect occurred at very early time of the experiment, unlike the linear reduction of  $\text{CO}_2$  fixation seen in controls. At lower concentrations,  $1 \times 10^{-5}$   $\mu\text{M}$  CT resulted in 10% inhibition of acetate formation, while  $1 \times 10^{-3}$   $\mu\text{M}$  CT resulted in 99% inhibition. Additionally, in cell-free extracts exposure to CT prevented the conversion of key compounds in the proposed pyruvate fermentation pathway, suggesting an interaction between CT these compounds specifically. CT inhibited acetate synthesis both by *Clostridium thermoaceticus* whole cell suspensions and cell-free extracts, indicating the interaction between CT and either methyltetrahydrofolate or the methylated corrinoid, key players in the proposed synthesis pathway<sup>22</sup>.

As discussed previously, inhibition by CT and CF may involve binding critical corrinoids or corrinoid enzymes of various microbial metabolic pathways<sup>27</sup>. In the case of OHRB, this would have implications for the efficiency of CE transformations since RDases require corrinoid cofactors to function<sup>78</sup>. It is also possible that the trichloromethyl radical binds indiscriminately to cellular materials such as phospholipids, which occurs in hepatic studies with mammalian tissues<sup>127,128</sup>. However, to the author's knowledge, this has not been studied in microbial systems. Despite the multiple possible mechanisms for inhibition or toxicity, several studies have demonstrated successful combined transformations of CEs and CMs.

## 5. CE/CM Co-contamination: Examples of Simultaneous Transformation

Despite the inhibition of CT and CF on microbial activity, some research has indicated the possibility for simultaneous transformation of CEs and CMs. Effects of one class of compound on the removal of another is pertinent to bioremediation schemes, especially since many sites harbor contamination from multiple chlorinated solvent classes. The ideal scheme would facilitate the removal of both classes of chlorinated solvents at a co-contaminated site. The following section provides some laboratory examples of this.

Adamson and Parkin<sup>129</sup> evaluated the simultaneous transformation of CT, PCE, and 1,1,1-TCA in batch studies with an acetate-fed methanogenic enrichment culture. CT transformation occurred within 2 days for the concentration ranges tested (0.59-4.6  $\mu\text{M}$ ) regardless of the presence of PCE or TCA, however, its pseudo first-order rates were slower when TCA was present. Data to determine the effect of CT and TCA on PCE transformation was scattered, and a statistically significant decrease in PCE transformation rate was only seen with a test combination of 0.8  $\mu\text{M}$  PCE, 2.7  $\mu\text{M}$  CT, and 2.2  $\mu\text{M}$  TCA. Additionally, control rates of PCE transformation were slow, suggesting that the culture had little PCE-degrading ability to begin with. Therefore the precise impact on PCE of CT alone could not be inferred, and it is likely that PCE did not affect CT transformation because PCE did not transform into toxic intermediates that could interfere with the culture performance.

In a column study with anaerobic digester cultures, PCE degradation acclimated to the presence of chlorinated methanes. CT additions caused an initial inhibition of PCE transformation that was eventually reversed by 35 days<sup>24</sup>. Each increase in influent CT concentration resulted in a faster recovery of PCE degradation to ethene, indicating the potential for recovery of cultures to long term CM exposure. The highest CT influent concentration of 13  $\mu\text{M}$  yielded consistent CF concentrations of about 3  $\mu\text{M}$  in most of the column, while DCM disappeared likely due to biodegradation. At all concentrations, CT degraded at short spatial distances from the influent. However, the ability of the system to quickly transform CT does not necessarily indicate that it was not toxic to the cultures. The CF concentration throughout most of the column was about 2.5  $\mu\text{M}$  when

CT influent was 6.6  $\mu\text{M}$  and only increased to about 3  $\mu\text{M}$  when the CT concentration was further doubled to 13  $\mu\text{M}$ .

Chung and Rittmann<sup>130</sup> evaluated the simultaneous CE/CM biotransformation ability of a Dehalococcoides-containing culture in a membrane biofilm reactor. Effluent concentrations of CF, TCE, TCA, and their intermediates indicated an improvement in transformation of all three compounds during 120 days. After successfully transforming lower concentrations at earlier time, the biofilm transformed influent concentrations of 21, 18.8, and 19  $\mu\text{M}$  of CF, TCA, and TCE, respectively, added at day 133 of operation. However, by day 180, effluent concentrations of 10  $\mu\text{M}$  chloromethane, 15  $\mu\text{M}$  chloroethane, and 2  $\mu\text{M}$  TCE were measured. While some inhibition of TCE and TCA transformation as well as competition for  $\text{H}_2$  by sulfate and nitrate-reducing populations was likely, the authors demonstrated the simultaneous CF/TCE transformation and successful  $\text{H}_2$  delivery to the system.

A sulfate-reducing bacteria (SRB), *Desulfovibrio vulgaris*, was found to transform 10  $\mu\text{M}$  CT at variable rates depending on batch reactor amendments in the presence of 40  $\mu\text{M}$  PCE<sup>25</sup>. Addition of vitamin B12 shifted the product distribution to consist primarily of  $\text{CS}_2$ , instead of CF or DCM seen to make up the majority of transformed CT mass in reactors without B12. Addition of Fe(III) shifted the relative proportions of CF and DCM when B12 was not amended, but its major contribution was for reductive dechlorination when PCE-degrading enrichment culture was added to the *D. vulgaris* at day 36. Only reactors with Fe(III) effectively transformed CEs, and those originally amended with B12 only increased CE transformation a little. The authors attribute this to the precipitation of free toxic sulfides by the Fe(III). VC and ethene were the resulting products at 46 days. Reactors that still contained CT did not transform PCE. Thus, an SRB was shown to lay the groundwork in stage one for the PCE transformation by OHRB in stage two of a co-contaminated setting. Discussion on the impacts of B12 from this work is discussed elsewhere.

Recent work with the Evanite culture used in the present project has demonstrated its ability to simultaneously transform CT and CEs in batch and column studies.

Vickstrom et al.<sup>26</sup> presented a transformation model for CT based on pseudo-first order kinetics for CT and products CF, CS<sub>2</sub>, DCM, and CO<sub>2</sub>. In batch tests with Evanite culture and chemostat supernatant, 50 μM TCE and 2.6 μM were added with formate as a H<sub>2</sub> supply. CT transformation was complete within 5 days. CF was the primary measurable product, however, CO<sub>2</sub> was suspected to be formed as 80% of the original CT mass by day 40. On day 14, more TCE was added to reactors, but CE transformation rates were slowed by about an order of magnitude.

In a column study<sup>7,131</sup>, PCE (0.1 mM), CT (0.015 mM), and formate (1.5 mM, electron donor) were added continuously to a column bioaugmented with Evanite culture that had been transforming PCE to ethene for 1640 days. Effluent concentrations were measured for 140 days after the start of CT addition and detected CT and CF for about 50 days after which only CF remained at 20% of CT mass added. Trace DCM and chloromethane were detected, but no methane, CS<sub>2</sub>, or CH<sub>4</sub> were detected. Acetate concentrations decreased, accompanied by an increase in formate and H<sub>2</sub>, indicating inhibition of homoacetogens. Incomplete CE OHR occurred during this stage. Column effluent measurements taken after halting the influent indicated that CE OHR was able to complete transformation with the longer reaction time this provided. When the column influent was restarted without CT addition and with lactate as the electron donor, CE OHR efficiency dramatically plummeted, with high levels of cDCE (50%) and VC (40%) present in the column effluent. H<sub>2</sub> had decreased below its detection limit, and despite lactate transformation, propionate and acetate levels built up, indicating the inhibition of propionate fermentation by CT transformation products remaining in the column. When lactate was replaced with formate, CE OHR was restored (97.8% ethene product), but acetate concentrations were below detection, indicating a long-lasting inhibition of homoacetogenesis as well. This was particularly notable because early column operation pre-CT exposure included the addition of lactate as the electron donor with successful CE OHR. Thus, poor PCE dehalogenation was linked with ineffective propionate fermentation. Various microbial populations and metabolic processes were evident throughout the stages of this experiment; however, PCE and CT transformation simultaneously occurred, with 20% CF product, no CS<sub>2</sub> product, and minor DCM

product. Complete PCE transformation depended on the electron donor present, functionality of which was subject to CM inhibition. This work made major contributions to understanding the dynamics of successful and inhibited CE/CM co-contaminated systems.

In a second experimental phase with the Evanite-bioaugmented PCE/CT column, Azizian and Semprini <sup>7</sup> demonstrated via <sup>13</sup>CT that 82-93% of the CT product in the column was non-toxic CO<sub>2</sub> and that effective lactate and propionate fermentation could be restored with a second bioaugmentation of the Evanite culture. On day 1950, electron donor was switched back to the original lactate. H<sub>2</sub> levels remained at formate-fed levels, acetate increased, and PCE transformation was effective (95% ethene). This performance was maintained during influent addition of 0.015 mM, 0.03 mM CT, and up to 0.2 mM sulfate until day 2336 of operation. CT broke through the column after influent concentration was increased to 0.03 mM, but it reduced below detection limit shortly thereafter. Pseudo-steady state CF levels were below detection within a couple of weeks after the influent increase to 0.03 mM CT. <sup>13</sup>CT was introduced to the column in order to quantify CO<sub>2</sub> product against background <sup>13</sup>CO<sub>2</sub>. According to first order rate constants from modeling kinetics with Evanite culture in batch reactors <sup>26</sup>, about 99% of CT would be able to transform, but only 30% of CF and 20% of CS<sub>2</sub> would be transformed. Thus, other factors likely contribute to the transformation and product distribution of CT in the column and may include spatial distribution, stronger reducing conditions, and presence of CF-respiring microbial populations. This work demonstrated the possibility of successful simultaneous CT and PCE transformations to non-toxic products in co-contaminated conditions via abiotic and biotic reaction mechanisms and its dependence on healthy fermenting populations.

Effective OHR is essential to *in situ* bioremediation, and its inhibition by CT, CT transformation, or CT products has been indicated but is not well understood. Factors contributing to CT product distribution can help inform design that aims to reduce the levels of toxic intermediates created. Mechanism(s) of CT-related inhibition or toxicity should be understood so that designs can be built to reduce their impact.

## CHAPTER 3 – METHODS

### 1. Chemicals

The following chemicals were used in calibration and experimentation: CT, 99% (Acros Organics); CF, 99.9% (OmniSolv); DCM, 99.9% (Fisher Scientific); CS<sub>2</sub>, 99.9% (Alfa Aesar); TCE, 99.5% (Macron Fine Chemicals); cDCE, 99% (TCI America); VC, 99.5% (Sigma-Aldrich); ETH, 99.5% (Airgas); L-cysteine, cell culture reagent (Alfa Aesar); vitamin B12 (cyanocobalamin), 99% (Sigma-Aldrich); sodium formate, 99% (Alfa Aesar).

### 2. OHRB Cultures

The Evanite – 5-liter (EV-5L) anaerobic dehalogenating culture was used for this study. Microbial cultures were originally collected at a TCE-contaminated site owned by Evanite Corporation (now Hollingsworth and Vose) in Corvallis, Oregon. Originally, EV-5L was maintained in batch reactors, operated by fill-and-draw, where PCE and butanol served as electron acceptor and donor, respectively. Reductive dechlorination, acetogenesis, and methanogenesis all occurred simultaneously, but the latter has stopped with OHRB enrichment<sup>132–134</sup>. Cultures were later switched to a closed continuous flow operating system (chemostat) with TCE and formate as electron acceptor and donor, respectively. Hydraulic retention time is approximately 50 days, and the chemostat has been operated since July 2007. Saturated TCE (8-10 mM) and sodium formate (45 mM) are supplied continuously to the reactor in mineral media described by Yang and McCarty, modified by the doubling of buffering capacity supplied by K<sub>2</sub>HPO<sub>4</sub> and NaHCO<sub>3</sub><sup>90</sup>. Complete reductive dechlorination of TCE to ethene occurs in EV-5L when sufficient electron donor is provided<sup>73</sup>.

Genetic characterization of EV-5L has revealed that it is highly enriched for *D. mccartyi*, with 90-99% of the bacterial community accounted for by *tceA* and *vcrA* abundance<sup>73</sup>. Other genera identified via 16S rRNA sequencing included *Geobacter* (1-10%), *Spirochaeta* (<1%), and *Desulfobacteria*<sup>73,103</sup>. Acetogenic activity is demonstrated by the production of acetate when abundant H<sub>2</sub> is supplied, indicating the presence of

acetogens, which use  $H_2$  as one of many electron donor substrates possible<sup>7,135</sup>. The EV-5L chemostat is unacclimated to the presence of chlorinated methanes; however, recent work has established ability of sampled cultures and media to transform carbon tetrachloride (abiotically) and chloroform (biotically), with concomitant slowing chlorinated ethene transformation<sup>26</sup>. However, column studies have suggested that EV-5L can completely transform CT and PCE with sufficient electron donor supply<sup>7</sup>.

### 3. Design of Kinetic Transformation Experiments

Prior to the onset of each experiment, empty 158 mL borosilicate glass reactors (Wheaton) were equilibrated for at least 24 hours in an anaerobic chamber with 3-7%  $H_2$  (balance  $N_2$ ). On day 0, the chemostat was pressurized with anoxic, furnace-treated (600 C) 75:25  $N_2/CO_2$  gas, allowing the anaerobic transfer of 50 mL of culture and media to each glass batch reactor (triplicate for each experiment unless stated otherwise). Residual volatile compounds were then sparged from the batch reactors with the same 75:25  $N_2/CO_2$  gas mix for 15 minutes, which was sufficient to achieve nondetect levels for all CEs and  $H_2$ .

With the exception of B12 amendment tests, every experiment began with the addition of approximately 50  $\mu M$  TCE, 2 mM formate, and some amount of CM, either CT or CF. TCE and its transformation products were measured throughout the experiment to obtain transformation rates. CT, CF, and their transformation products were measured as well, with transformation rates for CT and CF estimated according to first order kinetics (see Analytical Methods). In the case of CT addition, experimental reactors are referred to as CT-exposed reactors, even though CF is also produced. In the case of time zero addition of CF, reactors are referred to as CF-exposed.

Formate is a self-buffering fermentable substrate for microbial populations that produce  $H_2$ , the required electron donor for CE OHR<sup>91</sup>. Homoacetogens are likely formate fermenters here, as acetate production has been seen in prior studies with the Evanite culture<sup>131</sup>. Two mmol/L formate hypothetically yields 100  $\mu mol$   $H_2$  per reactor, only 12.5 of which are required for OHR of 50  $\mu M$  TCE. Because other populations are

able to compete for H<sub>2</sub>, this stoichiometric excess was supplied to ensure sufficient H<sub>2</sub> supply for *D. mccartyi*.

For the single addition CT/TCE or CF/TCE experiments, additional TCE/formate was delivered at 1 (CT/TCE only), 2 or 14 days. Select reactors were sparged at 49 days to remove CMs prior to further TCE/formate additions for recovery experiments. For the multiple delivery CT/TCE tests, the mass equivalent of CT from single addition experiments was split into separate additions over the course of the first 2 days, and TCE/formate was added on day 0 and 2. TCE/formate controls were established similarly without CT or CF addition to serve as a reference CE transformation profile for comparison with experiment (CM exposed) profiles. Controls were re-spiked with TCE/formate additions at the same day as experimental bottles to account for endogenous decay likely occurring in unfed batch reactors. In the B12 amendment experiment, reactors received additions accordingly: day 0 – formate and B12, day 1 and 2 as needed – formate, day 3 – formate and CT, day 4 as needed – formate, day 5 – formate and TCE. For all experiments, CE transformation data was collected following each addition of TCE. Figure 3 shows a simple schematic of the experimental design for Experiments 1-6, where the onset is marked by the first addition of TCE, formate, and inhibitor (CT or CF). Table 5 outlines the experiment design and purpose for each test, labeled according to its references throughout this document.

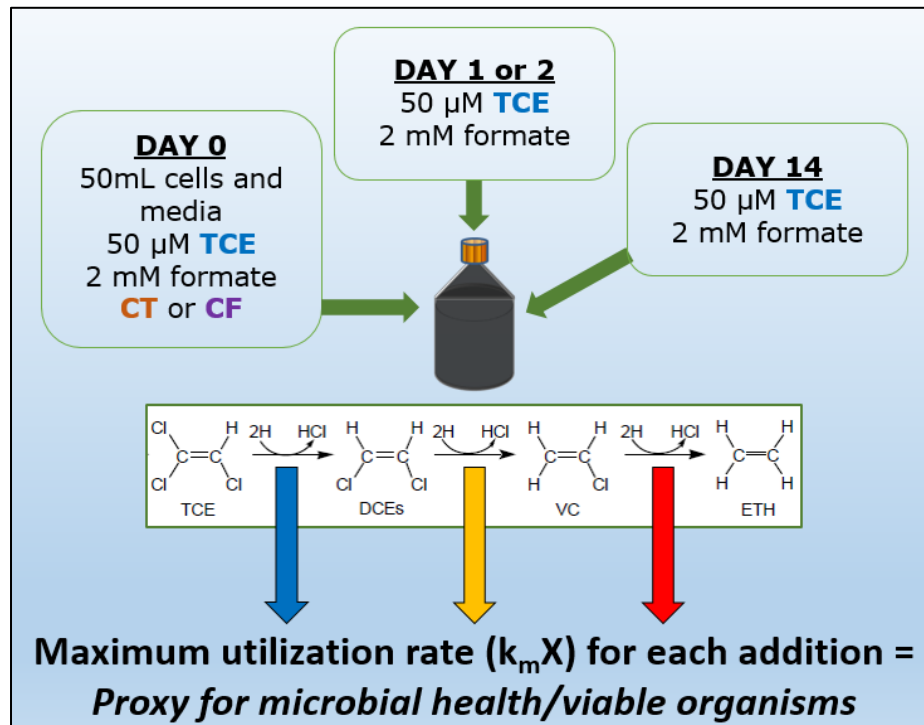


Figure 3. Simplified schematic of the design for Experiments 1-6.

Table 5. Experiments of this Project

Experiment	Purpose	First Addition	Further Addition(s)/Procedure(s)	
1	To establish long term effects of CT addition on CE transformation	<u>Day 0</u> 2 mM formate 50 $\mu$ M TCE 2.3 $\mu$ M CT	<u>Day 14</u> 2 mM formate 50 $\mu$ M TCE	
2	To establish short term effects of CT addition on CE transformation	<u>Day 0</u> 2 mM formate 50 $\mu$ M TCE 2.3 $\mu$ M CT	<u>Day 2</u> 2 mM formate 50 $\mu$ M TCE	
3	To establish short term effects of CT addition on CE transformation	<u>Day 0</u> 2 mM formate 50 $\mu$ M TCE 2.9 $\mu$ M CT	<u>Day 1</u> 2 mM formate 50 $\mu$ M TCE	
4	To establish long term effects of CF addition on CE transformation	<u>Day 0</u> 2 mM formate 50 $\mu$ M TCE 5.8 $\mu$ M CF	<u>Day 14</u> 2 mM formate 50 $\mu$ M TCE	
5	To establish short term effects of CF addition on CE transformation	<u>Day 0</u> 2 mM formate 50 $\mu$ M TCE 5.8 $\mu$ M CF	<u>Day 2</u> 2 mM formate 50 $\mu$ M TCE	
6	To evaluate CT concentration-dependence of CE transformation inhibition	<u>Day 0</u> 2 mM formate 50 $\mu$ M TCE 7.2 $\mu$ M CT	<u>Day 14</u> 2 mM formate 50 $\mu$ M TCE	
7	To evaluate CT mass of transformation dependence of CE transformation inhibition	<u>Day 0</u> 2 mM formate 50 $\mu$ M TCE 0.088 $\mu$ mol CT	<u>12 hours</u> 0.13 $\mu$ mol CT <u>24 hours</u> 0.13 $\mu$ mol CT	
8	To evaluate CT mass of transformation dependence of CE transformation inhibition	<u>Day 0</u> 2 mM formate 50 $\mu$ M TCE 0.068 $\mu$ mol CT	<u>12 hours</u> 0.094 $\mu$ mol CT <u>24 hours</u> 0.1 $\mu$ mol CT <u>36 hours</u> 0.098 $\mu$ mol CT <u>Day 2</u> 2 mM formate 50 $\mu$ M TCE	
9	To evaluate the potential for vitamin B12 amendment to mitigate the inhibition/toxicity of CT	<u>Day 0</u> 2 mM formate 15 mg/L (11 $\mu$ M) Vitamin B12	<u>Day 3</u> 2 mM formate 2-3 $\mu$ M CT (theoretical) <u>Day 5</u> 2 mM formate 50 $\mu$ M TCE	
10	To evaluate the potential for CE transformation recovery after CT addition (same reactors as Experiment 1)	<u>Day 49</u> 15 anaerobic gas sparge	<u>Day 50</u> 2 mM formate 50 $\mu$ M TCE	
11	To evaluate the potential for CE transformation recovery after CF addition (same reactors as Experiment 4)	<u>Day 49</u> 15 anaerobic gas sparge	<u>Day 50</u> 2 mM formate 50 $\mu$ M TCE	

#### 4. Analytical methods

Analytes were measured via gas chromatography (GC) throughout each experiment. Gas headspace samples were manually injected to GC with a Hamilton gas-tight syringe (100  $\mu$ L; 1700 series) All chlorinated compounds were measured on an HP 6890 Series GC System. Chlorinated ethenes (TCE, cDCE, VC, and ETH) were analyzed with a flame ionization detector (FID) with helium carrier gas at a flow rate of 15 mL/min with capillary column type Agilent 115-3234 30 m x 0.53 mm GS-Q. The following method was used for the FID: 150 C hold for 2 or 2.2 minutes, temperature ramp 35 or 45°C/min to 220 °C, hold 1.14 or 1.44 minutes. Chlorinated methanes (CT, CF, DCM) and CS<sub>2</sub> were analyzed with an ECD detector with helium carrier gas at a flow rate of 8 mL/min with capillary column type Agilent 30 m x 0.32 mm GS-Q. H<sub>2</sub> gas was analyzed with an HP-5890 GC thermal conductivity detector (TCD) on with argon carrier gas at a flow rate of 20 mL/min with a packed column (Supelco 15' x 1/8" SS support 60/80 Carboxen 1000). The method was isothermal at 220 °C.

Multi-point calibration curves for TCE, CT, CF, DCM, and CS<sub>2</sub> were established from saturated solutions of each in anaerobic mineral media containing no TCE or formate. A single-point cDCE calibration was also established using a saturated aerobic solution. Single-point VC and ETH calibration curves were performed similarly but with the addition of pure gases of each. Calibration curves yielded gas-phase concentrations for each compound which were then converted to aqueous concentrations and mass per reactor via Henry's Law equilibrium constants<sup>44,136,137</sup>. Experimental data is presented in figures throughout this document in mass per reactor.

#### 5. Data Analysis

As suggested by the schematic in Figure 3, each addition of TCE marks a data point at which CE transformation rates are obtained. Mass data from gas chromatography for TCE, cDCE, VC, and ethene create a CE transformation profile. Two types of transformation rates for TCE, cDCE, and VC were estimated from this mass data. The Multi-Fit Monod model estimates rates based on the Monod equation and incorporation

of competitive inhibition of more chlorinated ethenes on the transformation of less chlorinated ethenes<sup>134,138</sup>. The half-saturation constants ( $K_s$ ) were established for TCE controls based on the most recent kinetic work with these cultures. A property of the microbes, these were held constant for experiments. Observed maximum transformation rates were determined by plotting the sum of each CE's products (mass) versus time. The maximum slope of this plot ( $\mu\text{mol/d}$ ) was then corrected for batch reactor volume (50 mL) to obtain a rate in  $\mu\text{mol/L-d}$ , the same units as the zero order rate from the Multi-Fit Monod model. This process is shown in Appendix 4.

Transformation rates were the primary indicator of microbial performance in the batch reactors under various conditions. Sample standard deviations are reported in tables for all duplicate and triplicate reactors and are shown in figures as error bars. The percent reduction was used to demonstrate the difference in rates obtained in inhibited experimental conditions relative to control conditions. It is reported throughout this document and is calculated as follows:

$$(\text{rate}_{\text{control}} - \text{rate}_{\text{experimental}}) / \text{rate}_{\text{control}} \times 100\%$$

Percent reduction can therefore also be considered the percent inhibition.

Rates that were similar across different experimental conditions were evaluated using the MATLAB® version R2016b function `ttest2`, a command that the program uses to perform a two-sided t-test for equal means without assuming equal variances (also known as a Welch's t-test)<sup>139</sup>. The code for this program reads as follows:

```
[h,p,ci] = ttest2(x,y, 'Vartype', 'unequal')
```

where

“h” returns the number 0 to not reject the null hypothesis and the number 1 to reject the null hypothesis

“p” returns the probability that the result would occur by chance if the null hypothesis is true

“ci” returns the confidence interval for which there is a 95% confidence level that the difference of the population means falls within

“x” and “y” represent arrays containing experimentally obtained rate values for a single chlorinated ethene for duplicate or triplicate reactors

“Vartype” is a parameter label referring to the variance type assumed for the populations

“unequal” specifies that variances for compared populations are not equal

For this project, the p-value is reported and used to support conclusions regarding the similarity of rates from different populations of batch reactors. A population in this case corresponds to an infinite number of possible batch reactors made and tested under the same conditions (e.g. amount of CT or CF added). Each sample size is the number of reactor replicates. The value 0.05 is a common confidence level for the t-test, however adherence to absolute cutoff values is ill-advised. The smaller the p-value, the more likely that the observed difference in populations (e.g. average rates) is statistically significant. A p-value of 0.01 or less is usually considered very convincing evidence for a difference in populations, while the range around 0.05 is suggestive but not absolute<sup>140</sup>. This text will report the p-value and comment on the implications on a case by case basis.

Pseudo-first order transformation rates constants for CT and CF were obtained from a natural log-linear regression of chlorinated mass data with time in Microsoft Excel 2016. The same analysis was used by Vickstrom et al.<sup>26</sup> for similar experiments that used a first-order rate decay model for intermediates and products of multiple CT transformation pathways. Vogel et al.<sup>3</sup> state that “pseudo-first order kinetics are observed in aqueous solutions where water is dominant nucleophile.” This linearization is shown for some experiments in Appendix 1.

## CHAPTER 4 – RESULTS AND DISCUSSION

### 1. Overview

The impact of CT and CF on microbial performance in batch reactors was assessed and compared by the evaluation of chlorinated ethene (CE) transformation rates and hydrogen (H<sub>2</sub>) consumption (sections 2-4). With the discovery that CT had a more severe inhibition or toxicity on the system, experiments attempted to pinpoint the nature of its effect by increasing CT concentration and adjusting the delivery scheme (section 5). CT-exposed reactors were also amended with vitamin B12 to test the potential for B12 to mitigate the toxicity of CT (section 6). Finally, reactors exposed to either CT and products or CF and products were also evaluated for recovery potential after 50 days, which demonstrated that both CT and CF exert irreversible inhibition for the time frame evaluated (section 7).

### 2. Performance of the Evanite Culture with Carbon Tetrachloride Addition

Previous work with the enrichment culture and supernatant harvested from the Evanite (EV-5) chemostat demonstrated that addition of CT to batch reactors undergoing reductive dechlorination of TCE resulted in a significant decrease in transformation rates of each CE compound after 14-day exposures<sup>26</sup>. These results prefaced the current work, and inhibition of CE transformation by CT was evaluated after two different times of exposure. Batch kinetic tests were performed to measure CE rates at these 14-day (Experiment 1) and 2-day (Experiment 2) time exposures to elucidate a time-dependence of CT exposure.

For Experiment 1, triplicate batch reactors were established by sampling cells and supernatant from the EV-5 chemostat. Addition of 2.3-2.4  $\mu$ M CT, 50  $\mu$ M TCE, and 2 mM sodium formate marked the onset of each experiment. CE rates for day 0 were obtained for each triplicate to establish reproducibility of early time behavior with CM exposure. Further addition of 50  $\mu$ M TCE and 2 mM formate on day 14 resulted in a corresponding set of CE rates. CT was only added on day 0. Formate was added as a fermentable source of excess H<sub>2</sub>, as discussed in Methods. Reactors prepared with TCE

and formate additions (no CT) served as non-exposed controls. Comparison of control reactor (no CT) CE rates for day 2 or 14 with experimental reactor (CT present) demonstrated the CM effect at that day, correcting for impacts of endogenous decay and non-continuous feeding that may affect the active dechlorinating populations.

The CT transformation profile for Experiment 1 is shown in Figure 4. CT did not maintain its original concentration in the batch reactors because of its susceptibility to transform in anaerobic reducing environments (see Chapter 2, Section 3ii). CT almost completely transformed within 2 days, corresponding to an average pseudo first-order rate of  $2.33\text{d}^{-1}$  (standard deviation = 0.56, see Appendix 1), where 65% of CT original mass was CF product. The pseudo-first order CT transformation rate (Appendix 1) is approximately double the observed rate of  $1.05\text{d}^{-1}$  reported by Vickstrom et al., and the mass transformed to CF is higher than observed by the same authors<sup>26</sup>. This first transformation step to CF, CS<sub>2</sub>, and other products is primarily abiotic due to the reducing conditions of the media, as established previously<sup>26</sup>. Abiotic transformation of CT to CF was faster than the biotic CF to DCM step.

After an average maximum aqueous CF concentration of  $3.6\ \mu\text{M}$  ( $0.23\ \mu\text{mol}/\text{reactor}$ ) was reached, the CF concentration decreased to  $2.4\ \mu\text{M}$  by day 14, according to an average pseudo first-order rate of 0.0422 (standard deviation = 0.0044). This compares well with  $0.032\text{d}^{-1}$ , the combination of modeled rates for CF transformations to DCM and CO<sub>2</sub> previously reported<sup>26</sup>. DCM slowly built up as CF slowly transformed but does not decrease. This is consistent with previous findings<sup>26</sup> and suggests that DCM-fermenters are either not present or not active at the time of DCM accumulation<sup>141</sup>. The plot stops when reactors were sparged free of volatile compounds at day 49 (see Section 7), by which time 39% of maximum CF mass was transformed to DCM. The 59% loss in mass relative to the original CT mass added is attributed to the formation of CO<sub>2</sub>, as discussed previously for similar experiments showing approximately 67% mass loss<sup>26</sup>.

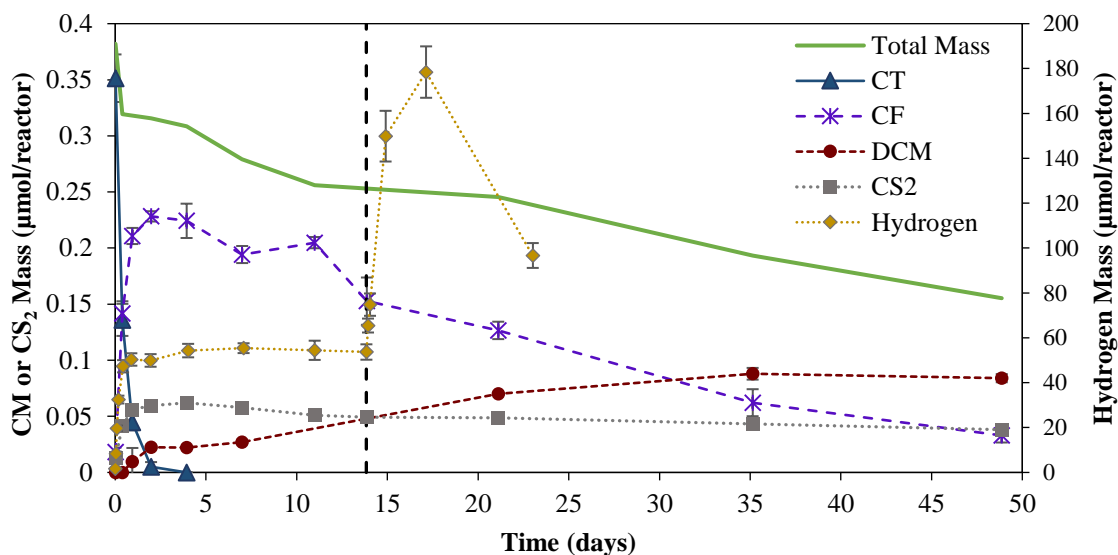


Figure 4. CM transformation profile for Experiment 1 (2.3 $\mu$ M CT addition), including production and consumption of H<sub>2</sub>. Rapid abiotic conversion of CT to CF and CS<sub>2</sub> is followed by slow CF biotransformation. DCM accumulates and is not transformed. The vertical dotted line indicates the day 14 addition of TCE and formate. H<sub>2</sub> produced early maintains a constant level until day 14, when more formate is added. Hydrogen data stops after the second CE transformation is complete. Error bars represent one standard deviation are not shown if smaller than the marker size.

As shown in Figure 4, H<sub>2</sub> levels increased from time zero as formate was fermented, reaching about 47  $\mu$ mol per reactor at 0.4 days. Formate supplies a theoretical 100  $\mu$ mol of H<sub>2</sub> per reactor, but complete TCE dechlorination to ethene in these reactors requires only 12.5  $\mu$ mol. Maximum H<sub>2</sub> did not exceed about 55  $\mu$ mol, indicating the uptake of about 45  $\mu$ mol by various microbial populations. However, the H<sub>2</sub> level did not decrease after 0.4 days. This H<sub>2</sub> levelling was found with this culture in previous work under conditions of similar CT exposure, where it was attributed to the presence of CF<sup>142</sup>. After the second addition of TCE and formate on day 14, H<sub>2</sub> levels increased to exceed 150  $\mu$ mol, the new theoretical total since 50 were left at the second formate addition. In contrast to behavior between days 0 and 14, H<sub>2</sub> decreased to approximately 100  $\mu$ mol by the end of the second TCE addition, which is double the quantity maintained in reactors between day 0 and 14. H<sub>2</sub> data was not collected beyond the time at which CE transformation completed. Implications for microbial inhibition are discussed further in Section 4.

Mass data for CEs and ethene in the same reactors was determined after TCE additions on day 0 and day 14 until TCE was completely transformed to ethene. Figure 5 shows the day 0 transformations of TCE and its intermediates for the control (CT free, Panel A) and CT-exposed (Panel B) reactors, along with the corresponding CT-exposed reactor CM profile for the same time period (Panel C). Note that Panel C has the same data presented in Figure 4, but with a truncated time axis. Typical CE transformation in controls is characterized by rapid TCE and cDCE transformation, which is complete by 0.1 days. At this time, VC reaches maximum mass and then rapidly transforms to ethene, marking complete TCE transformation by 0.3 days. Mass data obtained from CT-exposed reactors (Panel B) compares well with controls except during VC transformation, which takes longer. CT-exposed reactors reach complete TCE transformation between 0.4 and 1 days.

Zero order transformation rates for each chlorinated ethene were obtained through the Multi-Fit Monod model <sup>143</sup>, which predicts masses of transforming CEs and ethene product by microbial reductive dechlorination in batch conditions, according to Monod kinetics with the inclusion of substrate inhibition by more chlorinated ethenes on less chlorinated ethenes <sup>134,143</sup>. The model fit the control data well (Figure 5A), yielding zero order transformation rates for each CE shown in Figure 6. As shown in Figure 5B, this model also fit experimental data for the rapid transformation of TCE and production and transformation of cDCE to VC. Rates for TCE and cDCE were within the range of CT-free controls (Figure 6).

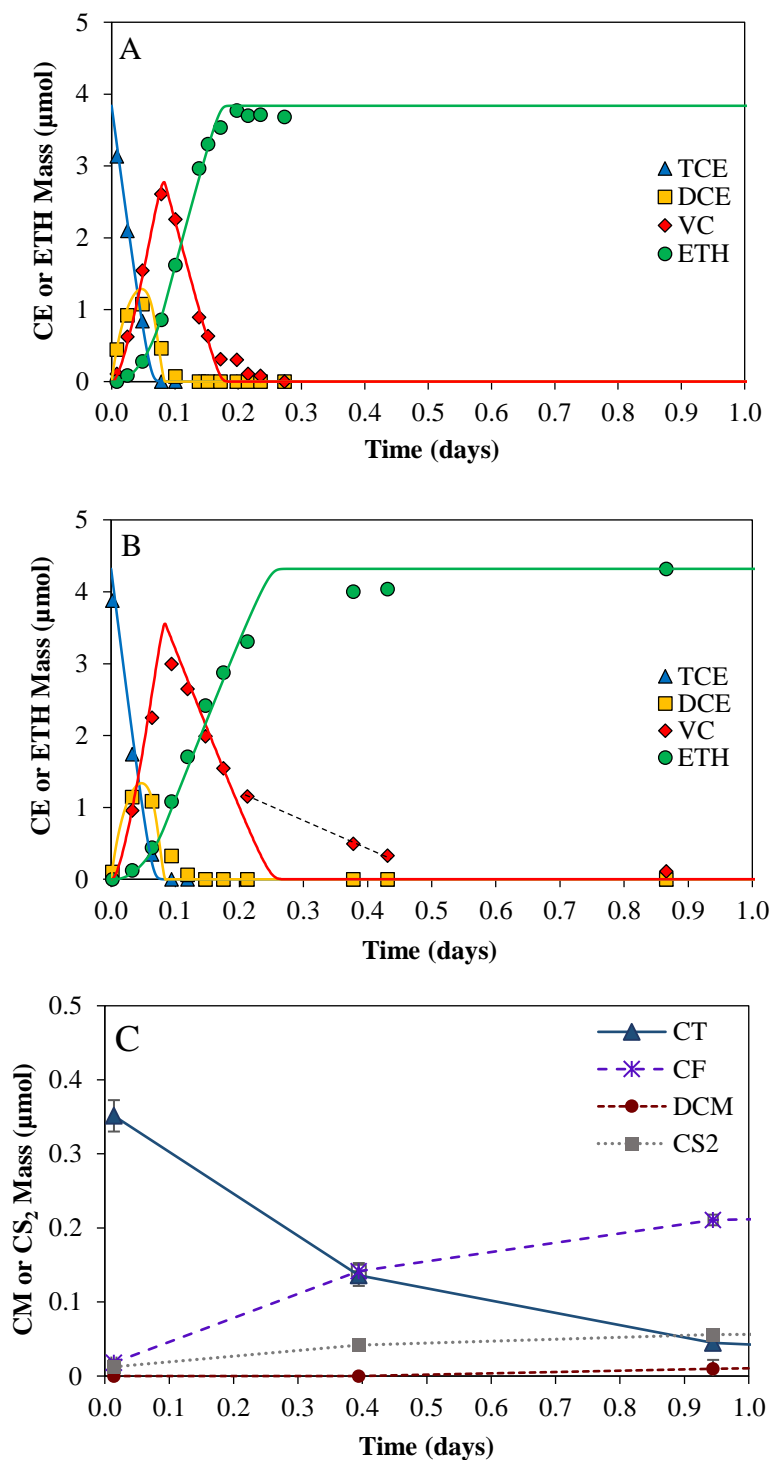


Figure 5. Day 0 CE transformation profile for a representative CT-free control (Panel A) and CT-exposed reactor (Panel B) after a  $2.3\mu\text{M}$  CT addition (Experiment 1). Panel C shows the CT transformation for the same time period, where error bars represent one standard deviation and are not shown if smaller than the marker size. Symbols represent raw data, and continuous lines represent the best fit to the Multi-Fit Monod model in Panels A,B.

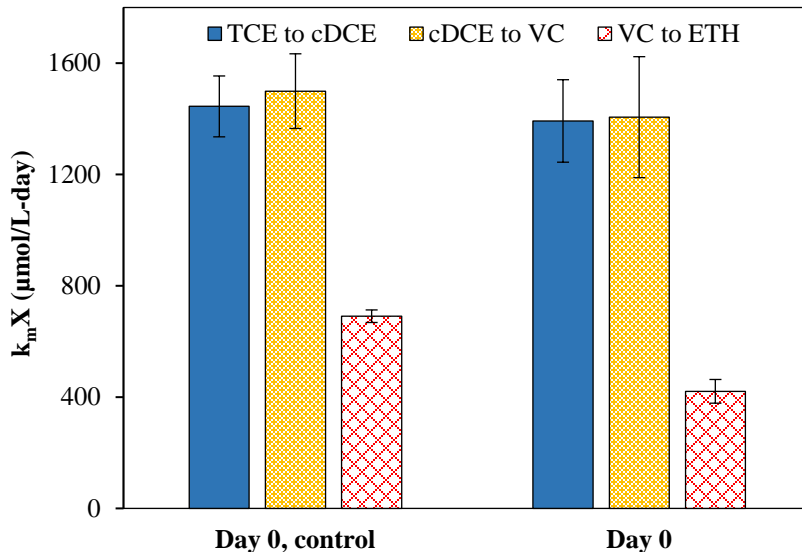


Figure 6. Modeled transformation rates for Day 0 control (CT-free) and CT-exposed (2.3 $\mu$ M CT) reactors of Experiment 1. Error bars represent one sample standard deviation of duplicate (control) or triplicate (CT-exposed) reactors. Differences between TCE and cDCE rates are assumed negligible, whereas the VC experimental rate is 39% reduced compared to the control.

In contrast, the transformation of VC to ethene in CT-exposed reactors has two major differences from controls. First, transformation was slowed, with a 39% decrease in modeled rates relative to controls (Figure 6). A Welch's t-test comparing modeled VC rates from control and CT-exposed reactors yielded a p-value of 0.0028. Such a small p-value indicates that these VC rates are statistically different from each other. Second, although the production and early decrease in VC mass follows the model fit, a discrepancy between data and model begins at approximately 0.2 days (4.8 hr) (Figure 5B). The deviation of the model indicates that the model cannot predict the reduction in the rate for VC under reactor conditions. Both of these findings indicate an effect from the presence of CT and/or its transformation.

The only difference in experimental design between controls and CT-exposed reactors is the addition of CT, thus it is likely that CT and/or its transformation results in a reduced VC transformation rate. Furthermore, because no deviation of the model occurs in CT-free controls, the lack of fit likely results from the presence of CT or CF, which is not incorporated into the model. Considering the model deviates from the data only after

a certain amount of exposure to CT and its transformation, it is likely that CT-related inhibition either A) does not begin until 0.2 days, or B) only affects *vcrA*-containing *D. mccartyi* that perform the VC to ethene transformation step. The model assumes a constant halo-respiring biomass as a function of time.

To describe the rate when the model did not fit the data, an observed zero order rate was calculated for that time interval from the slope of the VC mass data with time, corrected for a batch reactor volume of 50 mL. The region of the plot from which the rate was calculated is shown as a linear dotted line in Figure 5B. While the modeled VC transformation rate is 420.8  $\mu\text{mol/L-d}$ , the observed linear zero order rate between 0.2 and 0.5 days is 79.7  $\mu\text{mol/L-d}$ . This slowing in rate of VC transformation to ethene after 0.2 days was a reproducible phenomenon under day 0 CT transformation conditions, and rates from multiple experiments are included in Table A4.

First order CT transformation rates obtained by log-linear regression (see Appendix 1) predict the mass of CT present in the CT-exposed reactors at the time of model deviation from VC data of 0.221  $\mu\text{mol}$ , or about 63% of the original CT mass (37% has been transformed). This is visually apparent by comparison of Figure 5B and C. Complete TCE transformation to ethene occurred by approximately 0.5 days when approximately 67% of the original CT mass had been transformed. From analysis of day 0 rate data, it is likely that presence of CT, its transformation, and/or its transformation products (e.g., CF) inhibit VC transformation to some extent. Henceforth, inhibition referred to as CT-related will signify that it is likely due to CT itself, CT transformation, CT transformation product, or a combination of one or more of those factors.

On day 14 of Experiment 1, TCE and formate were added to the batch reactors to establish CE rates after long exposure to CT, CF, and their transformation products. By this time, CT had been completely transformed, and CF, DCM, and  $\text{CS}_2$  were present at the aqueous concentrations of 2.4  $\mu\text{M}$ , 0.8  $\mu\text{M}$ , and 0.4  $\mu\text{M}$ , respectively. Figure 7 shows the day 14 transformations of TCE and its intermediates for the CT-free control (Panel A) and CT-exposed (Panel B) reactors for the same time scales. Control reactors achieved complete TCE transformation within 0.3 days, similar to day 0 (see Figure 5A). In

contrast, in CT-exposed reactors, TCE decline takes much longer, and the cDCE and VC mass peaks occur at later times (Figure 7B). The complete transformation to ethene takes until day 22, or 8 days after the day 14 TCE addition (Panel C).

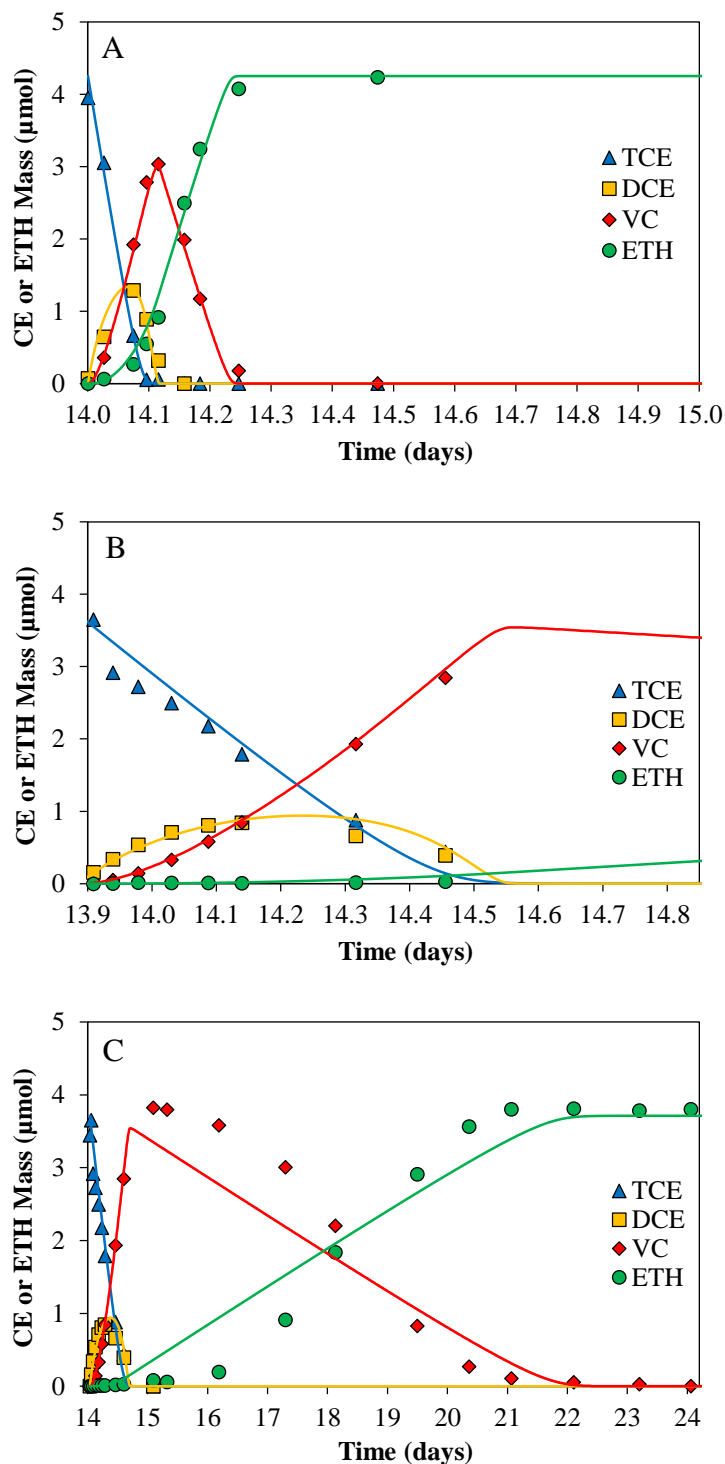


Figure 7. Day 14 CE transformation profile for a representative CT-free control (Panel A) and CT-exposed reactor (Panels B and C) with a  $2.3 \mu\text{M}$  CT addition (Experiment 1). Panel B displays the CE transformation over the same time as the control CE transformation, while Panel C displays data collected over the entire period of transformation in the same reactor. Panel B time axis is offset by about 0.2 days

due to the offset in the initiation of the TCE addition in control and CT-exposed reactors and is not expected to affect results.

After 14 days of exposure to CT and products, TCE transformation to ethene took 8 days instead of 0.5. TCE and cDCE took approximately 0.5 days to be transformed instead of 0.1 days in controls, while VC required a full day to reach maximum concentration. VC reached maximum at 0.1 days during day 0 transformations (Figure 5A and B), thus indicating a decrease in VC transformation rate by a factor of 10. The model simultaneously underestimates VC mass and overestimates ethene buildup from about 14 to 18 days (Figure 7C). From 18 to 21 days, the opposite occurs to a lesser extent. This behavior does not occur in either the control or day 0 CT-exposed reactor profiles. Thus, it is likely that this occurrence is CT-related (itself, its transformation, its products, or a combination).

Figure 8 displays the modeled control and CT-exposed rates for the day 14 CE transformation test. Percent reductions relative to the control for modeled TCE, cDCE, and VC rates were 84, 85, and 98%, respectively. CT-exposed reactors' TCE and cDCE rates decreased by an order of magnitude, consistent with the factor of 10 increase in time to achieve a maximum VC concentration. The control VC rate was 691  $\mu\text{mol/L-d}$ , but CT-exposed reactors only achieved a maximum rate of 10.3  $\mu\text{mol/L-d}$ , a difference of nearly two orders of magnitude.

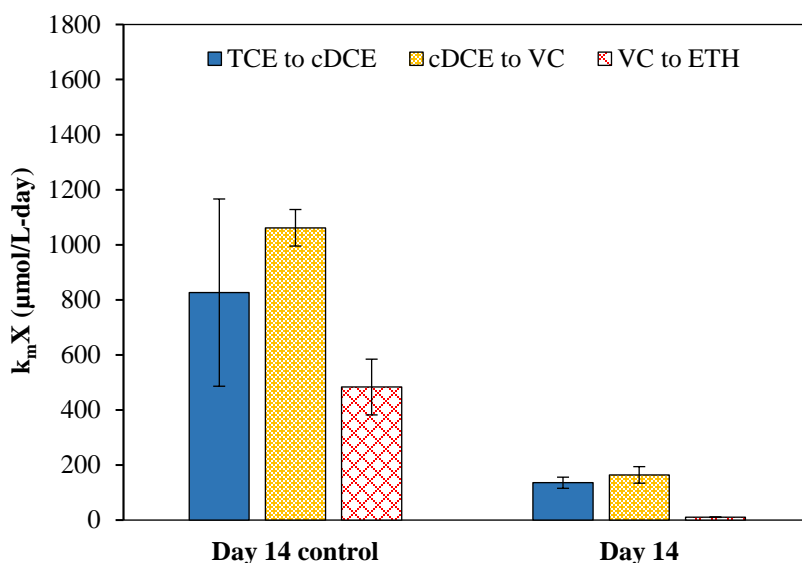


Figure 8. Modeled transformation rates for Day 14 control and CT-exposed reactors of Experiment 1 (2.3μM CT). Error bars represent one standard deviation of duplicate (control) or triplicate (CT-exposed) reactors.

The dramatic decrease in CE rates following CM exposure is consistent with Vickstrom et al.<sup>26</sup>, who recently reported a factor of ten decrease in CE rates under similar CT exposure conditions. They reported a VC transformation rate of approximately 10 μmol/L-d, which compares very well with the 10.3 μmol/L-d reported here. However, they reported TCE and cDCE transformation rates of about 80 and 60 μmol/L-d, respectively, after 14 days of CM exposure. In the present study, these rates were 135 and 164 μmol/L-d, respectively (see Figure 8), which does not signify as significant a decrease. Shifts in the chemostat culture over time could be responsible for the differences in reported rates.

The reduction in transformation rates demonstrates that exposure to CT and/or its transformation products severely impair the ability of OHRB to transform CEs. However, after Experiment 1, the precise source and timing of this inhibition was unknown. Between day 0 and 14, CF and DCM are also present at varying concentrations, and this transient behavior makes clear interpretation difficult. Determination of time-dependence of rate reductions was sought to gain insight regarding the mechanism of inhibition. Experiment 2 was therefore performed to obtain CE rates after a shorter CM exposure.

Elimination of long term exposure to high CF levels would partly remove this as a source of inhibition, potentially allowing an alternate mode of inhibition to be determined. TCE and formate were added on day 0 and day 2, when the maximum CF concentration had been observed. All other design parameters were the same as in Experiment 1. If CE rates from day 2 were similar to day 0, the long term exposure to CF would be indicated as a major factor in inhibition, as was suggested previously<sup>26</sup>. However, if day 2 rates were more comparable to those previously found for day 14, this would indicate primary inhibition at early time of exposure, likely due to CT itself or a non-CF product.

The behavior of chlorinated methane transformation and accumulation in Experiment 2 (Figure 9) was similar to that of Experiment 1. CT was rapidly transformed to CF and CS<sub>2</sub> and was completely transformed in less than 3 days. CF reached a maximum concentration of 3.8 μM at approximately 2 days. A comparison of CM transformation profile characteristics between the two separate experiments is shown in Table 6. Briefly, all points of comparison are similar, indicating reproducibility of experimental procedure as well as batch system behavior (microbial and abiotic factors). Although experiments were monitored across different timespans, similar mass loss occurred in both by the end of monitoring. In Experiments 1 and 2, respectively, 59% and 50% of the CT mass added could not be accounted for, which is slightly less than the 67% shown previously for similar experiments<sup>26</sup>. Similar initial CT concentrations were transformed within 3 days for each experiment, with first order CT transformation rates of -2.13 and -2.38 d<sup>-1</sup>. Mass of CT transformed to CF and rates of subsequent CF transformation compare well between the experiments, although as discussed above for Experiment 1, CF builds up to greater concentrations in the present study than was observed by Vickstrom et al.<sup>26</sup>.

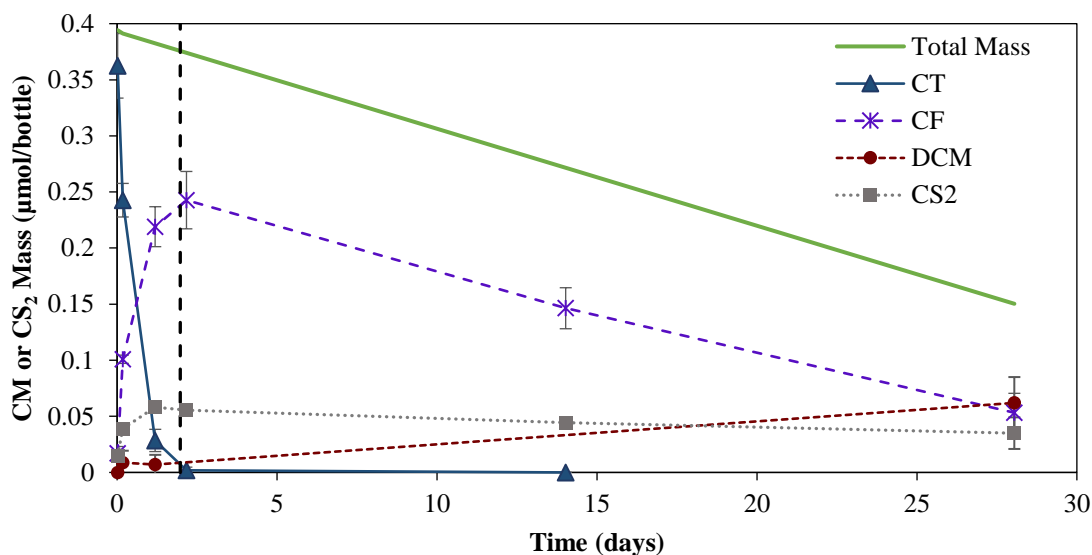


Figure 9. CM transformation profile for Experiment 2 (2.4 $\mu$ M CT addition). Rapid abiotic conversion of CT to CF and CS<sub>2</sub> is followed by slow CF biotransformation. DCM accumulates and is not transformed. The vertical dotted line indicates the day 2 addition of TCE and formate. Error bars represent one standard deviation are not shown if smaller than the marker size.

Table 6. Points of Comparison for Chlorinated Methane Transformation Profiles of Experiments 1 and 2.

Experiment	1	2
Timespan of data collection	49 days	28 days
Total mass loss over timespan	59%	50%
Initial aqueous CT concentration	2.3 $\mu$ M	2.4 $\mu$ M
Time to CT disappearance	about 2 days	< 3 days
1st order CT transformation rate (d <sup>-1</sup> )	-2.13	-2.38
Maximum CF mass (concentration)	0.23 $\mu$ mol (3.6 $\mu$ M)	0.24 $\mu$ mol (3.8 $\mu$ M)
CT mass transformed to CF	65%	67%
CT mass transformed (%) at the time the mass deviated from the model	0.22 $\mu$ mol/37%	0.24 $\mu$ mol/33%
1st order CF transformation rate (d <sup>-1</sup> )	-0.044	-0.059
CF mass transformed to DCM	0.39 $\mu$ mol	0.26 $\mu$ mol

Figure 10 presents the day 0 CE transformation profile for the CT-exposed reactors. TCE disappeared by 0.1 days, and cDCE followed shortly thereafter. The Multi-Fit Monod model, depicted in the figure by continuous lines, predicts both compounds accurately. VC mass peaks at approximately 0.1 days, and it is accurately predicted by the model until approximately 0.2 days, at which time its rate of transformation slows.

The observed rate between 0.2 and 0.5 days is approximately  $62.6 \mu\text{mol/L-d}$ . This behavior is identical to that seen in Experiment 1 for VC (see Figure 7 Panel B), and is likely CT-related. Modeled rates for the compounds are within  $\pm 7\%$  of the day 0 rates obtained in Experiment 1 and are shown in Table A4. Day 0 controls (CT-free) were not conducted for this experiment. Those from Experiment 1 one week prior were used for comparison with experimental CT exposures (See Figure 7A). This activity is consistent with the profile seen one week earlier in Experiment 1 (Figure 7B).

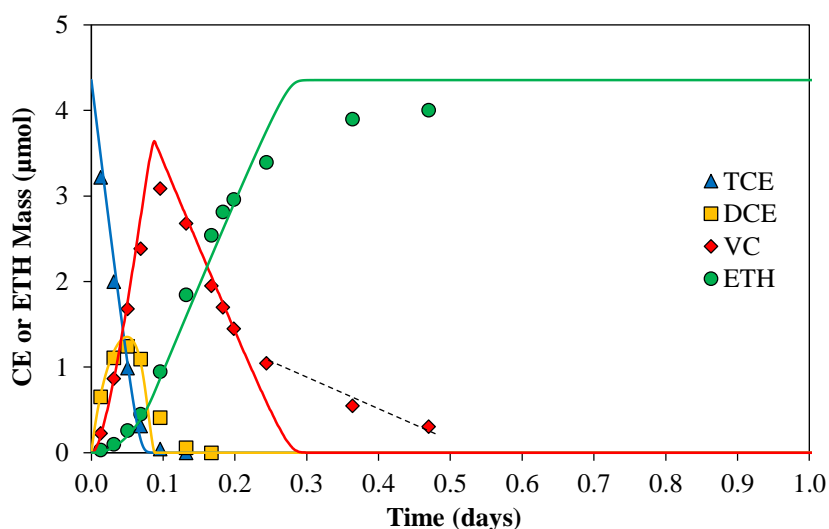


Figure 10. Day 0 CE Transformation Profile for a representative CT-exposed reactor after  $2.4 \mu\text{M}$  CT addition (Experiment 2). The dotted line represents the region for which an observed linear rate was obtained for VC transformation.

Experiment 2 differs from Experiment 1 in that the second addition of TCE and formate occurred at day 2 instead of day 14. By this time, CT had largely disappeared, as shown in Figure 9 at the dotted vertical line. CF had reached its maximum mass detected of  $0.24 \mu\text{mol}$ , or aqueous concentration of  $3.8 \mu\text{M}$ .

A CT-free control for day 2 was used from an experiment conducted one month later, which is recognized to bring some uncertainty to the results. However, this reactor's performance on day 0 compared well with the previous controls. TCE and VC rates were within 5% of each other, while the cDCE rate was 18% higher in the control used here. This reflects a consistent behavior in CE transformation rates for cultures sampled from

the chemostat over a period of 1.5 months. CE transformation profile for the day 2 control (CT-free) is shown in Figure 11A and is nearly identical to the day 0 control from Experiment 1, with a good model fit for all 4 compounds.

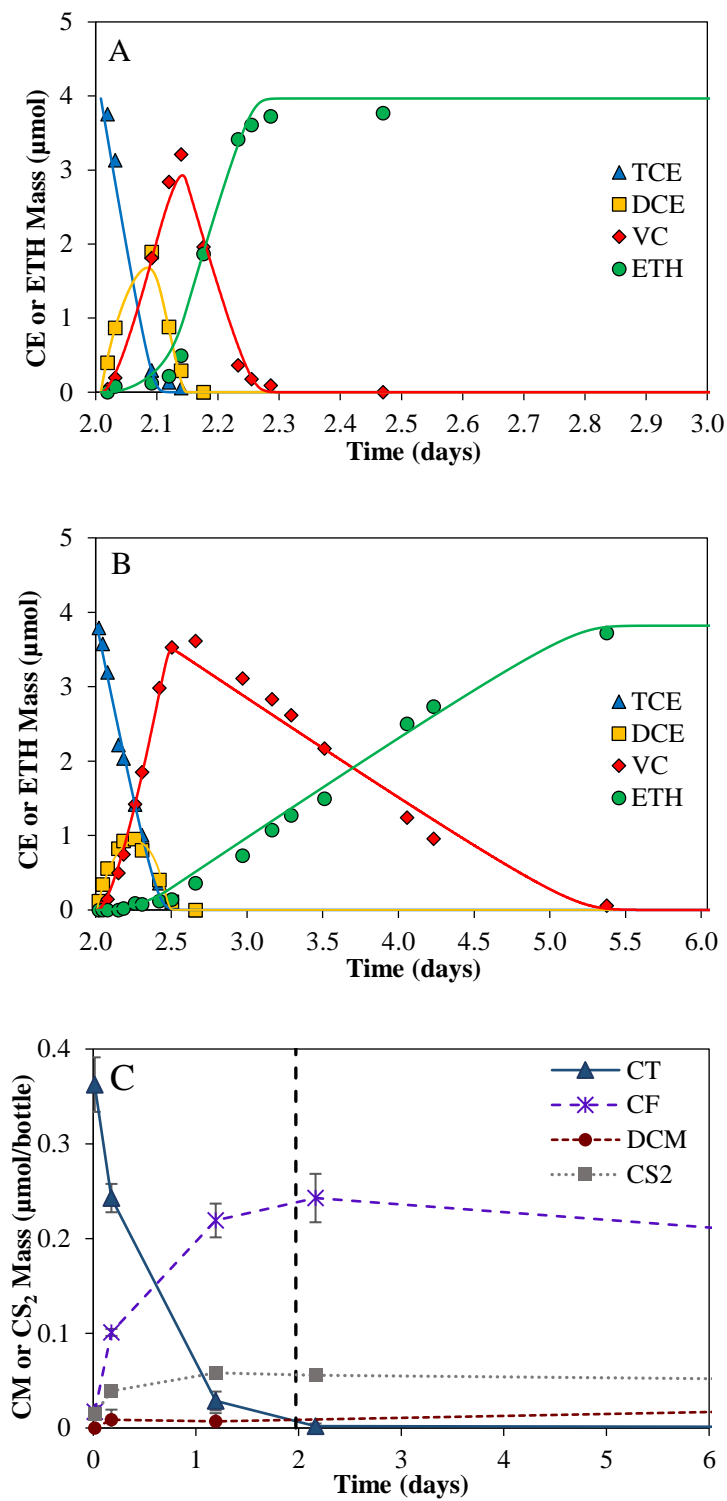


Figure 11. Day 2 CE transformation for a representative CT-free control (Panel A) and CT-exposed reactor (Panel B) with a 2.4 μM CT addition (Experiment 2). Panel C shows the CM transformation CT-exposed reactors for a truncated time period, where error bars represent one standard deviation and are not shown if smaller than the marker size.

As shown in Figure 11B, CE transformation in CT-exposed reactors were inhibited compared to the control, taking more than 3 days to completely transform TCE to ethene. After the second TCE addition, TCE and cDCE were not completely transformed until 0.5 days. This was about 5 times longer than the control but the same as after 14 days, indicating a similar reduction in transformation rates. The model fits the data for all 4 compounds for the entire duration of the test, indicating that the inhibition causing rates to decrease is proportional and constant for the duration of the experiment. Figure 12 displays the day 2 control and CT-exposed modeled CE rates. Relative to the control, CT-exposed reactors' rates decreased by 80, 67, and 96%, respectively for TCE, cDCE, and VC. These rate reductions are similar to those seen for day 14, suggesting that inhibition exerted by CT or its transformation is exerted primarily at early time of exposure.

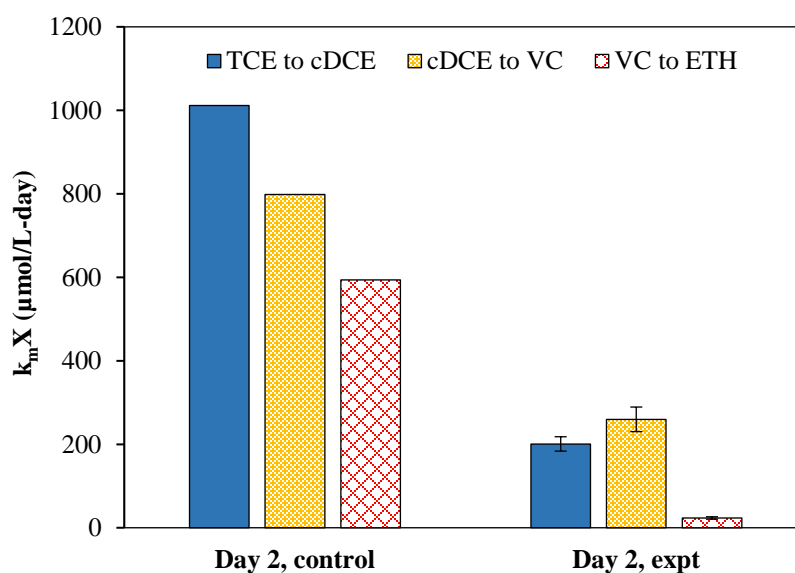


Figure 12. Modeled transformation rates for Day 2 control and CT-exposed reactors after addition of 2.4  $\mu\text{M}$  CT (Experiment 2). Error bars represent one standard deviation of triplicate (CT-exposed) reactors. “Expt” = CT-exposed. The control is a single replicate, so no error bars apply. Relative to the control, CT-exposed rates for TCE, cDCE, and VC are 80, 67, and 96% reduced, respectively.

The model fits the day 2 transformation data well over the entire time interval (Figure 11B), unlike the fit for the day 0 transformation test, where the model deviated from VC data. The observed zero order VC rate for transformation between 3.5 and 4.5

days is  $20.3 \mu\text{mol/L-d}$ , approximately equal to the modeled rate fit for the entire experiment duration ( $23.48 \mu\text{mol/L-d}$ ). Thus, it is proposed that inhibition of CE rates started after 0.2 days of CT exposure, when the VC data deviated from the model. Unlike rates obtained on day 0, on day 2 there appears to be a constant, proportional inhibition of all 3 CE transformations, which corresponds to complete transformation of CT and maximum concentration of CF. It is thus possible that the transformation of CT is responsible for the inhibition of OHRB dechlorination of CEs. CF may also inhibit CE transformation to some extent, as it reaches its maximum concentration on day 2.

The time interval between TCE additions was decreased to 1 day for triplicate reactors in Experiment 3, to which  $2.9 \mu\text{M}$  CT was initially added. This was the shortest exposure time tested for the batch experiments. On days 0 and 1, TCE and formate were added for transformation rate analysis. CT was not monitored beyond the initial time point, and  $\text{H}_2$  was not monitored. A control was not run for day 1, but rates were assumed to fall within other control day 0 and day 2 rates reported above.

Because CT was not monitored during the 24 hours before the day 1 addition of TCE, it is not possible to know how much it had transformed by this time. Based on data collected in Experiments 1 and 2, however, it is likely that transformation was underway but not complete. Using the first order transformation equation determined for Experiment 1 (Appendix 1), it is likely that the original CT mass of  $0.442 \mu\text{mol/reactor}$  ( $2.9 \mu\text{M}$ ) had been transformed to 9% of original mass by the time of the day 1 TCE addition. CF concentration at this time was not measured.

CE transformation after 1 day is shown below in Figure 13 for a representative reactor. Note that the model fits data points for all 4 compounds relatively well, and complete TCE transformation occurs at about 4 days. Rates with standard deviations are listed in Table A4. When compared to day 2 controls, day 1 CT-exposure rates represent reductions of 76, 62, and 95% for TCE, cDCE, and VC, respectively. This is consistent with very early time inhibition and toxicity of CE transformation by OHRB in batch systems as was indicated in Experiment 2, and resulting rates are within the range of those obtained during day 2 transformations.

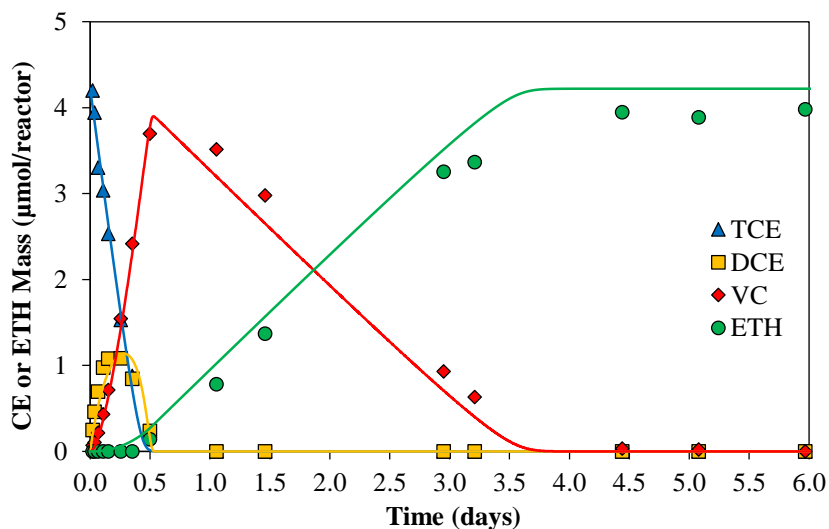


Figure 13. Day 1 CE transformation profile for a representative CT-exposed reactor after 2.9  $\mu\text{M}$  CT addition (Experiment 3).

Specifically, the modeled transformation rates for each compound on day 1 were 246, 301, 30.2  $\mu\text{mol/L-d}$  for TCE, cDCE, and VC, respectively. In comparison, day 2 rates were 201, 260, and 23.5  $\mu\text{mol/L-d}$ . Day 0 rates were 1390, 1410, and 421, with an observed rate of 76.5  $\mu\text{mol/L-d}$  for VC between 0.2 and 0.5 days (Table A4). This demonstrates a greater similarity in CT-related inhibition after days 1 and 2 of exposure than day 0, consistent with an early time decrease in the VC rate.

It is interesting to note that OHR apparently occurred in reactors in which  $\text{H}_2$  levels were constant at 50  $\mu\text{mol}$ . Because  $\text{H}_2$  is required for each step of OHR, this cannot be possible. Rather, it is likely that the  $\text{H}_2$  measurements were not sensitive enough to distinguish the relatively small change in  $\text{H}_2$  during the VC to ethene transformation. It is also possible that CT or CF slowed the rate of formate fermentation so that rates of production and consumption of  $\text{H}_2$  are equal and opposite, maintaining the  $\text{H}_2$  plateau observed. Furthermore, the decreased CE transformation rates are not attributed to low  $\text{H}_2$  supply because  $\text{H}_2$  was always in excess of a previously reported  $K_s$  value for *D. mccartyi* strain VS (7 nM, aqueous) <sup>144</sup>.

Figure 14 presents the modeled transformation rates for each exposure time in control (Panel A) and CT-exposed (Panel B) conditions. This comparison accentuates the relative impact of each exposure time on CE rates and highlights the importance of the first day of exposure. The results indicate most of the inhibition in rate and/or toxicity has occurred within 1 day. The day 1 rates and those showing VC slowing within the first day of exposure indicate an earlier time of inhibition in the rates.

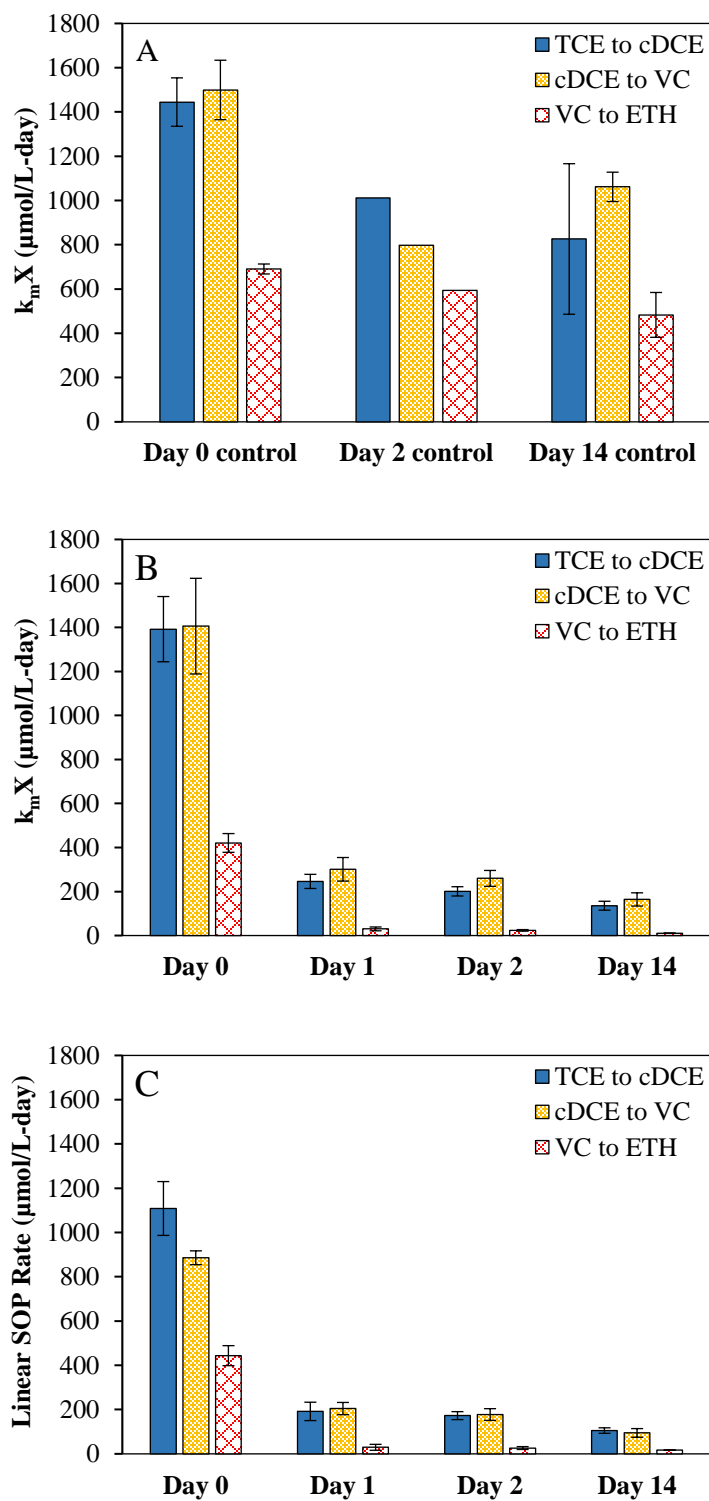


Figure 14. Zero order transformation rates determined by the Multi-Fit Monod model (Panels A and B) and SOP linearization (Panel C) for Experiments 1-3. Panel A displays CT-free control rates, while Panels B and C display CT-exposed reactor rates. Error bars represent one sample standard deviation.

In addition to the Multi-Fit Monod model, observed rates were obtained to compare the trend in rate reduction between methods of analysis. Observed maximum rates for each CE were determined by plotting the sum of each CE's products (mass) versus time. The maximum slope of this plot was normalized to batch reactor volume to yield a rate in  $\mu\text{mol/L-d}$  for comparison with modeled rates with the same units, henceforth referred to as the sum of products (SOP) linear rate. A schematic for this process is shown in Appendix 4. Maximum observed rates are shown in Figure 14C and demonstrate a similar trend in rate behavior with exposure time as modeled rates. Rates are presented in Table 7 and Appendix 3. Linear SOP rates for TCE and cDCE are lower than modeled rates in general because the model incorporates substrate inhibition of more chlorinated ethenes on the transformation of less chlorinated ethenes. Thus, the use of the Multi-Fit Monod model to evaluate CE rate reductions under CT addition is justified for the present work, despite discrepancies between the model and experimental data discussed earlier.

Table 7. Modeled and Linear SOP Transformation Rates<sup>a</sup> ( $\mu\text{mol/L-d}$ ) for various exposure times following addition of 2.3-2.9  $\mu\text{M}$  CT.

	2.3-2.9 $\mu\text{M}$ CT Exposure			
	Day 0 <sup>b</sup>	Day 1 <sup>c</sup>	Day 2 <sup>d</sup>	Day 14 <sup>b</sup>
	<b>Modeled Control Transformation Rates</b>			
TCE	1445 $\pm$ 109	N/A	1012	826.3 $\pm$ 340
DCE	1500 $\pm$ 134		798.1	1062 $\pm$ 66.3
VC	690.7 $\pm$ 22.6		593.7	483.3 $\pm$ 101
	<b>Modeled CT-Exposed Reactor Transformation Rates</b>			
TCE	1392 $\pm$ 148	246.0 $\pm$ 32.1	200.8 $\pm$ 21.1	135.6 $\pm$ 20.3
DCE	1406 $\pm$ 217	301.0 $\pm$ 53.5	259.7 $\pm$ 36.1	164.1 $\pm$ 30.0
VC	420.8 $\pm$ 42.6	30.24 $\pm$ 8.66	23.48 $\pm$ 3.51	10.3 $\pm$ 0.46
	<b>Linear SOP Rate</b>			
TCE	1109 $\pm$ 122	191.8 $\pm$ 41.5	172.6 $\pm$ 18	105.3 $\pm$ 12.4
DCE	885.9 $\pm$ 31.2	204.6 $\pm$ 27.7	177.7 $\pm$ 26.5	94.54 $\pm$ 19.6
VC	443.6 $\pm$ 45.3	29.52 $\pm$ 13.7	26.28 $\pm$ 6.40	16.58 $\pm$ 0.43

<sup>a</sup>  $\pm$  indicates one sample standard deviation from replicate mean.

<sup>b</sup>Data from Experiment 1.

<sup>c</sup>Data from Experiment 3.

<sup>d</sup>Data from Experiment 2.

A notable consideration of the Multi-Fit Monod model is that the equations that compose the model only contain one variable for active dechlorinating microbial biomass

<sup>143</sup>. This is represented by  $X$ , where  $X$  is the entire community of CE-dechlorinating OHRB composed of multiple populations that specialize in different steps of TCE transformation by the reductive dechlorination pathway. Because active biomass is not measured in the batch reactors for each time point,  $X$  is incorporated into the transformation rates solved by the model and reported here. Without the ability to distinguish between *tcra* and *vcrA*-containing populations, for example, it is not possible to know how CM inhibitors affect the active biomass specifically. Rather, the inhibition can only be inferred from the combined term  $k_m X$ , where  $X$  represents active biomass and  $k_m$  is the maximum substrate utilization rate.

The percent reduction in transformation rates demonstrate that CT-related inhibition of CE transformation by OHRB occurs during the time period of CT transformation. Reactors in which CT has been completely transformed and CF has reached maximum concentration at 2 days result in a very similar inhibition of CE transformation as those tested at 14 days, suggesting that the major inhibition event occurs at early time. Since CF was formed, it might be hypothesized that it is the primary inhibitor, which would agree well with findings in the literature <sup>17,123</sup>. However, since CT has also been reported to have toxic or inhibitory effects <sup>16</sup>, it is likely that this compound, its transformation, or its transformation intermediates also influences the reduction of CE rates. Also, while there is no report of confirmed measurement of the trichloromethyl radical in OHRB systems, this species as well as dichlorocarbene are possible intermediates formed in this scenario with uncertain impacts on OHRB functions<sup>9</sup>.

Other researchers have distinguished between presence of a given compound or its transformation products as the actual inhibitor. Weathers and Parkin <sup>111</sup> concluded that CF transformation products caused toxicity in methanogenic cultures, while Yang and Speece <sup>119</sup> reported that CF itself was responsible for a similar inhibition of methane production. However, no information in the literature is available regarding the inhibitory effect of CT compared to its non-CF transformation products in any microbial system, and the relative proportion of CT and CF impacts are thus far unknown for the present study. To investigate these knowledge gaps, experiments were performed with direct

addition of CF at the experiment start, thereby eliminating the inhibitory or toxic impacts of CT or other non-CF products such as the trichloromethyl radical formation. Isolation of the CT transformation process thus allowed for the comparison between CE transformation and H<sub>2</sub> consumption in systems with and without CT.

### 3. Performance of the Evanite Culture with Chloroform Addition

Kinetic transformation tests with addition of TCE and CF were performed using similar procedures as the CT exposure tests previously described. In Section 2, long and short term exposure to CMs after CT addition indicated that the CF formed from CT may not be primarily responsible for the reductions in CE rates. To assess this further, 14-day (Experiment 4) and 2-day (Experiment 5) tests were performed with the same design as in Section 2 except that an aqueous concentration of 5.8-6  $\mu\text{mol/L}$  CF (about 0.4  $\mu\text{mol/reactor}$ ) was substituted for CT at time zero. This quantity was approximately double the maximum concentration measured in Experiments 1 and 2. If previous CM-related inhibition was due to presence of CF, then doubling the exposure concentration and adding it directly at time zero should result in similar or even more pronounced CE rate reductions, especially during day 0 when CF concentration is the highest. Control reactors (CF-free) from Experiment 1 were used for rate data comparison.

H<sub>2</sub>, CF, and CF transformation products (DCM) in triplicate reactors were monitored for 49 days in Experiment 4 as shown in Figure 15. CS<sub>2</sub> was not formed because it is a transformation product of CT. CF was transformed with a first order rate of 0.0639 d<sup>-1</sup> (standard deviation = 0.0018) (Appendix 1). The CF concentration decreased to 3.5  $\mu\text{M}$  by day 2 (40% transformation) and 2.15  $\mu\text{M}$  by day 14 (63% transformation). Overall, CF converted approximately 40% to DCM, which was not further degraded, consistent with earlier results. By day 49, 56% of original CF added had been lost (compared to 59% in Experiment 1), and this was again attributed to formation of CO<sub>2</sub>. A comparison of first order rate coefficients calculated for CF transformation in CT-exposed (0.0422 d<sup>-1</sup>, Table 6) and CF exposed (0.0639 d<sup>-1</sup>) reactors

indicate the CF transformation is faster in CF exposed reactors ( $p = 0.005$ , Welch's t-test).

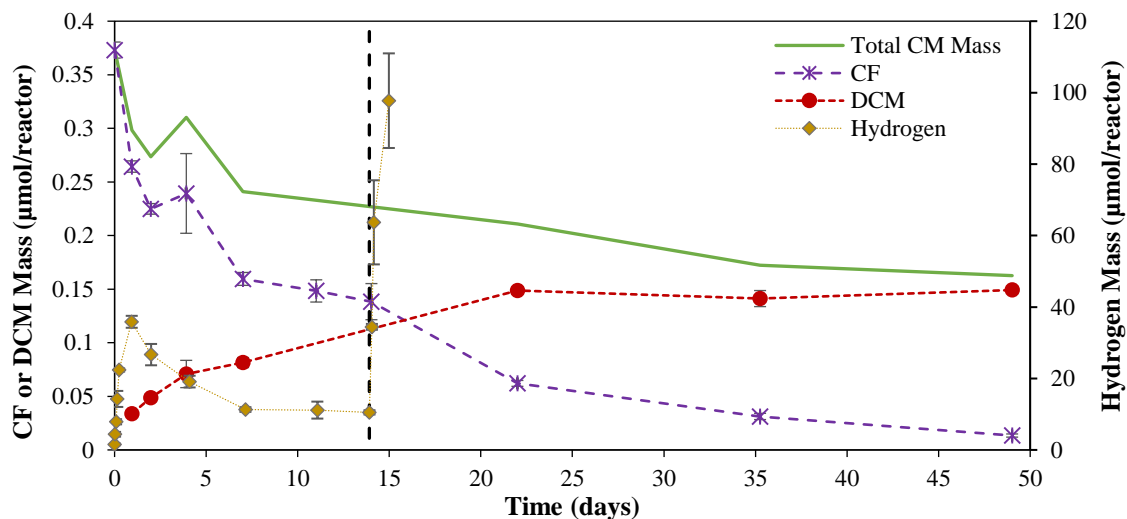


Figure 15. CF transformation profile for Experiment 4 ( $5.8 \mu\text{M}$  CF addition), including production and consumption of  $\text{H}_2$  until completion of the second CE transformation on day 14. DCM accumulates and does not transform for the experiment duration.  $\text{H}_2$  reaches a maximum mass at 0.9 days and is consumed until day 7. The vertical dotted line indicates the day 14 addition of TCE and formate. Error bars represent one standard deviation are not shown if smaller than the marker size.

$\text{H}_2$  plotted in Figure 15 applies to Experiment 4 reactors to which TCE and formate were added on day 0 and day 14, indicated by the dotted line. The  $\text{H}_2$  mass peaked at  $36 \mu\text{mol}$ , or 36% of the theoretical amount produced by  $2\text{mM}$  formate, and was consumed to  $10 \mu\text{mol}$   $\text{H}_2$  by day 7, where it remained until the second TCE/formate addition. Previous work had indicated that CF concentration above  $0.8 \mu\text{M}$  inhibits  $\text{H}_2$  consumption in this culture when  $2.1 \mu\text{M}$  CF is added at time zero<sup>142</sup>. However,  $\text{H}_2$  consumption began after about 1 day in the present study (Figure 15), corresponding to a CF level below about  $0.25 \mu\text{mol/reactor}$  ( $4 \mu\text{M}$ ). It is possible that this difference is due to the addition of TCE in the present study, which stimulated OHRB to consume  $\text{H}_2$  in addition to homoacetogens in the culture. Implications for microbial inhibition are discussed further in Section 4.

The transformation of all CEs slowed with time of CF exposure. Figure 16 shows the horizontal elongation of transformation data for each compound from top (day 0) to bottom (day 14) for similar time scales of 1 day. The spread in the peaks of cDCE and

VC data are particularly noticeable with increasing CF exposure time. Maximum VC mass is achieved at later time intervals from top to bottom of the figure, and TCE reaches undetectable levels at increasing time after each addition.

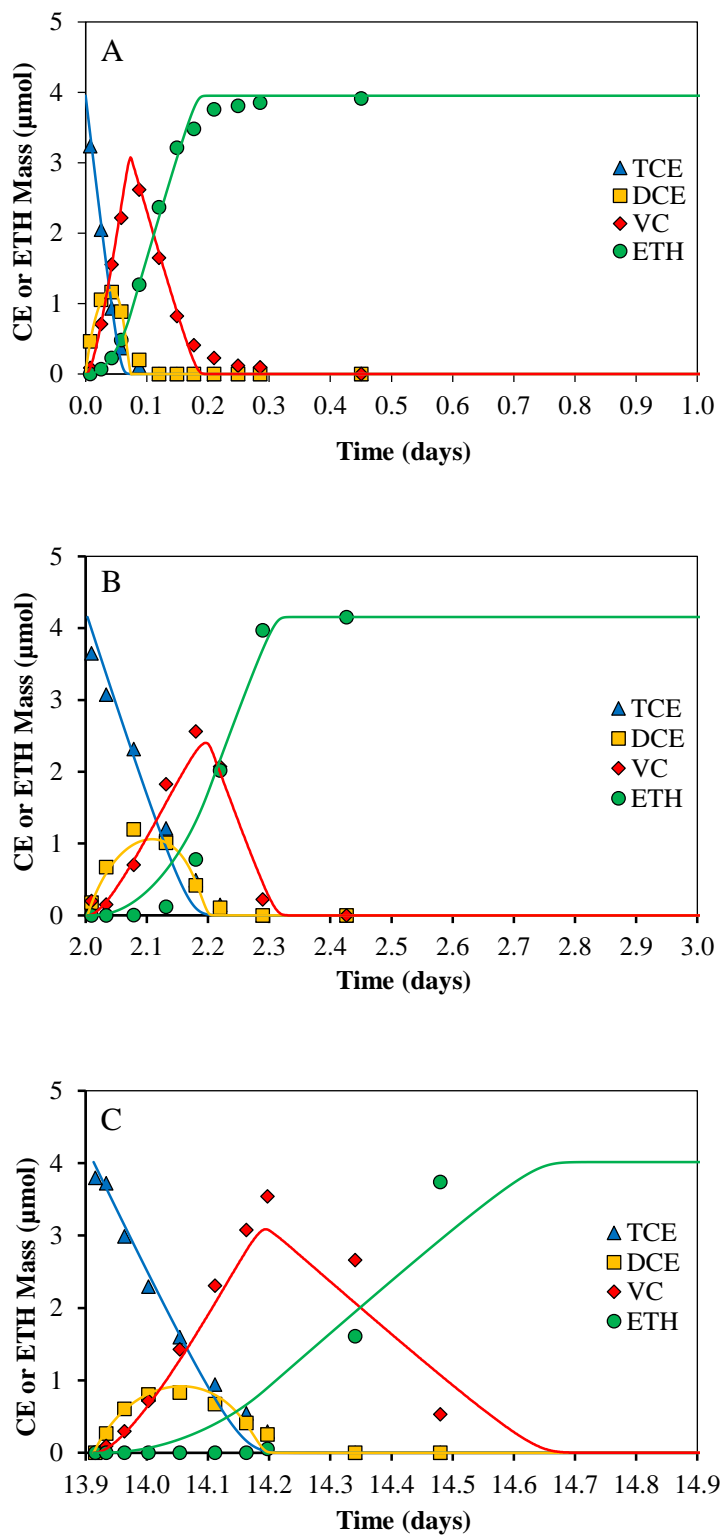


Figure 16. Representative CE Transformation profiles for Experiments 4 and 5 with CF exposed on day 0 (Panel A), day 2 (Panel B), and day 14 (Panel C), with 1-day time scales beginning at TCE addition.

On day 0, CF-exposed reactors performed like CF-free controls, with the disappearance of TCE and cDCE occurring at approximately 0.1 days along observation of maximum VC mass. As shown in Figure 16A, the Multi-Fit Monod model predicts the data accurately, and the transformation of TCE to ethene is complete by 0.3 days. Day 2 behavior is similar, however, the time of TCE and cDCE disappearance and VC maximum shifts to 0.2 days following TCE addition, shown in Figure 16B. Although the time to reach 50% ethene is about 0.1 days in day 0 and 0.25 days on day 2, time to 100% ethene in both scenarios is approximately 0.3 days. The model fits to experimental observations well with the exception of ethene production, which is predicted to occur more quickly than observed at early time. Finally, the transformation profile for day 14 TCE addition is shown in Figure 16C. TCE and cDCE disappear in 0.3 days accompanied by the maximum VC mass, and complete transformation to ethene is delayed compared to days 0 and 2. The model deviates from VC and ethene data more dramatically here than for day 2, as discussed further below.

Modeled estimated rates for each exposure time are compared in Figure 17B to control rates from Section 3 (Panel A). On day 0, the average control and CT-exposed VC rates are within 3% of each other, while the TCE and cDCE rate is slightly higher than the control. This is attributed to day-to-day microbial variability since controls and experiments were not sampled on the same day. On day 2, CE transformation rates for TCE, cDCE, and VC were only 50, 19, and 23% reduced from day 2 controls. By day 14, they were 57, 53, and 73% reduced from controls. As for CT-exposure experiments (Figure 14), linear SOP rates for Experiments 4 and 5 displayed in Figure 17C demonstrate a similar trend in rate reduction as modeled rates. Therefore, the use of the model to compare rate inhibition is appropriate. Corresponding modeled and SOP linear rates for each stage in control and CF-exposed reactors are also included in Table 8 and Table A5.

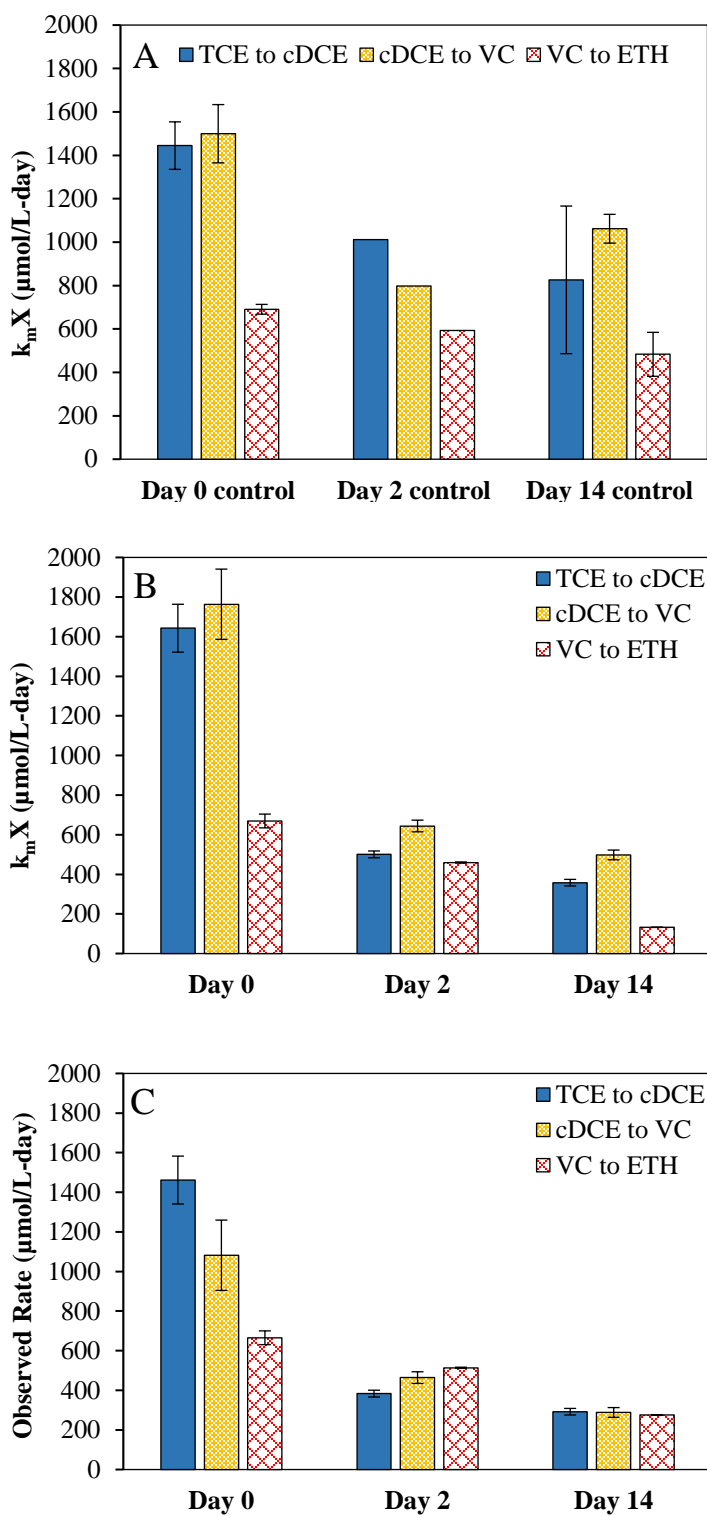


Figure 17. Zero order transformation rates determined by the Multi-Fit Monod model (Panels A,B) and SOP linearization (Panel C) for Experiments 4 and 5. Panel A displays CT-free controls, while Panels B and C display CF-exposed reactor rates. Error bars represent one standard deviation and are small enough to not be visible for some sets.

Table 8. Modeled and Linear SOP Transformation Rates<sup>a</sup> ( $\mu\text{mol/L-d}$ ) for various exposure times following addition of 5.8-6  $\mu\text{M}$  CF.

	5.8-6 $\mu\text{M}$ CF Exposure		
	Day 0 <sup>b</sup>	Day 2 <sup>c</sup>	Day 14 <sup>b</sup>
	Modeled Control Transformation Rates		
TCE	1445 $\pm$ 109	1012	826.3 $\pm$ 340
DCE	1500 $\pm$ 134	798.1	1062 $\pm$ 66.3
VC	690.7 $\pm$ 22.6	593.7	483.3 $\pm$ 101
	Modeled C- Exposed Reactor Transformation Rates		
TCE	1643 $\pm$ 102	500.6 $\pm$ 67.3	357.9 $\pm$ 6.37
DCE	1764 $\pm$ 99.5	644.0 $\pm$ 61.5	497.9 $\pm$ 14.0
VC	669.2 $\pm$ 66.1	459.7 $\pm$ 93.9	132.2 $\pm$ 28.8
	Linear SOP Rate		
TCE	1462 $\pm$ 127	383.4 $\pm$ 31.5	292.1 $\pm$ 24.5
DCE	1082 $\pm$ 125	464.1 $\pm$ 65.9	288.4 $\pm$ 12.7
VC	665.4 $\pm$ 55.8	513.7 $\pm$ 69.6	274.8 $\pm$ 32.1

<sup>a</sup>  $\pm$  indicates one sample standard deviation from the mean

<sup>b</sup>Data from Experiment 4

<sup>c</sup>Date from Experiment 5

The model deviates from the production of ethene during day 2 transformation (Figure 16B), and this becomes more apparent after the day 14 TCE addition (Figure 16C). This finding is consistent with the discrepancy seen in Section 2 during day 14 transformation (Figure 7C), but its cause is unclear. Since day 14 controls are well-predicted by the model (Figure 16A), it is unlikely that factors such as endogenous decay influence the model deviation. Since the model discrepancy for VC transformation and ethene production occurs in both CT-exposed and CT exposed reactors, it may be related to the presence of CF at different concentrations.

Specifically, in Experiment 1 (2.3  $\mu\text{M}$  CT addition), CF rose to a maximum of 3.55  $\mu\text{M}$  by day 2, after which it transformed. The day 2 CE mass data was fit well by the model (Figure 11), but by day 14, the model did not accurately predict VC and ethene for the first 5 days (Figure 7C). In comparison, in Experiment 4 (5.8  $\mu\text{M}$  CF addition), CF concentration began at 5.8  $\mu\text{M}$  and had decreased to 3.5  $\mu\text{M}$  by day 2, at which time model deviation at early time is evident for ethene data (Figure 16B). For the day 14 transformation, ethene buildup is overpredicted from the start and the profile after the time of VC maximum looks similar to the day 14 for CT exposure on a shorter time scale. That the model deviation occurs at short time in CF exposed reactors, but not at short time in CT-exposed reactors, is consistent with differences in CF concentrations present.

Direct addition of CF to OHRB-containing reactors did not yield the same CE transformation inhibition as did CT exposure. As shown in Table 8, modeled day 2 rates were still greater than half of the day 2 control rates. TCE transformation was the most decreased by day 2, relative to control rates. By day 14, rates from CF exposed reactors had fallen to approximately half of the value in day 14 controls. Thus, CF exerted some inhibition on CE transformation. The following discussion will compare it more extensively with CT.

#### 4. Comparison of Evanite Performance in Reactors Exposed to CT or CF

While CE rates decreased with time under exposures to both inhibitors, microbial cultures behaved very differently in reactors amended with CT and only CF, even though CF was present in both scenarios. Long exposure time to CT, its transformation, and its transformation products resulted in more significant CE transformation rate decreases than did exposure to CF and its transformation. Additionally, H<sub>2</sub> production and consumption patterns differed from control reactors under either amendment. CT-exposed reactors displayed a greater inhibition of H<sub>2</sub> consumption than did CF exposed reactors. These differences are described in more detail below.

Direct CF addition resulted in higher CE rates than CT exposure for all three exposure times evaluated. Figure 18 illustrates this with modeled zero-order transformation rates for each CE, inhibitor, and time of exposure. Table 9 provides corresponding average rate values and the percent reduction relative to controls, or percent of inhibition. During day 0, CE rates with CF addition are equivalent to controls, with negative or small percent reductions in rate. However, in CT-exposed reactors, the VC rate decreased on day 0, indicated by the 39% reduction from control shown in Table 9. After 2 days of exposure to CT and its transformation rates for TCE, cDCE and VC were reduced from the control by 80, 67, and 96%, respectively, indicating significant inhibition. CF reactor percent reductions were not nearly as large in comparison (Table 9). For example, the day 2 VC rate under CF exposure is 459.7  $\mu\text{mol/L-d}$ , reduced by 23% from the control. This rate is 20 times larger than the CT exposure (23.48  $\mu\text{mol/L-d}$ ).

d), which was 96% reduced from the control. This difference strongly indicates that the early time inhibition of CE transformation in CT-exposed reactors is not due to the presence of CF, but rather CT itself, its transformation, or some other unidentified product.

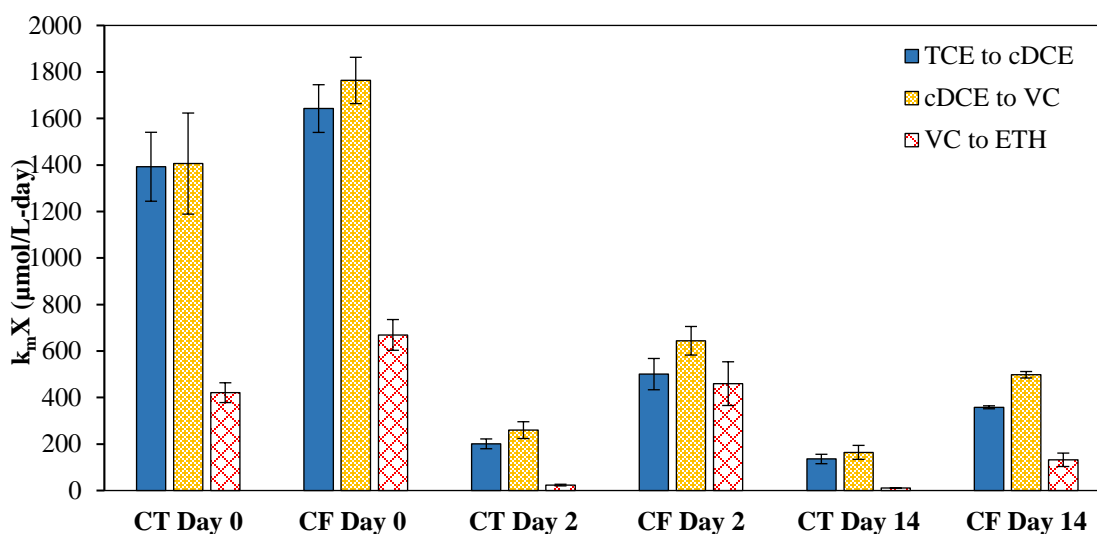


Figure 18. A side-by-side comparison of modeled CE transformation rates for each exposure time under CT and CF additions. Error bars represent one standard deviation of triplicate batch reactors.

Table 9. A Comparison of CE Transformation Rates for Evanite cultures with CT and CF Exposures

Inhibitor, to	Day of Exposure	Modeled Transformation Rate, μmol/L-d			% Reduction from Control		
		TCE	cDCE	VC	TCE	cDCE	VC
3 μM CT	0	1390 ± 148	1410 ± 217	421 ± 42.6	4%	6%	39%
	2	201 ± 21.1	260 ± 36.1	23.5 ± 3.51	80%	67%	96%
	14	136 ± 20.3	164. ± 30.0	10.3 ± 0.46	84%	85%	98%
5.8 μM CF	0	1640 ± 102	1760 ± 99.5	669 ± 66.1	-14%	-18%	3%
	2	501 ± 67.3	644 ± 61.5	460 ± 93.9	51%	19%	23%
	14	358 ± 6.37	498 ± 14.0	132 ± 28.8	57%	53%	73%

However, by day 14, CF-exposed rates indicated 57, 53, and 73% inhibition of TCE, cDCE, and VC rates, respectively, illustrating the significant inhibition exerted by CF exposure over the long term that was not evident at early time. For example, the VC rate decrease from 460 to 132 μmol/L-d from day 2 to 14 in CF-exposed reactors, which represented a major contribution to the 73% reduction from control shown in Table 9.

This suggests that a significant proportion of the inhibition observed in CT-exposed reactors may be due to the presence of CF over the long term. However, complicating factors make it difficult to tease apart the proportional contributions of CT and CF in reactors where they are both present. In the present study, CF concentrations differed. Addition of CT resulted in a maximum aqueous concentration of about 3  $\mu\text{M}$  CF, whereas CF-exposure experiments began with the addition of 5.8  $\mu\text{M}$  CF.

One might hypothesize that the contribution of CF to the inhibition observed in CT-exposed reactors is the fraction of CF inhibition divided by total inhibition observed. For example, day 14 CF inhibition may constitute 57/84 of the total inhibition observed. These values are percent reductions taken from Table 9 for day 14. However, that analysis assumes that the CE transformation rates decrease linearly with time of exposure to both CT and CF. If instead inhibition affected rates according to a first order relationship, the same relationship would not hold for all times of exposure.

Direct inhibition by either CT or CF did not appear to cause a linear reduction in CE rates with time (Figure 18). Early times of exposure yielded dramatically decreased rates, especially in the case of CT addition. A kinetic model describing disinfection in engineered systems was used in an attempt to evaluate toxicity for the present system according to a first order relationship. The Chick-Watson model predicts a disinfectant's ability to reduce the concentration of viable microorganisms, which follows a logarithmic decrease with time<sup>145</sup>. For the present study, a comparison was made to the simplest version of this model, shown below.

$$\ln \frac{X(t)}{X(0)} = -k[D]^n t^{145}$$

X(t) = number or concentration of viable organisms at time t

X(0) = number or concentration of viable organisms at time 0

k = pseudo-first-order reaction rate constant with respect to D

D = disinfectant concentration

n = order of reaction with respect to disinfectant

t = time

Viable organisms were not quantified for the present study. However, CE transformation rates serve as a proxy for OHRB health because some of the microbial populations, *D. mccartyi* included, depend upon the anaerobic dechlorination pathway for cell growth and metabolism. Thus, the CE transformation rates at each time of exposure were used to approximate the  $X(t)$  of the Chick-Watson expression. The disinfectant of the Chick-Watson expression was either inhibitor of the present study, CT and CF. The order of reaction,  $n$ , was assumed to be 1.

To approximate this relationship for the present data, rate values from Table 9 and Experiment 3 (day 1 CT exposure) for each CE were transformed by calculating the natural log and plotted against time of exposure for both inhibitors (CT and CF). The resulting curves were evaluated for a linear fit, which would indicate that inhibition by the corresponding CM could be described by the Chick-Watson expression. In CT-exposed reactors, the day 0 VC transformation rate observed after model deviation was considered here as a separate time of exposure. Thus, CT-exposed reactor plots including data from Experiments 1 and 2 have four time points for TCE and cDCE transformation rates (0, 1, 2, and 14 days) and five time points for VC (0, 0.2, 1, 2, 14). Experiments 4 and 5 supplied original CF inhibition data. However, also included for this analysis are rates obtained from a separate experiment in which 5 TCE/formate additions were made to the same triplicate reactors spanning days 0 to 33. Bar graphs containing original rates for this experiment can be found in Appendix 5.

The attempted Chick-Watson analysis for CT-exposed reactors is shown below in Figure 19. The linear fit was poor for TCE, cDCE, and VC rates. This is because the early time decrease in rates are too large compared to those at later time. This is consistent with CT-related inhibition or toxicity occurs at early time, and thereafter rates decrease more slowly. Figure 20 shows the Chick-Watson analysis for CF-exposure rates obtained from Experiments 4 and 5 (Panel A) and an additional CF-exposure experiment in which CE rates were evaluated on days 0, 3, 6, 15, and 33 (Panel B). The fit is also poor for all rates except for the VC rate in the CF-exposed reactors of Experiments 4 and

5 (Panel A). This suggests that CF inhibition of VC-respiring OHRB populations occurs according to Chick-Watson kinetics, however it was not reproducible in the data shown in Panel B. Slopes of rate changes with time of exposure are not comparable between the tests. However, the transformed rate data from both CF-exposure tests illustrate an early CF inhibition on CE transformation, similar to what is observed in CT-exposed reactors (Figure 19).

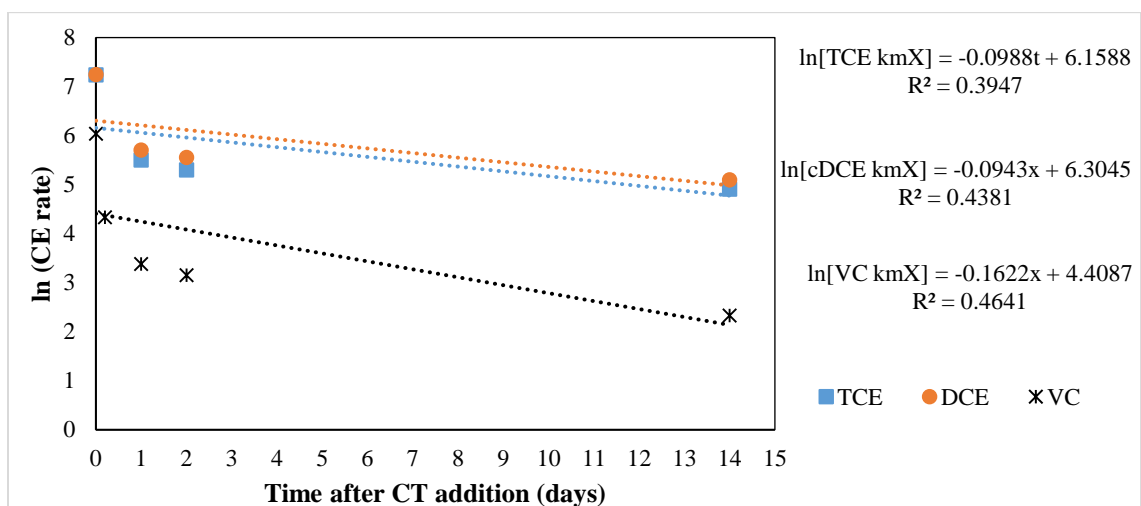


Figure 19. CT exposure log transformed average CE rates from Experiments 1 and 2.

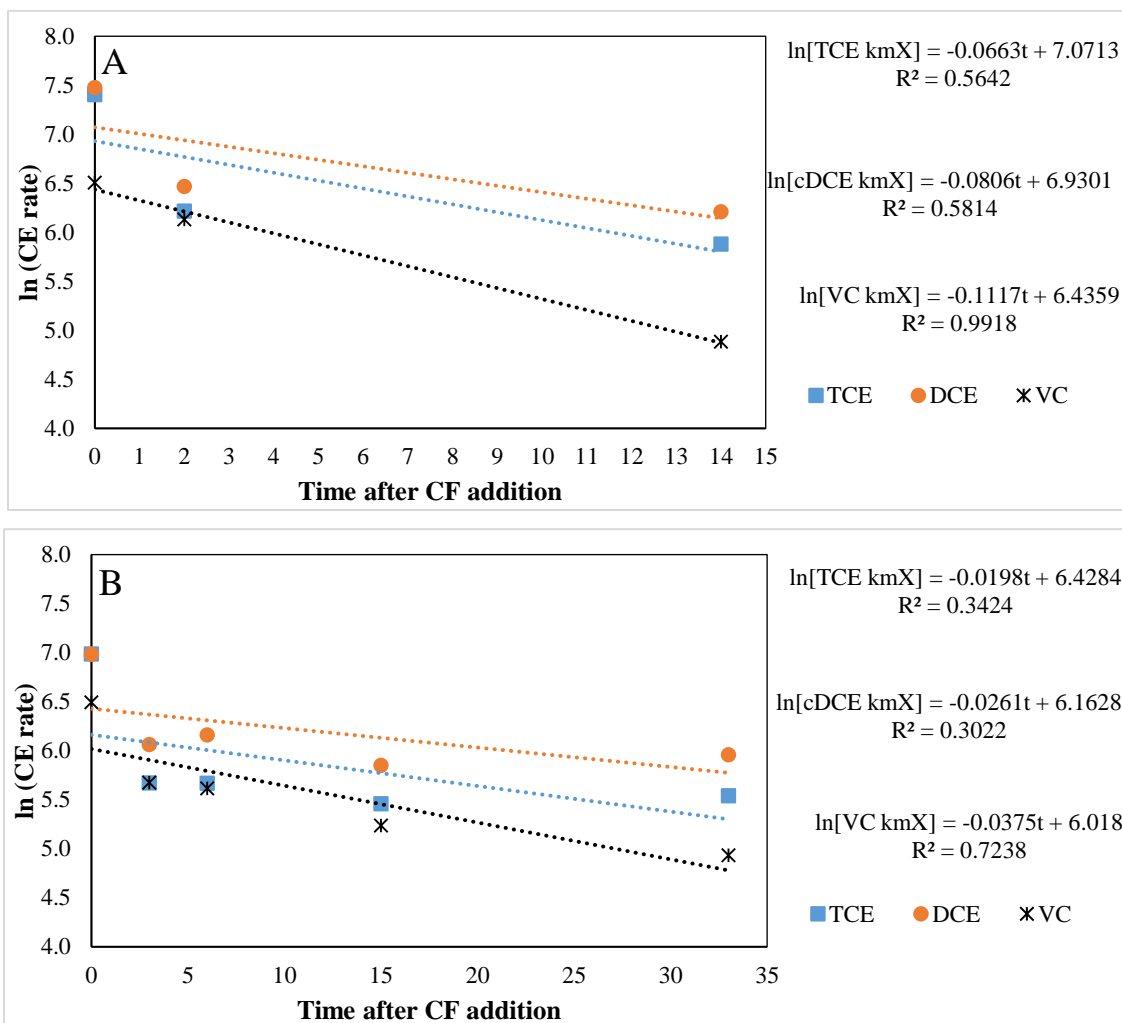


Figure 20. Natural log transformation of CE rates with exposure time to CF. Panel A contains 3 time points from Experiments 4 and 5. Panel B is from a single separate experiment with 5 time points. All points were transformed from an average rate.

In addition to slowing CE transformation rates, CT and CF have an effect on H<sub>2</sub> consumption by the microbial cultures. Previously described H<sub>2</sub> production and consumption data for CT-exposed reactors (2.3 μM, Figure 4) and CF exposed reactors (5.8 μM, Figure 15) is compiled below in Figure 21 with a typical control reactor profile.

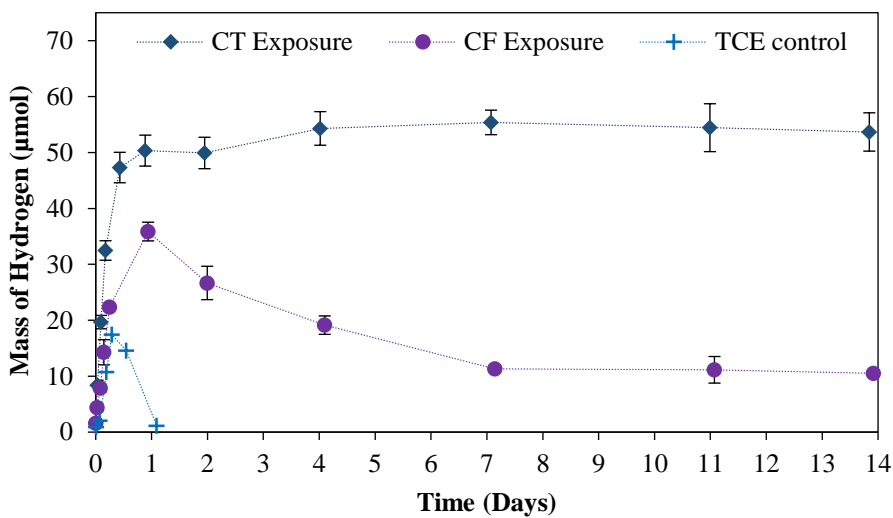


Figure 21. H<sub>2</sub> production and subsequent consumption in reactors exposed to CT addition, CF addition, or TCE only. Control reactors consume H<sub>2</sub> rapidly within 1 day. CM exposure results in a higher maximum concentration and a longer consumption time. CT reactors completely plateau. Error bars represent one standard deviation for triplicate reactors and are not shown if smaller than marker size.

Following a formate injection, H<sub>2</sub> levels quickly rose in all the reactors. The theoretical H<sub>2</sub> mass supplied (100 µmol) was never reached, indicating simultaneous production and consumption. Control reactors performing uninhibited reductive dehalogenation of TCE, cDCE, and VC quickly consumed H<sub>2</sub> within 1 day after reaching a relatively low maximum concentration at about 0.3 days. Transformation of 50 µM TCE for each addition only requires 12.5 µmol of H<sub>2</sub>, this leaves an excess of 87.5 µmol. Because CE transformation is complete by about 0.5 days, the rapid decline in H<sub>2</sub> mass after 0.5 days can be attributed to consumption by other microbes, such as homoacetogens or *Geobacter* strains, which have been reported in the Evanite enrichment culture<sup>73,104</sup>.

CT and CF-exposed reactors reached a higher maximum H<sub>2</sub> mass and experienced a levelling of H<sub>2</sub> at detectable levels. Figure 21 displays maximum masses of approximately 35 and 50 µmoles per reactor for CF and CT-exposed reactors, respectively. A lag time in consumption could cause these greater maximum masses, likely due to some type of inhibition exerted by CMs. In CT-exposed reactors, H<sub>2</sub> levels stayed stationary at approximately 50 µmol, even after the complete transformation of

TCE to ethene. This suggests a nonspecific, community-wide inhibition effect of the CMs on H<sub>2</sub> consumption by the culture and could be partially responsible for the slowing of CE rates in the presence of CT. However, since the consumption of H<sub>2</sub> does not rapidly decline, CT likely affects other microbial populations.

In CF direction addition reactors, H<sub>2</sub> levels decrease after the maximum to 11 μmoles per reactor by day 7 with no further decrease. Because CE transformation in CF exposed reactors did not experience a reduction in rates, it is likely that OHRB had little trouble with H<sub>2</sub> consumption. Therefore, the slower uptake seen in the profile may be attributed to a CF effect on non-OHRB populations. This could have longer-term implications for OHRB indirectly if they rely on cross-feeding with these apparently compromised non-OHRB populations, but the inhibition is not as dramatic as what is seen in CT reactors.

Since *D. mccartyi* relies on other microbial populations for nutrients and cofactors like H<sub>2</sub> and cyanocobalamin, it is prudent to understand the effect that CT or CF may have on these populations. H<sub>2</sub> consumption is thus a loose proxy for the overall health of the microbial culture. After complete TCE transformation in CT-exposed reactors, 50 μmol of 87.5 μmol available to other processes remained. Inhibition of homoacetogens in the culture could potentially be evaluated with acetate measurements throughout the experiment, however, high background levels of acetate in the supernatant did not permit any acetate product to be assessed.

Previous work with this culture indicated that aqueous CF concentrations above 0.4 μM result in an inhibition of H<sub>2</sub> consumption<sup>142</sup>. However, in the present study, H<sub>2</sub> consumption occurs at concentrations of 4 μM CF or below in CF-exposed experiments but levels at 50 μmol in CT-exposed reactors with similar CF concentrations. Thus, there is evident CT-related inhibition of H<sub>2</sub> consumption, even after CT transformation is complete. Adamson and Parkin<sup>16</sup> reported a similar inhibition of H<sub>2</sub> consumption by a reductively-dehalogenating, methanogenic culture in the presence of CT. However, they found H<sub>2</sub> consumption to resume following CT disappearance, unlike the present study.

Experiments conducted with CT and CF added separately to cultures performing reductive dechlorination of TCE revealed major differences in the impacts that each CM has upon these batch systems. At concentrations tested, CT displayed a greater inhibition of CE transformation and H<sub>2</sub> consumption than CF alone, where the largest magnitude of impact was measured after very brief exposure to CT and its transformation. CF addition yielded some reductions in CE rate and H<sub>2</sub> consumption, however these effects were produced more gradually and never mirrored CT effects for the time durations tested. Inhibition of CE transformation and H<sub>2</sub> consumption persists after CT transformation is complete, and the majority of the rate reduction occurs at early time. Thus, the results indicate that the transformation of CT, and not its presence alone, is responsible for the reduction in CE transformation rates and that the CT-related inhibition can be more accurately described as toxicity. Additional experiments were designed to further evaluate these impacts on the OHRB and community.

##### **5. Probing the Mechanism of Carbon Tetrachloride Inhibition**

Presence of CT and its transformation clearly altered the microbial ability to transform CEs, but its mechanism of toxicity is unclear. To further probe the unique impact that CT exerts on the EV5 culture, additional tests were performed and are discussed in this section. If CT itself exerts toxicity upon microbes transforming CE and using H<sub>2</sub>, inhibition of CE rates should display a dependence on CT concentration, which can be evaluated by increasing concentration of CT in similar batch tests to those discussed above. In addition, non-CF CT transformation products such as the trichloromethyl radical could be responsible for the inhibition, in which case a CE rate dependence on CT concentration may not be evident. Experiments with a high initial CT concentration were performed, and results were compared to prior experiments at lower concentration to examine a CT concentration-dependent inhibition. In addition, a multiple delivery strategy was used for CT addition to evaluate inhibition due to CT mass transformed.

*i. High level CT (HiCT) tests*

To evaluate the potential for CT concentration-dependent inhibition of CE transformation, Experiment 6 was performed with 7.2  $\mu\text{M}$  CT, 3 times the original (Experiment 1) concentration of 2.3  $\mu\text{M}$ . CE rates under each concentration for day 0 and day 14 transformations were compared.

A CM transformation profile accompanied by  $\text{H}_2$  formation and consumption profile is shown in Figure 22. As expected, CT was transformed rapidly in batch reactors, with an average pseudo-first order rate constant of  $1.11 \text{ d}^{-1}$  (standard deviation: 0.127). This rate was about half the rate of that observed in Experiment 1, however, the CT is still mostly transformed by day 2. CF gradually built up to a maximum mass of 0.28  $\mu\text{mol}$  (3.8  $\mu\text{M}$ ), similar to the maximum achieved in Experiment 1 (0.23  $\mu\text{mol}$ ). Unlike earlier experiments, this CF maximum occurred after 5 days and only accounted for 25% of the original CT mass. However, it is possible data between days 2 and 5 is inaccurate, which would be consistent with the total mass at 2-5 days dipping below the total mass recorded on day 6. Thus, it is difficult to confidently report either the time of CF maximum or the actual maximum mass achieved. Notably, CF concentration between day 5 and day 14 was not seen to decrease, unlike in low level CT experiments.

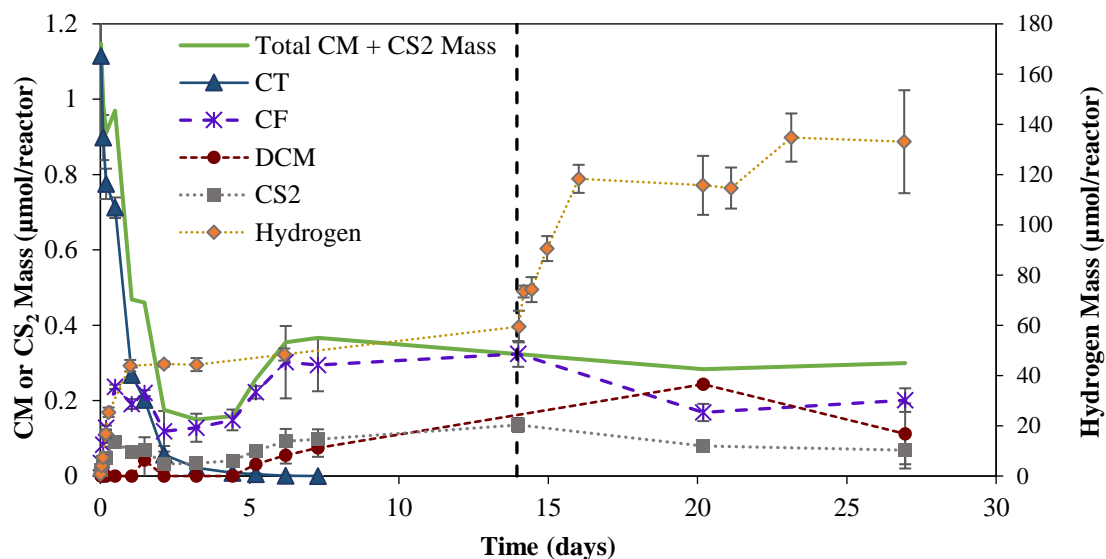


Figure 22. CM transformation profile for Experiment 6 with production and consumption of H<sub>2</sub>. Rapid abiotic conversion of CT to CF and CS<sub>2</sub> is followed by slow CF biotransformation and DCM accumulation. CF does not significantly decrease during the experiment time frame. The vertical dotted line indicates the day 14 addition of TCE and formate. H<sub>2</sub> produced early maintains a constant level until day 14, when more formate is added. Error bars represent one standard deviation are not shown if smaller than the marker size.

The H<sub>2</sub> profile in HiCT reactors is also similar to low level CT experiments. H<sub>2</sub> mass plateaus between 40 and 50 μmol/reactor by 1 day. Thus, only 50 μmol is consumed by microbial populations between day 0 and 14. TCE control reactors experience complete H<sub>2</sub> consumption within about 1 day. A more pronounced increase in H<sub>2</sub> occurs after the day 14 TCE/formate addition. H<sub>2</sub> increases to an average of 133 μmol by day 27, which indicates that of the 200 μmol of H<sub>2</sub> supplied to batch reactors from both formate additions, only 34% is ultimately used. In comparison, Experiment 1 H<sub>2</sub> levels dropped to 100 μmol before day 25, indicating that 50% of the 200 μmol supplied in both additions was consumed.

Day 0 CE mass data for HiCT reactors in Experiment 6 is shown in Figure 23 for the CT-free control (Panel A) and CT-exposed (Panel B) reactors. Panel C displays the same data as presented in Figure 22, truncated to 1 day. The trend from left to right in the top panels of the figure demonstrates that high levels of CT shift of the VC transformation curve, with increasing time to reach the maximum mass compared to the control profile, which resembles those previously discussed.

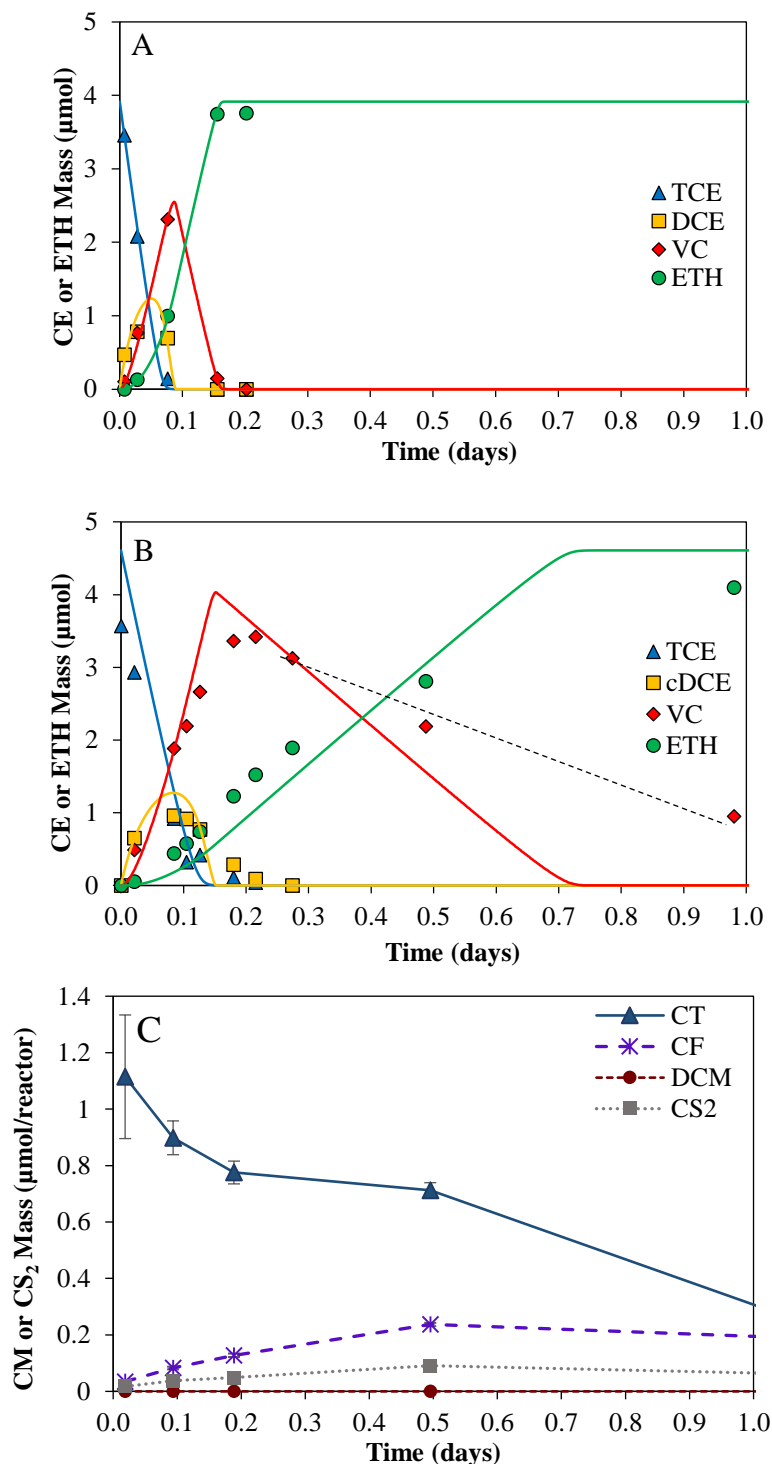


Figure 23. Day 0 CE transformation profile for a representative CT-free control (Panel A) and CT-exposed reactor (Panel B) after a 7.2  $\mu\text{M}$  CT addition (HiCT, Experiment 6). Panel C shows the CT transformation for the same time period, where error bars represent one standard deviation and are not shown if smaller than the marker size. Symbols represent raw data, and continuous lines represent the best fit to the Multi-Fit Monod model in Panels A,B.

As shown in Figure 23 Panel B, complete TCE transformation to ethene took more than 1 day in HiCT reactors. TCE and cDCE disappeared and VC peaked at 0.2 days, twice the time required in controls. The Multi-Fit Monod model poorly predicts data beyond 0.1 days, after which it underpredicts ethene and overpredicts VC until somewhere around 0.4 days. Shortly after the VC mass peak, the model deviates from data, and the slope of the raw data gives the impression that VC transformation is slower in HiCT reactors. However, the average observed VC rate between 0.3 and 1 day (shown by the dotted line in Panel B) is 50  $\mu\text{mol/L-d}$ , which is similar to low CT concentration experiments (Figure 5B). The reason for this discrepancy is likely related to slower transformations of TCE and cDCE, precursors to VC, due to the HiCT exposure. Thus, greater concentrations of CT resulted in a slowing of CE transformation on day 0 that was apparent in the earlier transformation steps of TCE and cDCE.

Modeled rates are shown in Figure 24. CE transformation is slower in HiCT reactors than in low level reactors. HiCT rates as a percentage of low CT exposure rates were 59, 65, and 41% for TCE, cDCE, and VC, respectively. Welch's t-tests (p-values in Table 10) confirmed that differences in TCE and VC rates were statistically significant, however, the large standard deviation in cDCE rates for the low level triplicate yielded a p-value on the confidence level of 0.05. T-tests were also performed on controls from the low level and HiCT experiments to verify that uninhibited cultures performed similarly despite the 5-month interlude between Experiments 1 and 6. Resulting p-values are shown in Table 10, all of which are above the confidence level of 0.05, indicating reproducible Evanite culture performance in both experiments.

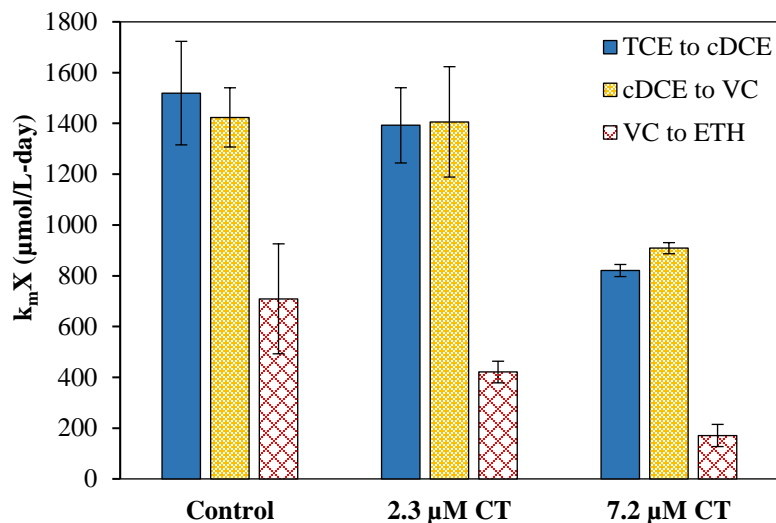


Figure 24. Modeled transformation rates for Day 0 control (CT-free), low, and high CT-exposed reactors of Experiments 1 and 6. Error bars represent one sample standard deviation of duplicate (control) or triplicate (CT-exposed) reactors. HiCT reactors have smaller rates than in low CT exposure.

Table 10. T-test Analyses Comparing CE Day 0 Transformation Rates Between CT Exposures and Between Associated Controls

Transformation Rate	Low vs High	Controls
TCE	0.0195	0.3387
cDCE	0.0568	0.6732
VC	0.0021	0.8419

In earlier experiments, CT inhibition was proposed to begin at the time when the model deviated from VC data because day 0 rates for TCE and cDCE were similar to control day 0 rates, indicating those steps were not yet affected by CT. In HiCT reactors, however, transformation of all three CE compounds was slowed relative to the control and low level reactors, indicating an earlier (or possibly immediate) CT-related inhibition to the OHRB. Thus, the time at which the model deviates from VC data is no longer an accurate indicator of the start of inhibition. Because slowing of the TCE rate began soon after CT addition, it difficult to estimate the mass of CT transformed at the start of inhibition, but it is possible that the earlier reduction corresponds to more CT mass transformed since time zero.

TCE and formate were added to the reactors again on day 14. At this time, CT products were present at aqueous concentrations of 1.05  $\mu\text{M}$  ( $\text{CS}_2$ ), 2.95  $\mu\text{M}$  (DCM), and 3.79  $\mu\text{M}$  (CF). Figure 25 displays the CE transformation profiles for control (Panel A) and CF-exposed (Panels B, C) reactors. All steps of the CE transformation pathway are visibly slowed in comparing Panels A and B, which are shown with the same time scale and highlight the elongation of data points in CT-exposed reactors. Control behavior was consistent based on prior experiments, with a rapid time of completion and a good model fit to the data. Decreases in rates from day 0 and day 14 are again attributed to endogenous decay and delayed feeding.

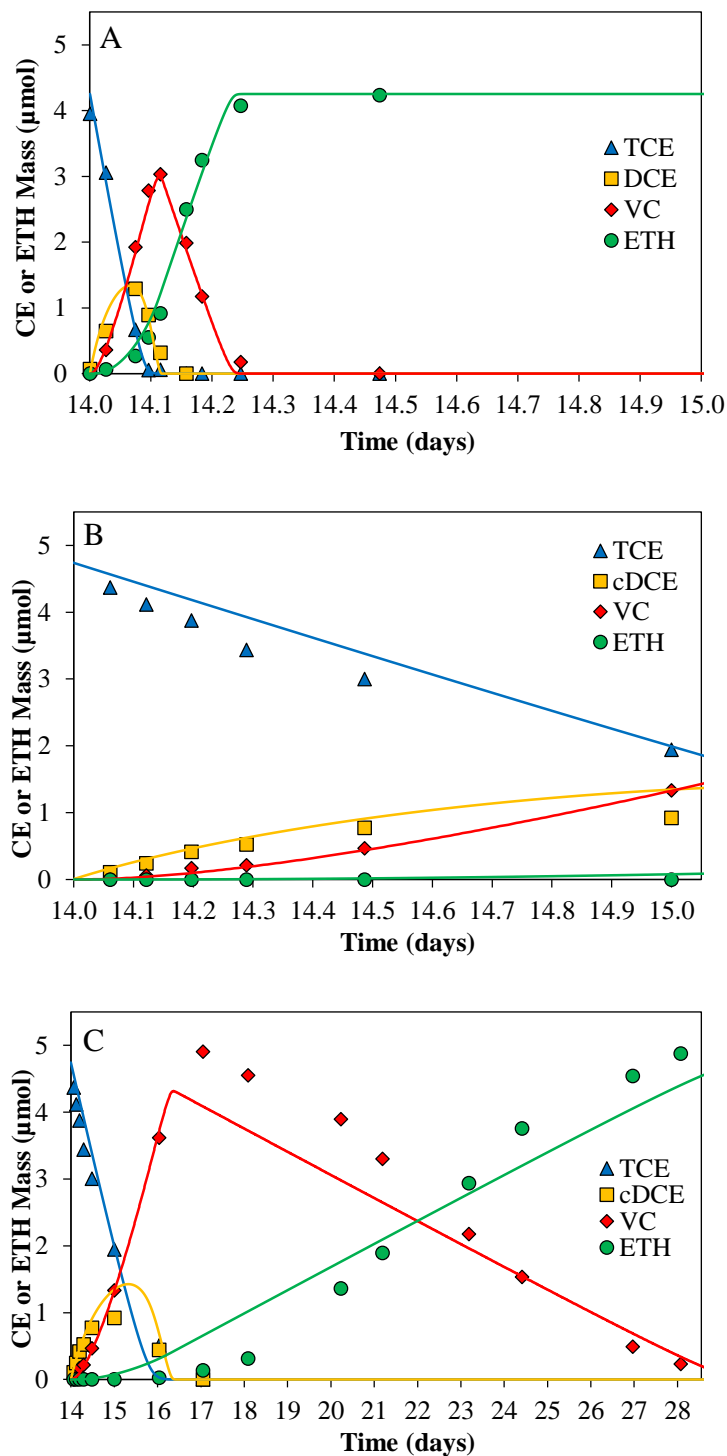


Figure 25. Day 14 CE transformation profile for a representative CT-free control (Panel A) and CT-exposed reactor (Panels B and C) 14 days after 7.2  $\mu\text{M}$  CT addition (Experiment 6). Panel B displays the CE transformation over the same time as the control CE transformation, while Panel C displays data collected over the entire period of transformation in the same reactor.

As expected based on low level experiments, HiCT reactors experienced a dramatic decrease in transformation rates for TCE, cDCE, and VC. When TCE was added, the CF concentration in reactors was 60% higher than in Experiment 1. TCE and cDCE were transformed by 16 and 17 days, respectively, corresponding to 2 and 3 days after the second addition of TCE. Maximum VC mass occurred on day 17, or 3 days after TCE addition. The model fits TCE and cDCE reasonably well, but between days 15 and 22, ethene production is overestimated and VC mass is underestimated.

The CT concentration of 7.2  $\mu\text{M}$  in Experiment 6 was triple the concentration in low level exposure (Experiment 1). Modeled transformation rates for the control, low level, and high level CT exposed reactors are shown in Figure 26. The rates are displayed on a logarithmic scale so the difference between CT concentrations is visible. The rates are also presented in Table 11. A reduction by about 2 orders of magnitude in TCE and cDCE rates relative to the day 14 control is apparent. Rates differ between HiCT and low level CT exposures by a factor of 3, and Welch's t-test p-values for these TCE, cDCE, and VC rates were 0.0056, 0.0168, and 0.0298, respectively. This agrees with day 0 analysis that suggested that CT concentration does significantly influence the inhibition of OHRB.

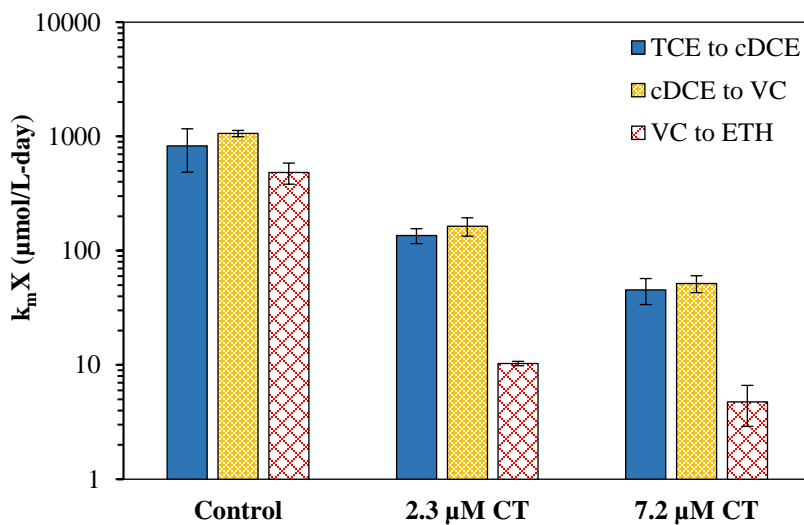


Figure 26. Modeled transformation rates for Day 14 control (CT-free), low, and high CT-exposed reactors of Experiments 1 and 6. Error bars represent one sample standard deviation of duplicate (control) or

triplicate (CT-exposed) reactors. HiCT reactors have smaller rates than in low CT exposure. Note the log scale of the y-axis.

Transformation rates and their percent reduction from controls from Experiments 1 and 6 are also displayed in Table 11 for a side by side comparison. Greater reductions in rate are apparent when the CT concentration is higher. CF concentration on day 14 was 60% greater in Experiment 6 (HiCT) than 1 (low CT), which could contribute to the lower rates in day 14 HiCT reactors. However, CT toxicity likely responsible for the majority of the rate reduction.

Table 11. A Comparison of CE Transformation Rates in Low Level CT and HiCT Exposures

CE Rate	Day 0		Day 14	
	Expt 1 (2.3 $\mu$ M CT)	Expt 6 (7.2 $\mu$ M CT)	Expt 1 (2.3 $\mu$ M CT)	Expt 6 (7.2 $\mu$ M CT)
	<b>Modeled Transformation Rate</b>			
TCE	1390 $\pm$ 148	821 $\pm$ 23.9	136 $\pm$ 20.3	45.4 $\pm$ 11.7
cDCE	1410 $\pm$ 217	909 $\pm$ 21.9	164 $\pm$ 30.0	51.7 $\pm$ 8.71
VC	421 $\pm$ 42.6	171 $\pm$ 43.7	10.3 $\pm$ 0.46	4.76 $\pm$ 1.86
	<b>% Reduction from Control</b>			
TCE	8.4%	83.6%	46.0%	94.5%
cDCE	1.2%	84.5%	36.2%	95.1%
VC	40.7%	97.9%	75.9%	99.0%

ii. *Multiple CT Additions*

HiCT tests demonstrated a CT concentration-dependence of CE rate reduction, but whether results could be entirely explained by that was unclear. This is because a greater CT concentration in a single addition necessarily increases the mass of CT transformed. In order to evaluate whether the reduction in rates was dependent on the mass of CT transformed, a multiple CT delivery strategy was employed in Experiments 7 and 8. The design for these tests was similar to Experiment 2, with TCE and formate addition to Evanite batch reactors on day 0 and day 2 for CE transformation analysis under CT exposure. However, CT was delivered to the batch reactors in 3 (Experiment 7) or 4 (Experiment 8) separate additions, injected every 12 hours after time zero. The total

mass of CT delivered to reactors was approximately equal to the single addition mass delivered in Experiments 1 and 2. Thus, the initial CT concentration in multiple addition experiments was lower than in single addition, but the total CT transformed in 2 days was approximately the same. A comparison of day 2 CE transformation rates in single and multiple CT addition reactors could therefore indicate whether initial CT concentration is a major factor in inhibition of CE transformation, or if an equal inhibition can be achieved in reactors that transform the same amount of CT. A 2-day exposure was used to reduce the effects of long term CF exposure on the cultures. All other components of experimental design were the same.

In Experiment 8, CT was added 4 times separated by 12-hour intervals, and the chlorinated methane profile is shown below in Figure 27 Panel A. CT rapidly decreased after each addition, however, a first order rate analysis indicated CT transformation slows with each addition, shown in Appendix 6. A slowing in CT rate is consistent with previous work suggesting a CT transformation capacity of the system<sup>142</sup>. The average total CT exposed to the batch reactors over 4 additions was 0.36  $\mu\text{mol}/\text{reactor}$ , the same as single addition experiments (Table 12). By day 2, 0.108  $\mu\text{mol}$  CT remained and CF had gradually accumulated to about 1.19  $\mu\text{M}$  aqueous concentration, and DCM and  $\text{CS}_2$  accumulated up slowly throughout the experiment.

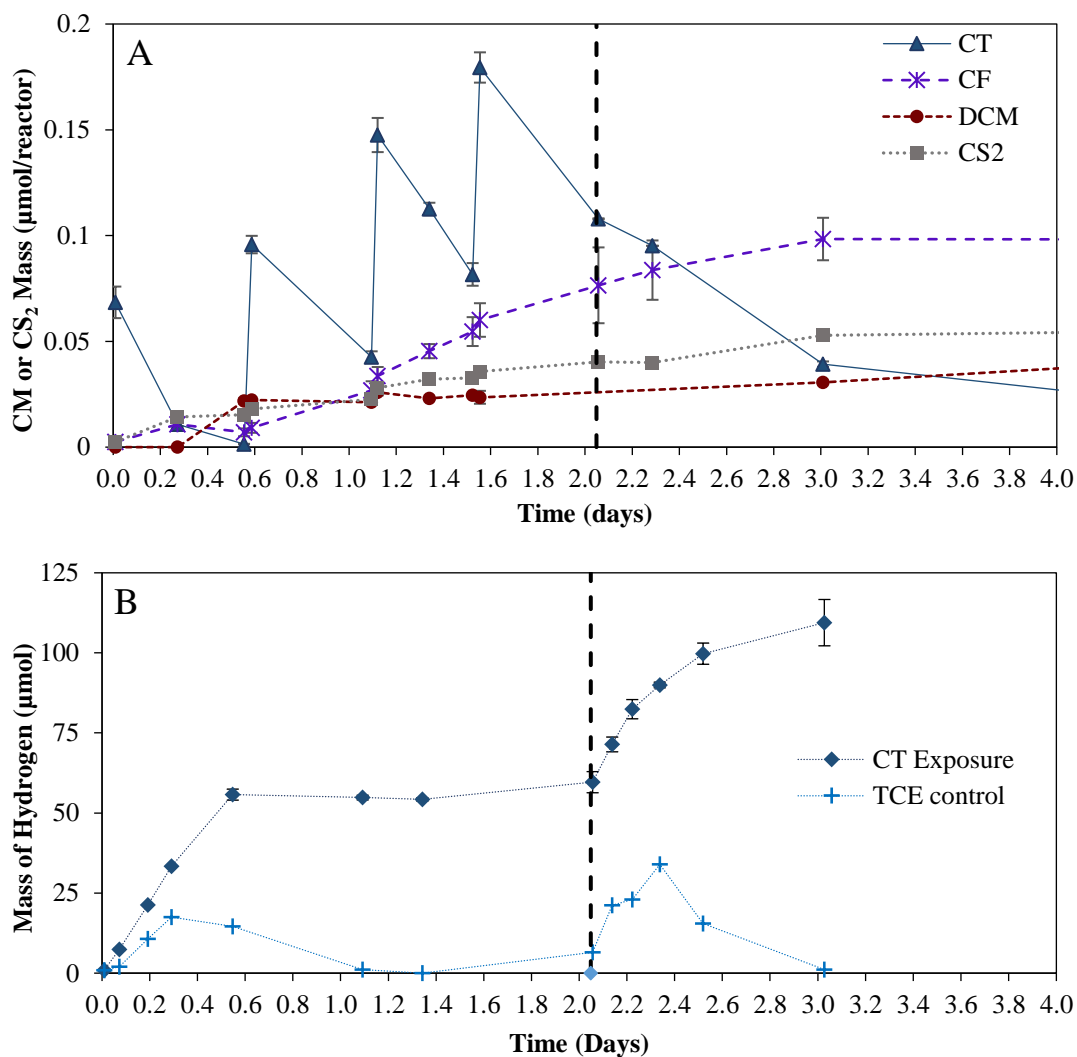


Figure 27. CM transformation and addition profile (Panel A) and H<sub>2</sub> production and consumption (Panel B) for Experiment 8 beginning 4/25/17. CT is added 4 times within the first 48 hours, during which CF slowly accumulates (Panel A). H<sub>2</sub> consumption is inhibited (56 µmol) in CT-exposed reactors, and H<sub>2</sub> increases after the second TCE/formate addition, denoted by the dotted line. Error bars represent one standard deviation and are not shown if smaller than the marker size. The TCE control was a single reactor and has no error bars.

Table 12. CT Mass Introduced to Reactors in Single and Multiple Addition Experiments

Experiment Type	Single Addition	Multiple Addition	
	2	7	8
Experiment	2	7	8
CT Addition 1	0.36	0.088	0.068
CT Addition 2	N/A	0.13	0.094
CT Addition 3	N/A	0.13	0.10
CT Addition 4	N/A	N/A	0.098
Total CT Added	0.36	0.34	0.36
CT Transformed by Day 2	0.36	0.30	0.26

Shown in Figure 27B, H<sub>2</sub> production and consumption in Experiment 8 is consistent with previous CT-exposure experiments. Inhibition of H<sub>2</sub> consumption does not appear change because of alternate delivery of CT. In CT-exposed reactors, H<sub>2</sub> reached a maximum of 56 μmol at 0.5 days, which was maintained until the next formate addition. The CT or its transformation inhibits the complete consumption of H<sub>2</sub>, which apparently halted at 0.5 days. Day 2 addition of formate caused H<sub>2</sub> to increase again in all reactors. Control reactors consumed day 2 H<sub>2</sub> similarly to day 0. H<sub>2</sub> in CT-exposed reactors built up to 109 μmol, approximately double the level prior to the second formate addition. Thus, CT-related inhibition of H<sub>2</sub> consumption is persistent into the second TCE addition and unaffected by the multiple additions of CT.

TCE transformation was rapid and accurately modeled on day 0. Figure 28 presents the nearly identical transformation profiles for control and CT-exposed reactors, where the disappearance of TCE and cDCE is coupled with the VC maximum at 0.1 days or before. VC was detectable for 0.5 days in both controls and CT-exposed reactors, and the reason for this is unknown, but modeled zero order rates compare well with previous controls and are shown in Figure 29. Rates in were not statistically different between control and CT-exposed reactors for any CE (p-values greater than 0.05, not shown). Most notably, the day 0 VC transformation rate is not reduced by the presence and transformation of 0.5 μM CT added at time zero. In contrast, in single addition experiments, the initial CT concentration of 2.3 μM was sufficient was inhibit VC transformation starting on at 0.2 days. This difference demonstrates the CT concentration-dependence indicated from HiCT tests discussed above.

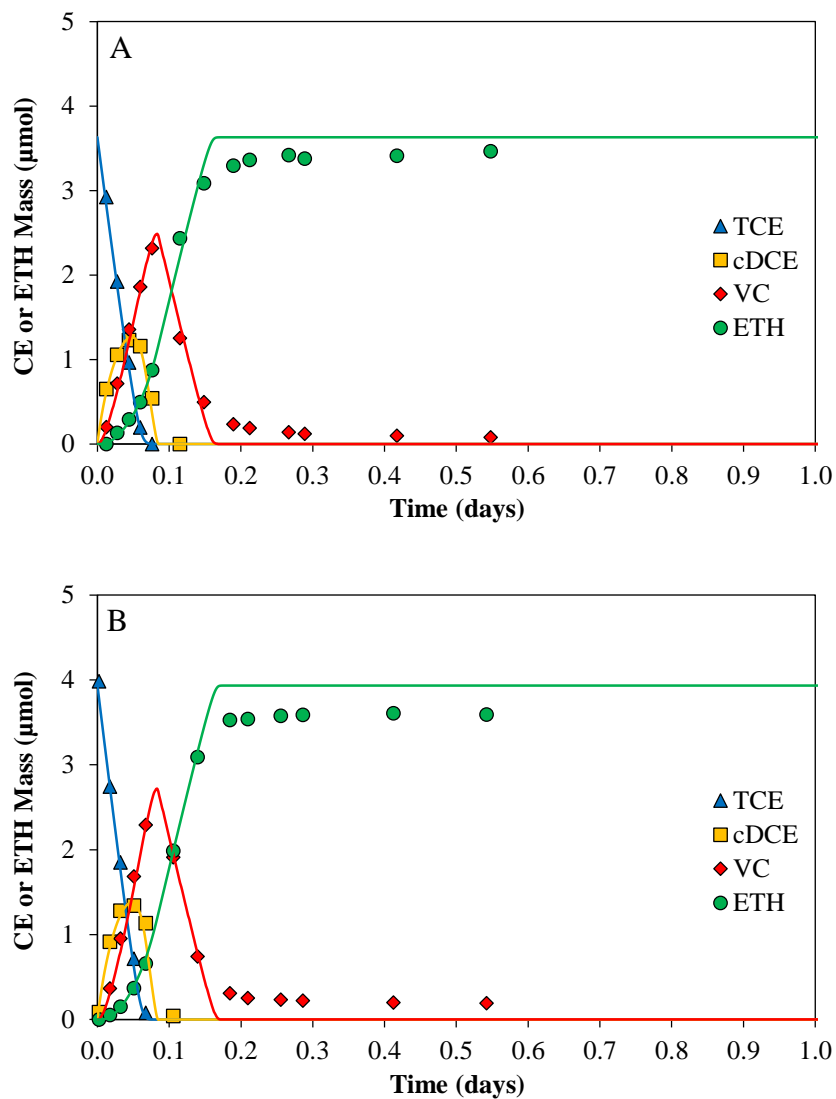


Figure 28. Day 0 CE transformation profile for a CT-free control (Panel A) and representative CT-exposed reactor (Panel B) subject to CT addition at 0, 0.5, and 1 days (Experiment 8). Profiles are essentially identical, with no inhibition of VC transformation observed.

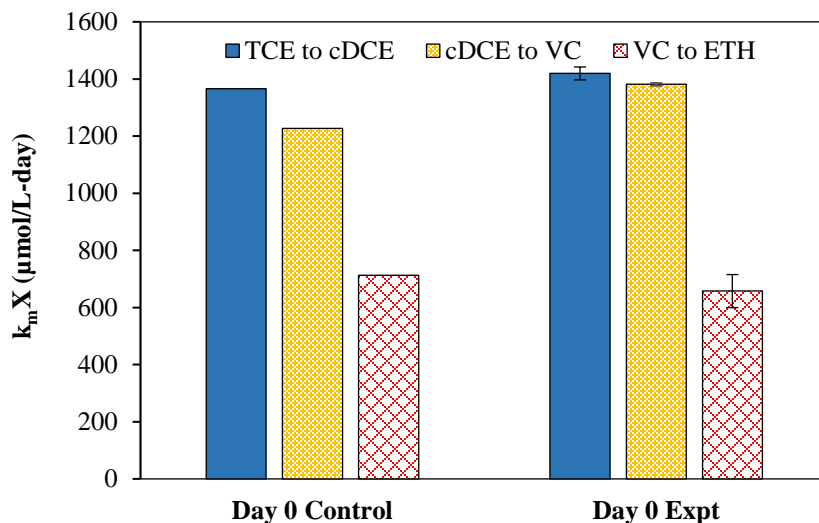


Figure 29. Modeled transformation rates for day 0 control and CT-exposed reactors of Experiment 8 (multiple CT addition). Error bars represent one standard deviation. There is only one control reactor. “Expt” = CT-exposed. There are not significant differences between control and CT-exposed reactor rates for any compound.

Transformation profiles for control and CT-exposed reactors are shown in Figure 30. Complete TCE transformation occurred by 2.3 days in controls and 3.4 days in CT-exposed reactors (1.4 days after second addition). In comparison, the process took until about 5.5 days (3.5 after second addition) in Experiment 2, when the same CT mass was delivered as a single addition (see Figure 11B). By day 2, 0.108 μmol CT remained, or 0.6 μM aqueous concentration. This was unlike Experiment 2, in which CT had been fully transformed by this time. The presence of CT at the start of the day 2 TCE transformation could partially contribute to the slower rates under the multiple delivery design because its transformation continued throughout the day 2 CE transformation (Figure 27A).

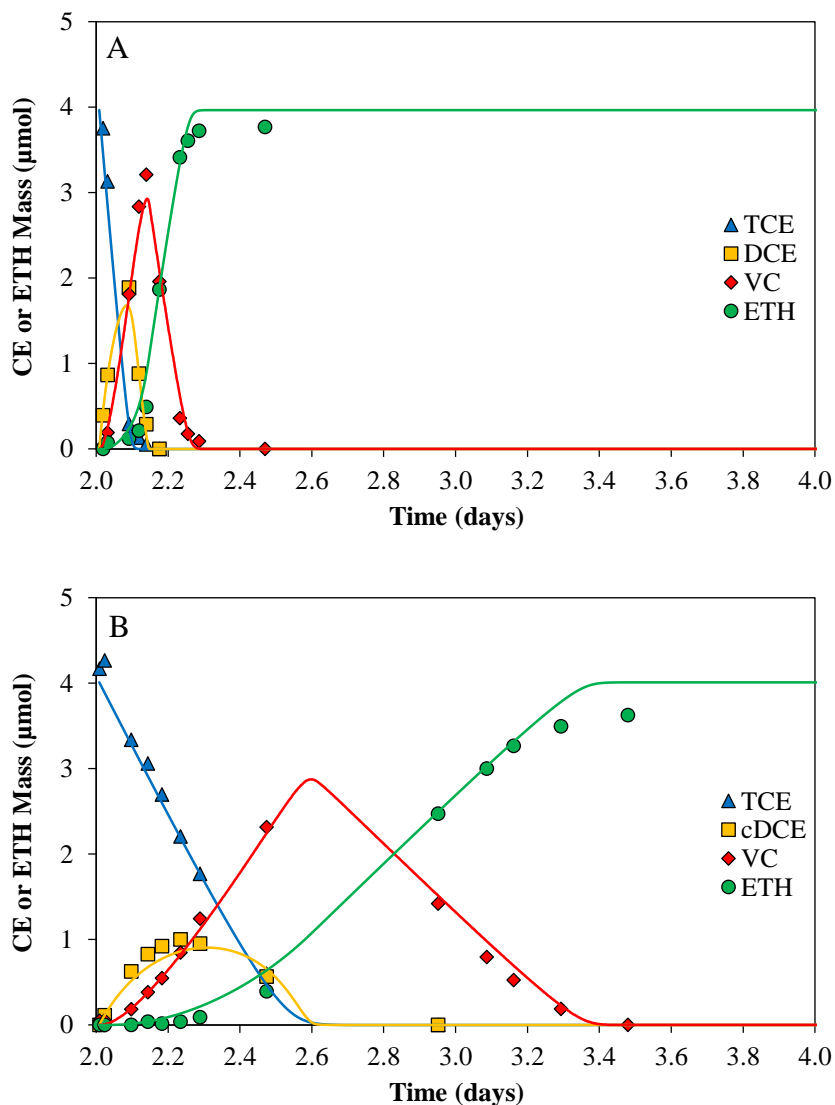


Figure 30. Day 2 CE transformation profile for a CT-free control (Panel A) and representative CT-exposed reactor (Panel B) following 3 separate additions of CT (Experiment 8).

The Multi-Fit Monod model fits the data well, indicating that toxicity slows rates proportionally for the experiment time span and that the effect of toxicity has already occurred. Nearly all of the CT mass delivered to the system has transformed by day 2, so if the inhibition of CE transformation is related to CT or a product, that is consistent with CT being completely transformed. Zero-order transformation rates are shown in Figure 31 and Table 13 along with day 2 single addition rates from Experiment 2 for comparison. Single or multiple addition of CT significantly reduces all CE rates relative

to the control, and Welch's t-tests with a 0.05 confidence level yielded no significance difference between rates from systems inhibited by single and multiple delivery designs (Table 13).

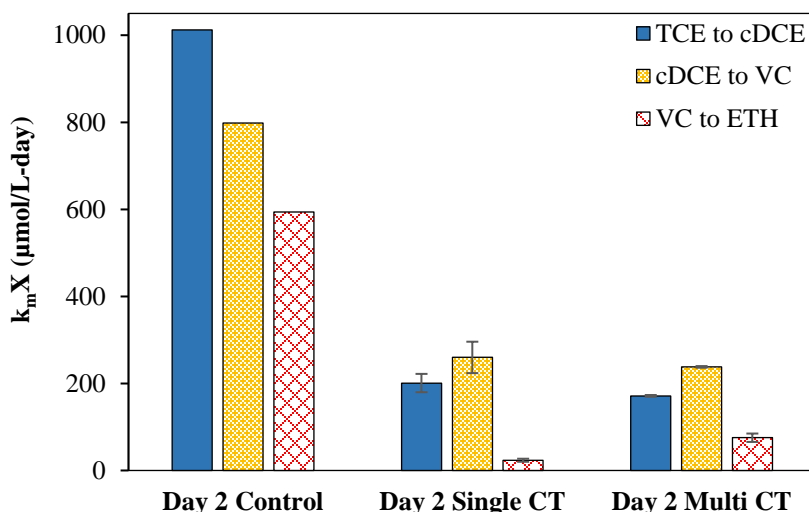


Figure 31. Modeled CE transformation rates for Day 2 control (CT-free), single CT addition, and multiple CT addition reactors (Experiment 8). Error bars represent one standard deviation from triplicate (single) and duplicate (mult) reactors. There is one control. Despite visual differences between VC rates, CT delivery strategy does not result in statistical differences between transformation rates of any compound.

Table 13. Comparison of CE Transformation Rates in Single Addition and Multiple Addition CT Exposures

CE Rate	Single CT Addition		Multiple CT Addition		Comparison	
	Day 0	Day 2	Day 0	Day 2	Day 0	Day 2
	Modeled Transformation Rate				Welch's t-test p-value	
TCE	1453 ± 118	200.8 ± 21.1	1419 ± 31.9	171.4 ± 2.03	0.786	0.135
cDCE	1503 ± 207	259.7 ± 36.1	1381 ± 6.48	238.0 ± 1.85	0.861	0.406
VC	406.9 ± 15.0	23.48 ± 3.51	657.4 ± 81.9	75.21 ± 9.67	0.111	0.064
	% Reduction from Control					
TCE	-6.4%	80.2%	-3.9%	83.1%		
cDCE	-22.5%	67.5%	-12.6%	70.2%		
VC	43.0%	96.0%	7.8%	87.3%		

CT delivery scheme at these concentrations did not influence the toxicity of 0.3 μmol CT to cultures respiring 50 μM TCE on days 0 and 2. Statistical tests confirmed

that day 0 and day 2 rates between reactors of different CT delivery were not significantly different. Thus, CT toxicity appears to be more dependent on the mass of CT transformed.

## 6. Vitamin B12 Amendment

Up to this point, the mechanism of CT toxicity was unclear, however, results had demonstrated that non-CF factors were primarily responsible for CE rate reduction at early exposure times and that CT toxicity continued to affect cultures after the disappearance of CT. Experiment 9 was designed with vitamin B12 amendment to simultaneously investigate both the mechanism of CT toxicity and potential protectant against it.

It is generally assumed that CT transformation in reducing systems proceeds via the trichloromethyl radical intermediate, from which multiple parallel products may be formed. This radical has been proposed to bind with the cobalt atom of corrinoid compounds<sup>8,9,25,106</sup>, and addition of vitamin B12 has been reported to increase CT transformation rates<sup>10,11</sup>. Microbial reduction of vitamin B12 facilitated the transformation of CT by the reduced B12 to non-halogenated products in a *Shewanella* strain<sup>13</sup>. The current experiment was modeled with these results in mind and aimed to evaluate the effect of vitamin B12 amendment on CT toxicity to OHRB after 2 days of exposure.

Experiment 9 reactors were amended with 15 mg/L cyanocobalamin (vitamin B12) and 2 mM formate after cultures and supernatant were sampled from the Evanite chemostat. Modeled after the concepts of Workman et al.<sup>13</sup>, the cultures were given three days without CE or CM addition to reduce the B12 if possible, however the potential for this was unknown. During this time, analytical techniques such as spectrophotometry were not used to evaluate the oxidation state of B12, as was performed in the Workman study. H<sub>2</sub> from formate fermentation was monitored from the start, and formate was added again on day 1 and 2 when H<sub>2</sub> levels were measured to be less than 10 μmol/reactor. On day 3, 2-3 μM CT was added to reactors. Due to analytical limitations

at the time, its transformation was not monitored. Two days of CT exposure was assumed to deliver a similar toxicity to OHRB as had been previously observed. Experiment 1 CT transformation was complete by day 2 (Figure 4), however in light of catalytic properties of B12 on CT transformation reported by other researchers, it is possible that transformation was complete at an earlier time. On day 5, after 2 days of CT exposure, TCE (30  $\mu$ M) and formate (2mM) was added to reactors at, and resulting CE transformation was evaluated similarly to prior experiments. These reactors are henceforth referred to as the B12/CT/TCE Expt. Single reactor controls were performed on the same day and are named according to the control condition as follows: TCE (TCE addition day 5), B12/TCE (B12 addition day 0, TCE addition day 5), CT/TCE (CT addition day 3, TCE addition day 5). All reactors received formate at the same time as B12/CT/TCE Expt reactors.

The addition of 15 mg/L B12 to reactors caused a color change in the media from clear to light pink. This voided use of resazurin as a redox indicator in the reactors, however, reactors without B12 addition maintained a clear color throughout the experiment, indicating a consistently anaerobic design. Photographs of reactors on days 3, 5, 7, and 14 are shown in Figure 32. B12/CT/TCE, consistently shown on the right, change within the first 5 days to a browner shade of pink compared to the B12/TCE reactor, shown on the left in the photos. However, by day 14 (bottom right), similar shades of brown/yellow are seen in both B12/TCE and B12/CT/TCE reactors. Color changes may be due to the reduction of B12 by media components such as  $\text{Na}_2\text{S}$  or cell components of the supernatant.



Figure 32. Color observations in B12 amendment tests (Experiment 9). Clockwise from top left: Day 3, Day 5, Day 14, Day 7 post-B12 addition. In the top photos, the single reactor on the left (blue label) is the B12/TCE, and reactors on the right are B12/CT/TCE (red label). The Day 7 photo shows the CT/TCE and TCE reactors on the left, with clear coloration maintained throughout the experiment. The Day 14 photos shows anaerobic mineral media freshly amended with B12 for visual comparison of what reactors looked like on Day 0.

Hydrogen behavior for Experiment 9 in Figure 33, where arrows denote formate (2 mM) additions. TCE and B12/TCE reactors behaved similarly to each other for the entire period, with rapid  $H_2$  consumption following each addition.  $H_2$  never accumulated past 27  $\mu\text{mol}$  in either reactor. Production and consumption was nearly identical in all reactors until day 3. After day 3,  $H_2$  began to build up in reactors to which CT was added. The CT/TCE control  $H_2$  reached 90  $\mu\text{mol}$  and decreased to 50  $\mu\text{mol}$ , which was maintained until the day 5 addition of formate increased  $H_2$  to 122  $\mu\text{mol}$  within the next day. This is similar to behavior reported in Experiments 1, 6, 8 (CT addition). Interestingly,  $H_2$  in the B12/CT/TCE reactors accumulated to 50  $\mu\text{mol}$  after the day 3 formate addition, but it did not plateau there. Instead,  $H_2$  was consumed to approximately 20  $\mu\text{mol}$  by day 5. In B12/CT/TCE reactors, the day 5 formate addition resulted in a maximum  $H_2$  mass of 40  $\mu\text{mol}$ , which was then consumed. This profile indicates improved  $H_2$  consumption in B12-amended reactors relative to unamended, CT-exposed reactors.

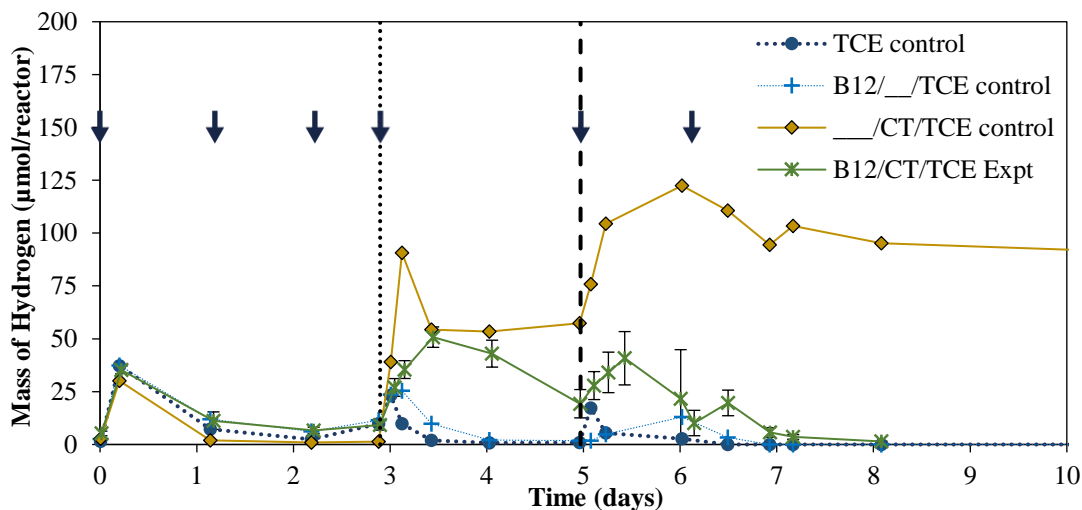


Figure 33. H<sub>2</sub> profiles for B12 amendment (Experiment 9). Arrows represent addition of formate to all reactors except for day 6, on which only B12/CT/TCE reactors were amended. The Day 3 dotted line represents CT addition to CT/TCE control and all B12/CT/TCE reactors. The Day 5 dotted line represents addition of TCE to all reactors. By day 8, B12/CT/TCE reactors had completed TCE transformation and had completely consumed H<sub>2</sub>. On day 10, the CT/TCE control reactor still has about 100 μmol H<sub>2</sub> and VC is still at detectable levels. The major difference in H<sub>2</sub> consumption between CT/TCE control and B12/CT/TCE reactors is likely due to the presence of vitamin B12. Error bars represent one standard deviation from the mean of triplicate reactors. If not shown, there is only one reactor.

Day 2 CE transformation profiles for each reactor condition are shown in Figure 34. Panels A and B illustrate the rapid transformation of TCE, cDCE, and VC in CT-free reactors, and complete ethene mass is achieved by 5.5 days or less (0.5 days from TCE addition). The B12-amended reactor performs slower transformations than the TCE only reactor, and the Multi-Fit Monod model fits data well for the entire period. In reactors with CT addition (Panels C and D), transformation is significantly slower. TCE was transformed by about 5.5 days in both types of reactors, however, cDCE (model prediction) and VC transformation were much slower in reactors without B12 (Panel C). In B12/CT/TCE reactors, complete transformation to ethene occurred by day 8, at which time VC mass was 1.8 μmol in the CT/TCE reactor. The model fit the data well for all CEs, and corresponding zero-order rates are displayed in Figure 35 and Table 14.

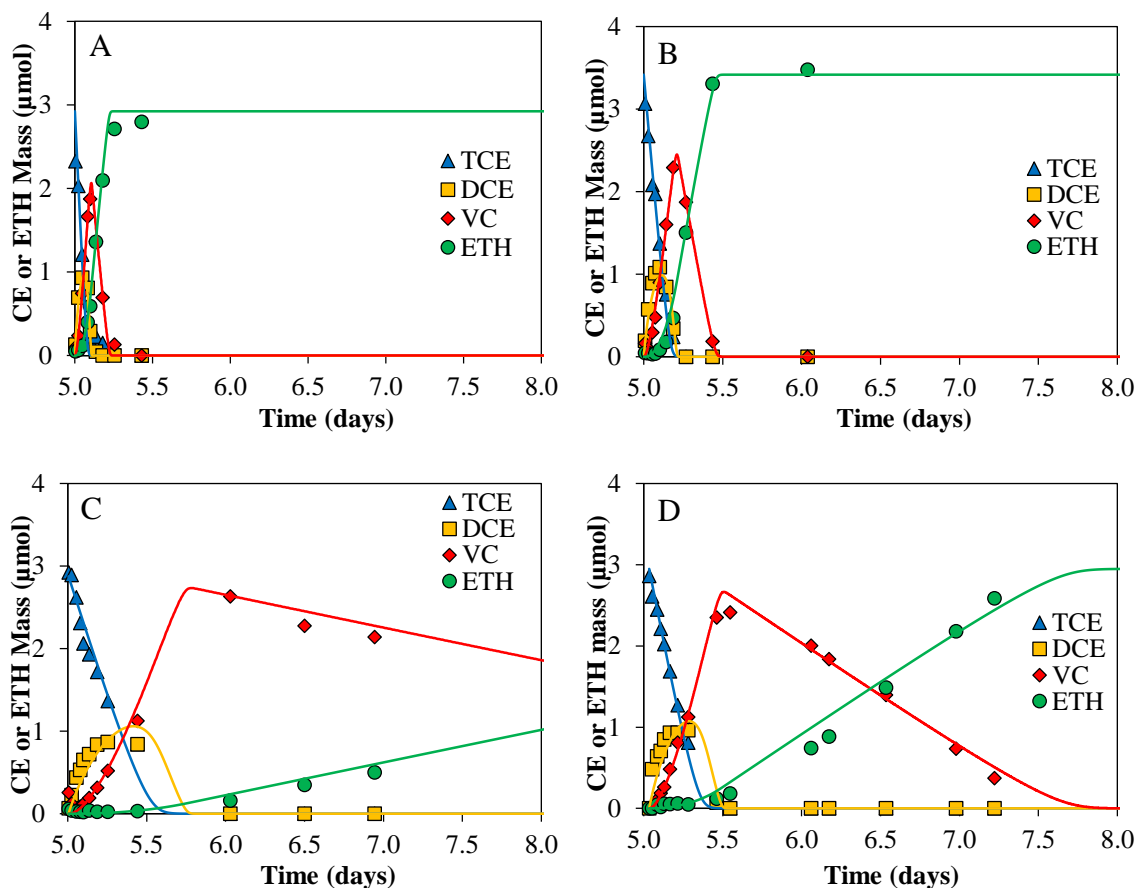


Figure 34. Day 5 CE Transformation Profiles for Various Reactor Conditions of the Vitamin B12 Amendment (Experiment 9). Panel A, TCE. Panel B, B12/TCE. Panel C, CT/TCE. Panel D, B12/CT/TCE (representative reactor of triplicate).

Table 14. Comparison of CE Transformation Rates in Various Reactors of the B12 Amendment Experiment

CE Rate	TCE	B12/TCE	CT/TCE	B12/CT/TCE
	Modeled Transformation Rate			
TCE	840	454	127	228 ± 20.4
cDCE	860	527	115	216 ± 25.9
VC	399	219	8.08	32.5 ± 6.38
% Reduction from TCE Reactor				
TCE		45.9%	84.9%	72.9%
cDCE	N/A	38.7%	86.7%	74.9%
VC		45.0%	98.0%	91.9%

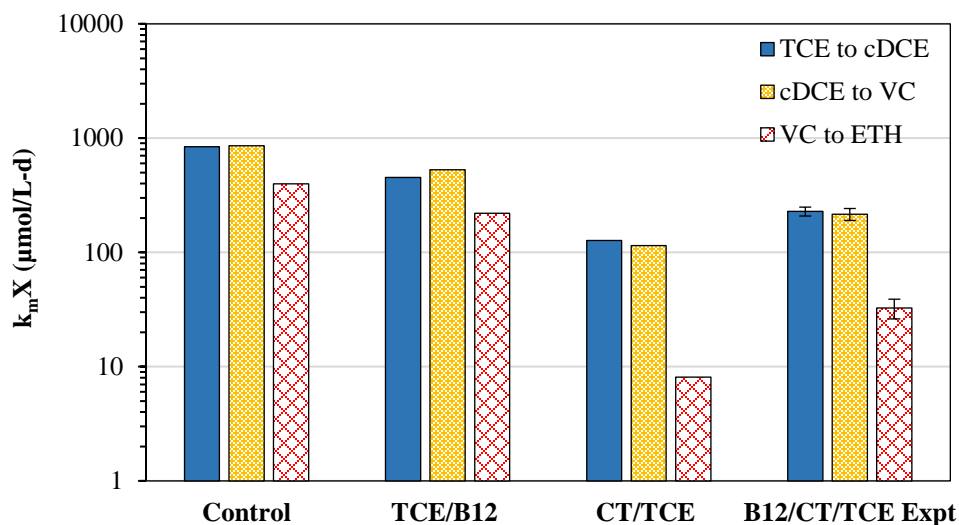


Figure 35. Day 5 CE Transformation Rates for Reactors in the B12 Amendment Experiment (9). Control = TCE only. Note the log scale.

Rates in the TCE/B12 reactor were about half the rates of TCE. The reason for this is unknown. It is possible that 15 mg/L B12 was toxic to the culture, however this quantity was chosen based on literature values between 7 and 68 mg/L B12 amendments for similar tests<sup>11,13,25</sup>. The difference in rates does suggest that B12 amendment does not catalyze CE transformation; if it had, the B12/TCE reactor may have achieved faster rates than the TCE reactor. If B12 amendment did protect against CT toxicity, it did so without being used in CE RDase-catalyzed reduction. It is also possible that oxygen was introduced into the reactor via the syringe injecting either B12 or formate and that this was not detectable with resazurin because the B12 had changed the media color to light pink.

TCE and cDCE rates in B12/CT/TCE reactors are about a factor of 2 greater than those in CT/TCE reactors, and VC rates in B12 amended reactors are about 3 times greater. T-tests were not performed because there was only a single CT/TCE reactor. However, this difference in rates, coupled with the enhancement of H<sub>2</sub> consumption under B12 and CT exposure, suggest that B12 may have some potential as a protectant against CT toxicity towards OHRB and their community.

## 7. Post-Exposure Recovery Potential

Results reported thus far focused on the inhibition of chlorinated ethene (CE) transformation rates and H<sub>2</sub> consumption by the presence and/or transformation of chlorinated methanes (CMs), and findings are supported by earlier observations of inhibition of OHRB CE transformation<sup>16,17,26</sup>. However, these results do not differentiate between inhibition and toxicity because CT and/or CF are always present during CE transformation. In the case of CT-related CE rate inhibition, toxicity may be responsible mechanism because decrease in CE rates established for early CT exposure time is maintained even after the disappearance of CT. The mechanism of toxicity was suggested to involve CT transformation and possible interaction with essential cofactors (see Section 5). However, if the CT-related inhibition was due, in part or entirely, to the presence of a non-CF volatile product of CT transformation, its removal may allow for recovery of transformation rates. Where bioremediation is employed, it would also be important to know if CE degradation could recovery after exposure to CMs. This would help establish prioritization in a design, such as the removal of CMs prior to focusing on CE dechlorination. In order to evaluate if toxicity was the primary mechanism behind the inhibition of CE transformation, recovery tests were performed, where recovery potential of long-term batch reactors was assessed after the removal of CF, DCM, and CS<sub>2</sub>.

Recovery will be defined as the ability of the culture to display increased CE rates after the removal of CMs relative to rates obtained under CM exposure. Recovery was evaluated in the CT and CF-exposed reactors 50 days after the start of the experiment (Experiments 1 and 4). Day 49 control rates represent the best-case scenario of recovery, where factors contributing to decreased rates are unrelated to CM inhibition. Achieving day 49 control rates in a previously CM-exposed reactor would therefore correspond to 100% recovery according to this method of analysis. Recovery would indicate that CM-related inhibition or toxicity is reversible for this system.

Experiments 10 and 11 involved the same batch reactors from Experiments 1 (CT exposure) and 3 (CF addition), respectively. Complete transformation of TCE to ethene had been achieved after addition both on day 0 and day 14. The reactors were shaken in the dark until day 49 without further substrate or nutrient additions. On day 49, reactors

were anaerobically sparged until CM concentrations were not detectable and then returned to the shaker table overnight. On day 50, 50  $\mu\text{M}$  TCE and 2 mM formate were added. CEs and  $\text{H}_2$  were monitored throughout CE transformation, and extra formate was added if  $\text{H}_2$  fell below about 2  $\mu\text{mol}$ /reactor. Modeled CE transformation rates were compared to rates obtained during CM exposure (day 0 and day 14). Day 50 rates less than day 14 rates could indicate effects from long term CF exposure and/or minimal recovery potential. Day 50 rates above day 14 rates would indicate recovery potential dependent on CM removal, or a reversible inhibition exerted by CT or CF.

Control reactor performance on day 49 is shown in Figure 36. The profile shows rapid TCE transformation after 49 days. The culture was maintained even though no electron donor or acceptor had been supplied since day 14. TCE and cDCE were transformed within about 0.2 days of TCE addition, and VC was transformed within 0.5 days of the TCE addition. The Multi-Fit Monod well predicts CE transformation behavior. Because the model only has one variable for CE-degrading biomass,  $X^{143}$ , the good fit suggests that factors such as endogenous decay and growth proportionally affect all OHRB populations involved in the CE RD pathway. Associated rates are shown in Figure 37 alongside day 0 and day 14 control rates. A Welch's t-test indicated no statistical difference between CE rates on day 14 and day 49, with p-values of 0.4, 0.1, 0.7 obtained for TCE, cDCE, and VC rates, respectively. These results demonstrate that the cultures are robust enough to tolerate a 5 week period (day 15 to 50) without feeding.

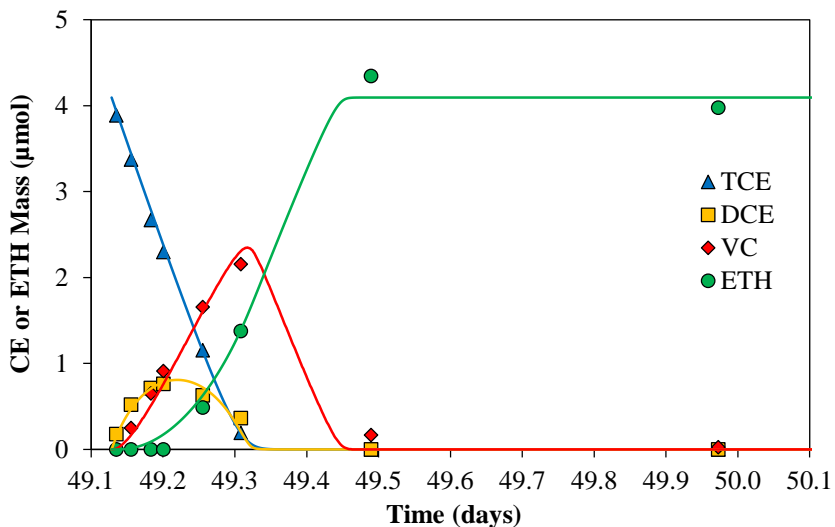


Figure 36. Day 49 CE transformation profile for a representative control batch reactor. Complete transformation occurs within 0.5 days of the day 49 TCE addition.

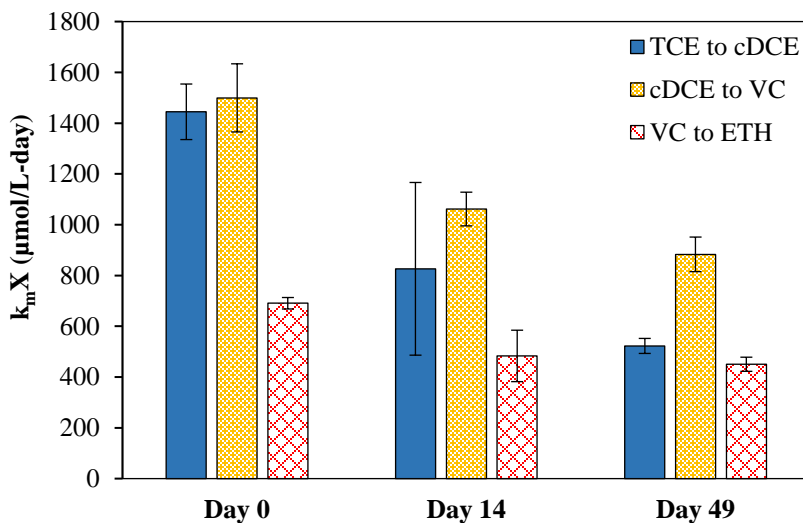


Figure 37. Control batch reactor CE transformation performance with time after sampling from the chemostat. Error bars represent one sample standard deviation. These duplicate reactors demonstrate the culture robustness despite periods without feeding or cell wastage.

In CT-exposed reactors, CF had decreased to 0.62  $\mu\text{M}$  by day 49 (Figure 4). Complete TCE transformation starting on day 50 took 17 days or more. One reactor of the triplicate had about equal masses of VC and ethene on day 17, after which no further data was collected. Figure 38 shows the mass data and model fits for 1-day (Panel A) and complete (Panel B) time scales. Transformation of all 3 CEs is slow, and ethene

production does not begin until after 24 hours. The model predicts the data well, yielding average rates of 120.8, 150.5, and 4.18  $\mu\text{mol/L-d}$  for TCE, cDCE, and VC, respectively. Shown in Figure 39, these rates are similar to day 14 transformation rates of 135.6, 164.1, and 10.3  $\mu\text{mol/L-d}$ . A Welch's t-test yielded p-values of 0.623, 0.647, and 0.0074 for TCE, cDCE, and VC transformation rates compared between day 14 and 50. Notably, these results show that the prolonged exposure to concentrations of CF, DCM, and  $\text{CS}_2$  present in reactors between day 14 and 50 (Figure 4) did not result in a further decrease of TCE or cDCE rates. However, the observed decrease in VC rate was statistically significant at an average 60% decrease relative to day 14.

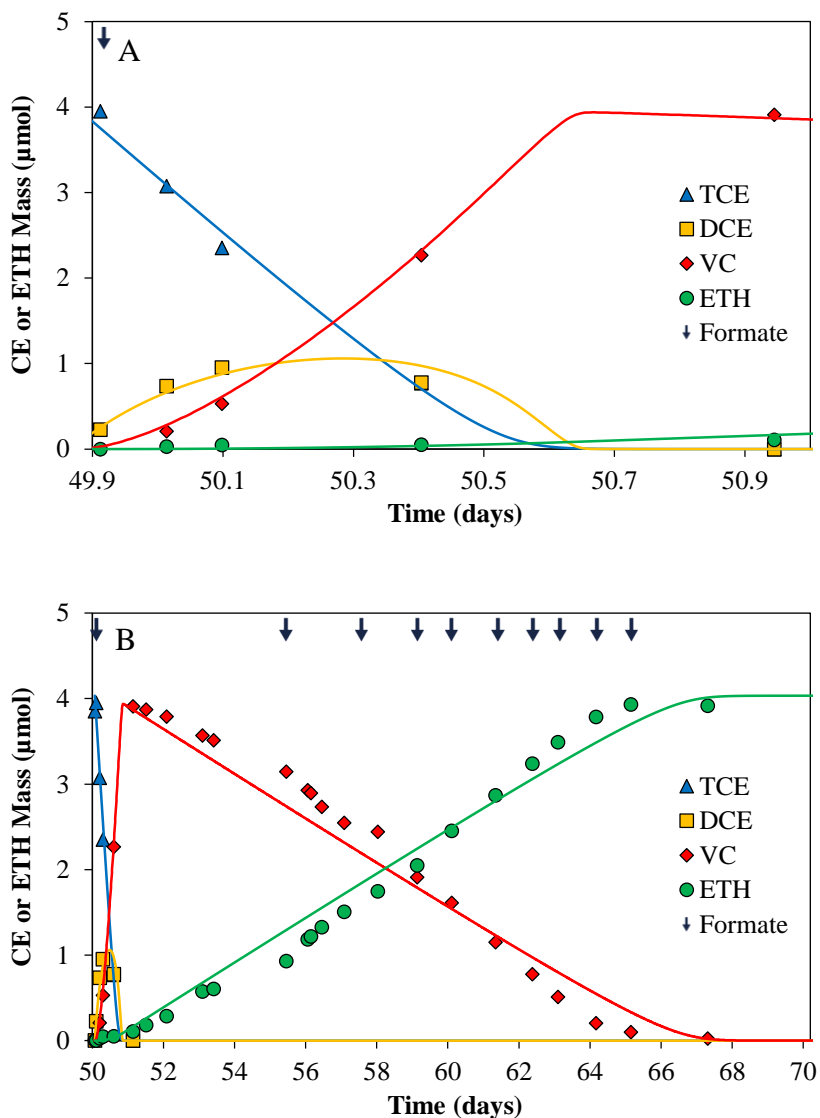


Figure 38. Day 50 CE transformation profile for a representative CT-exposed batch reactor. Sparging occurred prior to this data on day 49. Complete transformation occurs 17 days after the TCE addition. Arrows mark the addition of formate in response to a low  $H_2$  measurement.

The rates obtained on day 50 after reactors were sparged free of CF, DCM, and  $CS_2$  indicate removing CMs from these reactors does not allow recovery under the conditions tested. It is thus possible that inhibition of CE transformation was irreversible. However, results remain inconclusive because of the short time scale tested. It is possible that with longer times post-sparging cell recovery and growth could yield recovered rates.

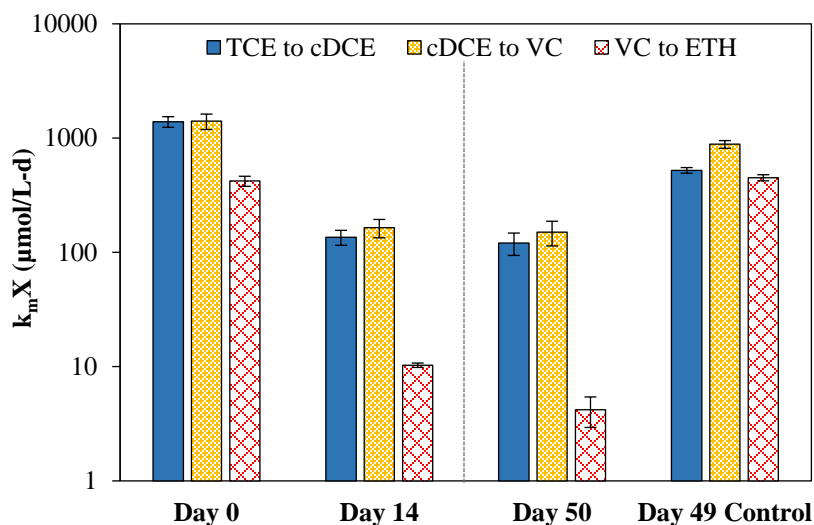


Figure 39. Modeled CE transformation rates occurring in CT-exposed reactors at various times before and after sparging. The day 49 control symbolizes the 100% recovery scenario. Rates do not improve immediately after sparging, denoted by the vertical dotted line. Error bars represent one sample standard deviation of triplicate (CT-exposed) or duplicate (control) reactors. Note the log scale of the y-axis.

Formate fermentation provided  $\text{H}_2$  to various microbial populations, including OHRB performing the CE transformations. Since OHRB require  $\text{H}_2$  as an electron donor, it is essential to maintain adequate  $\text{H}_2$  supply in the batch reactors. A hypothetical 12.5  $\mu\text{mol}$   $\text{H}_2$  is required for complete transformation of 50  $\mu\text{M}$  TCE. As shown in earlier sections, the presence of CMs partially inhibits  $\text{H}_2$  consumption, which results in an apparently high  $\text{H}_2$  supply that is maintained in reactors. Thus, additional formate additions were never required. For recovery experiments, however,  $\text{H}_2$  consumption increased after sparging. To maintain adequate excess of  $\text{H}_2$ , a total of 10 individual 2mM formate additions were required during the time of CE transformation. These additions are denoted in Figure 38B with small arrows.

Figure 40 shows the buildup and decline of  $\text{H}_2$  in response to formate additions to CT recovery reactors during the time frame for complete TCE transformation. While the first formate addition took about 5 days to deplete, subsequent additions were consumed faster. After day 59,  $\text{H}_2$  depleted so rapidly that collected data was not able to capture the rise and fall of  $\text{H}_2$  for each addition. It is possible that some formate did not completely

ferment to stoichiometric amounts of  $H_2$ , which would indicate incapacitation of the fermenting microbial populations and could contribute to the slow CE rate. However,  $H_2$  was measured between some additions to have reached 10-35  $\mu\text{mol}/\text{reactor}$ . So it is more likely that formate was fermented but that non-OHRB microbial populations were extremely competitive for this  $H_2$  relative to OHRB, causing its rapid depletion.

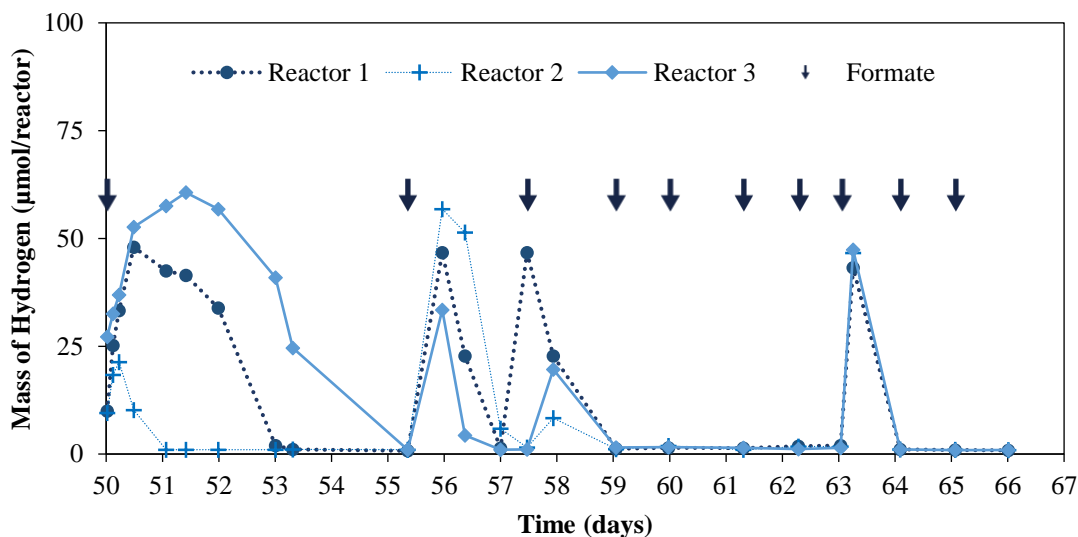


Figure 40.  $H_2$  production and consumption profile for recovery test (Experiment 10) with reactors from Experiment 1 during the transformation of TCE and products to ethene.

Dehalogenating bacteria have been established to compete best for  $H_2$  at low concentrations<sup>90</sup>, so it is possible that OHRB were not adversely affected by the rapid consumption of  $H_2$  to low levels by other microbial populations. However, since the CE transformation was slow, formate was added to ensure excess  $H_2$  was present for consumption by OHRB. This inconsistent  $H_2$  level made further TCE additions impractical, but use of a substrate that is fermented more slowly, such as propionate, may have avoided this issue<sup>90</sup>.

Thus far,  $H_2$  data suggests that CT exposure results in dramatic inhibition of  $H_2$  consumption that is reversible for some  $H_2$ -consuming microbial populations. It is not clear whether the reversibility is due to removal of the 0.62  $\mu\text{M}$  CF and 1.4  $\mu\text{M}$  DCM present on day 49 or if there was already recovery potential on day 23 or later.  $H_2$  was not measured between day 23 and 49. Thus, it is possible that this apparent recovery would

occur irrespective of sparging the reactors. However, as shown for CF-exposed reactors (Figure 21), about 2.2  $\mu\text{M}$  CF present in reactors corresponded to the plateau of  $\text{H}_2$  at 10  $\mu\text{mol}$ . While only 0.62  $\mu\text{M}$  CF was present by day 49 in CT-exposed reactors, it is likely that CF removal via gas sparging allowed for the full  $\text{H}_2$  consumption observed. Acetate measurements were not made at this time, although they may have yielded insights regarding the productivity of any  $\text{H}_2$ -consuming acetogens in the culture. No further TCE additions were performed due to questions regarding OHRB access to rapidly consumed  $\text{H}_2$ . It is ultimately unclear if OHRB recovery is possible, but it did not occur in the time frame tested.

At the start of the recovery experiment (11) for CF-exposed reactors, CF concentration had dropped to 0.2  $\mu\text{M}$ , about one third of the concentration in CT exposed reactors discussed above. DCM was present at 2.5  $\mu\text{M}$ . After reactor sparging on day 49, TCE and formate were added on day 50. Subsequent CE transformation was rapid and complete within 0.5 day. Two further additions were made on day 56 and 60 with similar results. Figure 41 displays collected and modeled data for a representative reactor for each addition. Figure 42 displays associated modeled transformation rates for each TCE addition. Table 15 shows these rates for TCE additions on days 14, 50, 56, and 60, accompanied by p-values for Welch's t-tests comparing rates at days shown to day 50 rates.

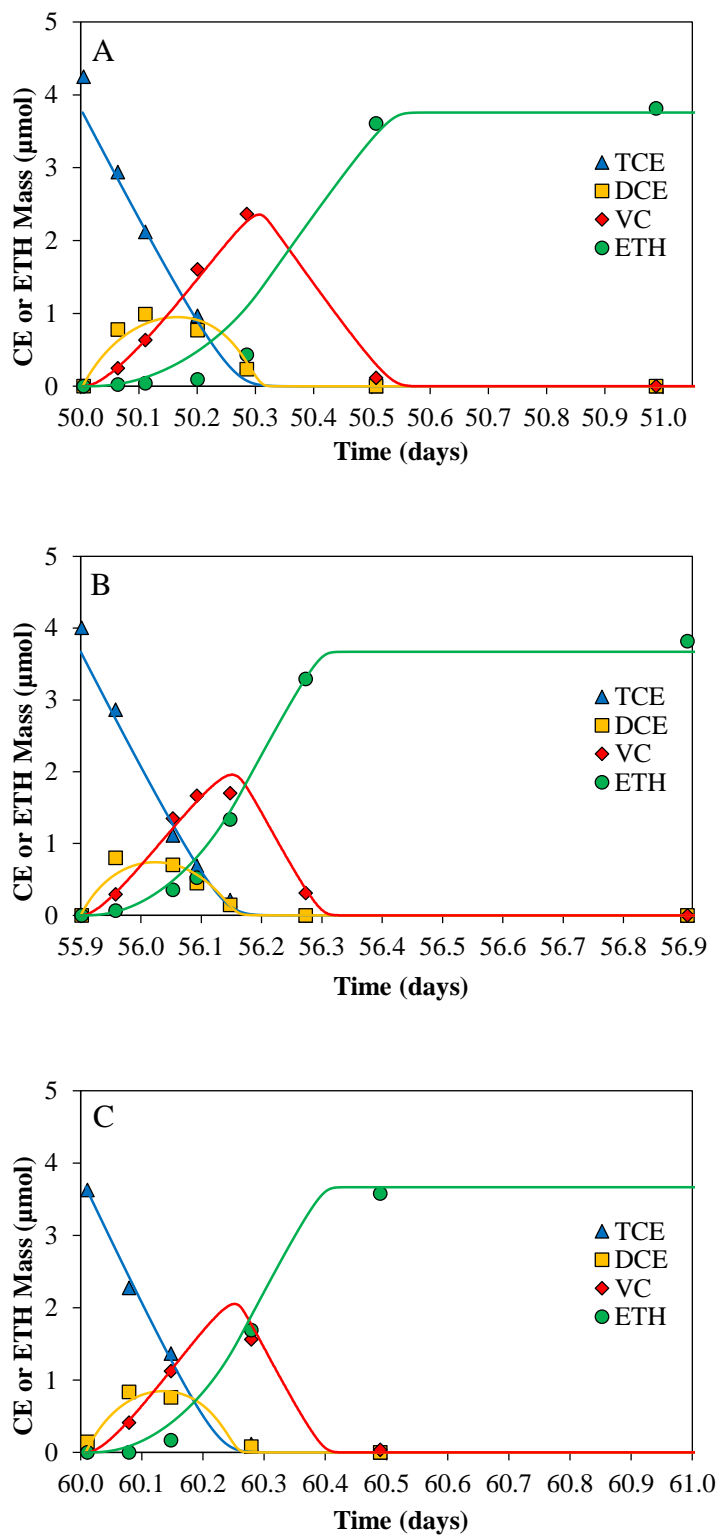


Figure 41. CF recovery days 50, 56, 60 TCE spikes and profiles. All similar, with complete transformation to ethene occurring in 0.5 days or less.

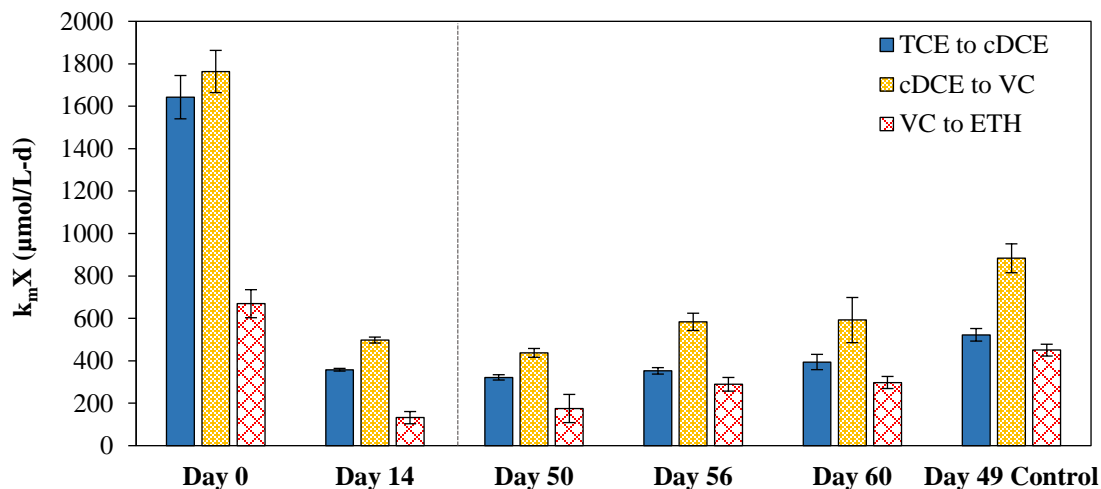


Figure 42. Modeled CE transformation rates occurring in CF exposed reactors at various times before and after sparging. The day 49 control symbolizes the 100% recovery scenario. Rates do not improve immediately after sparging, denoted by the vertical dotted line, however subsequent TCE additions result in similar CE rates each time. Error bars represent one sample standard deviation of triplicate (CF-exposed) or duplicate (control) reactors.

Table 15. Transformation Rates and Comparisons for Recovery Test of CF-Exposed Reactors from Experiment 4.

CE	Transformation Rate				T-test p-value*	
	Day 14	Day 50	Day 56	Day 60	Day 14	Day 60
TCE	358 ± 6.4	322 ± 12	353 ± 15	394 ± 36	0.022	0.061
cDCE	498 ± 14	437 ± 21	584 ± 41	592 ± 100	0.018	0.123
VC	132 ± 29	175 ± 66	289 ± 32	298 ± 28	0.386	0.069

\*Reported for Welch's t-test performed between rates from Day 50 and the Day listed.

In general, the rates for each CE are similar across times of exposure. This is visually apparent in the transformation profiles and bar graph. According to Welch's t-tests performed for CE rates between day 14 and 50, TCE and cDCE rates decreased by 10% (p-values < 0.05, Table 15), with the VC rate maintained. This is different from the CT reactors, for which day 50 rates were statistically the same as day 14 except for VC, which had decreased.

To determine if CE rates recovered between day 50 and 60, t-tests were performed to compare rates for these additions. As shown in Table 15, all p-values are greater than the common 0.05 confidence level, however the value of 0.06 is largely

inconclusive. This warrants further investigation of recovery potential for CF-exposed reactors, because it is likely that OHRB could recovery with longer time post-sparging. Thus, CF inhibition leads to toxicity, but it remains unclear whether this toxicity is reversible.

For each TCE/formate addition, resulting  $H_2$  was sufficient to support complete TCE transformation without additional formate. Figure 43A shows the production and consumption of  $H_2$  for the entire time period of the 3 separate TCE transformations. Consumption of  $H_2$  occurred more quickly with each addition, similar to behavior in CT-exposed recovery reactors, shown again in Figure 43B with the same time scale as CF exposed recovery reactors. The longer length of time required to reach complete  $H_2$  consumption after the first addition suggests a lag time in stimulation following the several weeks without substrate amendments. More  $H_2$  was required to maintain detectable levels in reactors that had experienced CT exposure, which suggests that non-OHRB were less inhibited by CT than OHRB, which seems to have experienced a toxicity from CT and/or its transformation. In reactors only inhibited by CF, OHRB were better able to be stimulated alongside other  $H_2$ -consumers and complete rapid TCE transformation. It is currently unknown if further additions could increase the CE transformation rates to control reactor rates and achieve full recovery.

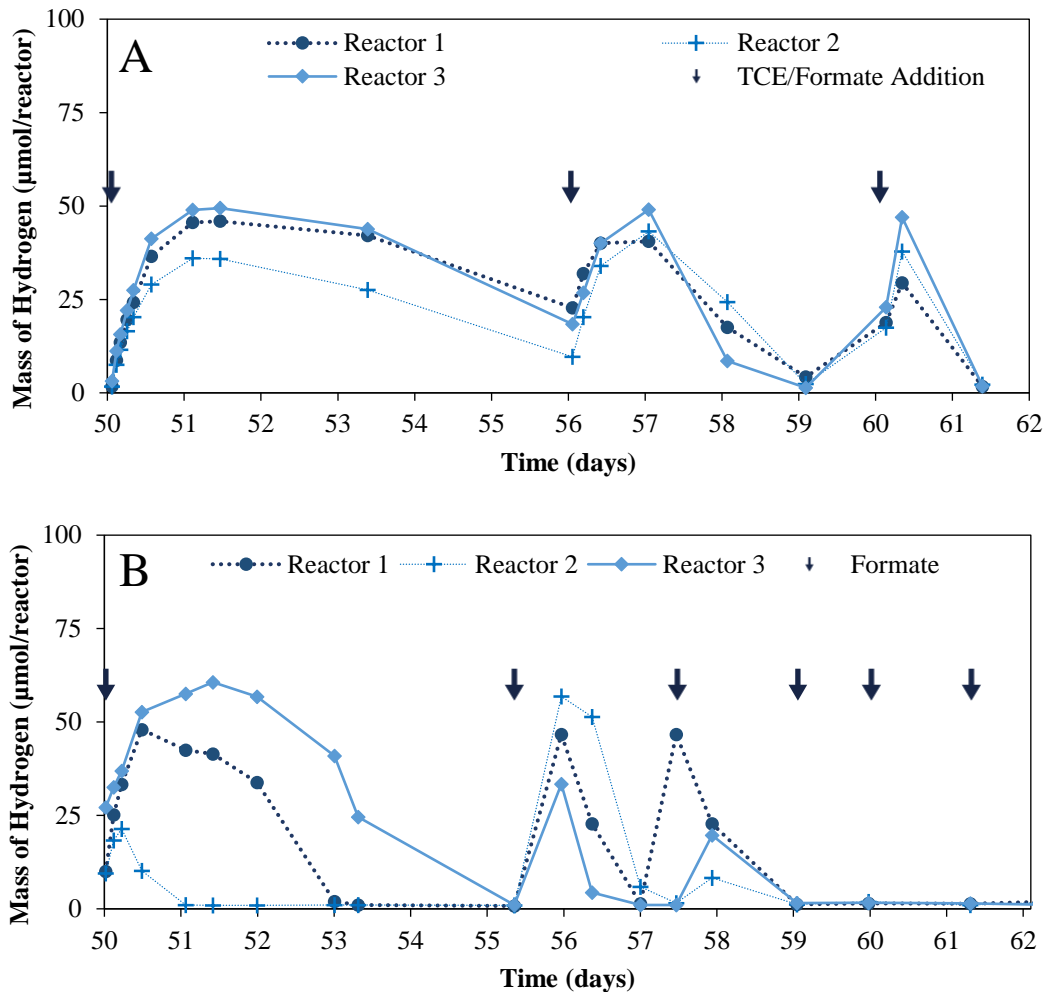


Figure 43. Same time scale H<sub>2</sub> profiles during recovery tests for Experiment 4 (Panel A, CF exposed) and Experiment 1 (Panel B, CT exposure). Consumption of H<sub>2</sub> faster in reactors originally exposed to CT.

Sparging reactors did not allow for CE rate recovery in CT or CF-exposed reactors. Thus, both inhibitors contribute toxicity to the systems evaluated. Exposure to CF – both as direct addition and as CT product – between 14 and 50 days had a minimal effect upon the CE transformation rates. This could be because of the relatively low CF concentrations in reactors at this time or could indicate an acclimation of OHRB to originally toxic levels of CF. Such acclimation has been reported for methanogens and sulfate-reducing bacteria<sup>119,120,126</sup>. It remains unclear whether rate recovery would be observed at longer time points after sparging. Thus, the reversibility of CT and CF toxicity is unknown as of yet.

At the time of writing, the author is aware of only two studies that have evaluated the recovery of microbial activity after CM exposure, and of these, only CF was tested. In a methanogenic culture, CF (50 or 200 mg/L) was removed after either 1 or 24 hours of exposure by exchanging the bottle supernatant<sup>119</sup>. Acetate consumption and methane production were compared between bottles with original supernatant and exchanged (no CF) supernatant. The initiation of methane production was delayed in bottles exposed to CF, but gas production rates eventually reached uninhibited levels, indicating full recovery.

In OHRB systems, the thesis of Kai Wei describes recovery of the KB-1 OHRB culture after 15-20 days of exposure to 230-250  $\mu\text{M}$  CF<sup>124</sup>. Minimal or no OHR of TCE, cDCE, and VC occurred during CF exposure, and CF was not transformed. After sparging the reactors with a  $\text{H}_2/\text{CO}_2$  mixed gas, OHR potential was evaluated. Additions of cDCE, and VC were transformed after a lag period of 20-40 days. TCE transformation began after about 5 days. Only one addition post-sparging occurred, so improvement over time was not assessed. Taken with the current study, these data demonstrate the need for further experimentation regarding OHRB recovery from CM exposure.

## CHAPTER 5 – CONCLUSIONS

Time-dependent inhibition of CE transformation was established using OHRB batch reactors exposed to CT and CF. CE transformation rates decreased with time of exposure to either inhibitor; however, differences in CE transformation and H<sub>2</sub> consumption were identified for CT and CF exposed reactors. The CT-related inhibition slowed all 3 transformation steps in the TCE OHR pathway within 1 day of CT addition, as demonstrated by similar CE transformation rates after day 1, day 2, and day 14 exposures. VC transformation was slowed as early as 0.2 days after the initial exposure. Rates for TCE, cDCE, and VC were reduced by an order of magnitude after 1 day of exposure (by 75, 62, 95%, respectively, from control). This represented the majority of the rate decrease observed in this study, which did not recover after CT completely transformed. H<sub>2</sub> consumption was inhibited, as indicated by the build up of 50% of the H<sub>2</sub> supplied for each addition.

In contrast, rate reduction was more gradual in reactors with CF initially added at twice the maximum concentration achieved in CT reactors. After 14 days of exposure to CF and its transformation, CE transformation rates were still 2.6, 3, and 13 times greater than rates observed in CT-exposed reactors over the same time period. H<sub>2</sub> levels were depleted to 10% of the available supply by day 14 by the microbial community, indicating less H<sub>2</sub> inhibition due to the presence of CF without CT. Thus, this work indicated that CT-related inhibition was not due to its CF product alone. Further, since the CT-exposed rates did not improve after complete CT transformation, a more permanent, toxicity was indicated, resulting in a more significant rate inhibition that observed in CF-exposed reactors.

CT toxicity was evaluated further with experiments at higher exposure concentrations and multiple delivery. Tripling the initial CT exposure concentration resulted in slower CE transformation, with day 14 TCE, cDCE, and VC rates decreased from controls by 95, 95, and 99%, respectively. HiCT rates were 2-3 times smaller than 2.3 μM CT exposure rates on day 14. However, rates did not slow proportionally to the increase of CT exposure. In experiments with multiple CT additions, an equal mass of CT

addition was found to decrease transformation rates by a similar amount, regardless of initial CT concentration. Day 2 CE transformation rates were similar in reactors receiving 0.3  $\mu\text{mol}$  CT in a single addition or divided into several additions, with p-values above 0.06 in a Welch's t-test. Together, the concentration and transformed mass experiments indicate that CT-related inhibition or toxicity is affected by the amount of CT transformed.

Because CT and its transformation intermediate, the trichloromethyl radical, have been proposed to interact with the cobalt atom of essential corrinoid cofactors, vitamin B12 (15 mg/L; 11  $\mu\text{M}$ ) was amended to cultures 3 days prior to CT exposure to test the cobalamin as a potential protectant against CT-related inhibition. On day 5, after 2 days of CT transformation (assumed complete), CE transformation was assessed. Relative to unamended reactors exposed to CT, only VC transformation was appreciably faster, by a factor of 3. However,  $\text{H}_2$  consumption was significantly enhanced in B12-amended reactors, which indicated B12-related improvement of OHRB community function.

Batch reactors purged of volatile compounds 7 weeks after CM additions were unable to regain control-type CE transformation rates in the time frame tested. CF exposed reactors maintained rates similar to those obtained on day 14 after 3 TCE additions, consumption of the day 50  $\text{H}_2$  supply was slower than for subsequent additions. Similarly, CT-exposed reactors also maintained rates similar to day 14; however, during the 17-day CE transformation, a total of 1000  $\mu\text{mol}$  of theoretical  $\text{H}_2$  was consumed, indicating a potential recovery of  $\text{H}_2$  consumption during this time period. Thus, recovery potential was not confirmed in either CT-exposed or CF exposed reactors. This demonstrates that both compounds exert permanent, potentially irreversible toxicity on the OHRB community, although results indicated that CT has a more potent impact.

This work led to the following conclusions regarding inhibition and toxicity by CT and CF on OHRB:

- CT exerts a stronger toxicity upon OHRB than CF, measurable by early time CE transformation rate reductions and 50% inhibition of  $\text{H}_2$  consumption, both sustained after CT transformation is complete.

- CF is not primarily responsible for the CT-related inhibition of CE transformation and H<sub>2</sub> consumption, but it does exert inhibition or toxicity upon OHRB with an early time effect that most dramatically reduces TCE and cDCE rates.
- CT exerts toxicity on the OHRB that is dependent both on the CT concentration present and the mass of CT transformed in the system.
- Mitigation of CT toxicity by vitamin B12 may be possible. At the conditions tested, H<sub>2</sub> consumption was dramatically increased, but only the VC transformation rate showed potential for slight improvement.
- VC-respiring *D. mccartyi* are apparently more sensitive to CT exposure and B12 amendment than TCE- and cDCE-respiring populations.

## CHAPTER 6 – FUTURE WORK

This work could be furthered with multiple approaches. Sections 1-4 could be expanded with experiments at multiple inhibitor concentrations. Chemostat-level toxicity experiments could yield insight regarding the ability of the Evanite culture to acclimation to various concentrations of CT or CF, which would have implicates for field sites.

A series of approaches could inform questions from Section 5. To further clarify the mechanism of CT toxicity, the presence and toxicity of the trichloromethyl radical could be evaluated with the use of a radical trap, as was used by McCormick and Adriaens<sup>12</sup>. Molecular approaches, such as the use of real-time RNA sequencing of RDase-encoding genes would yield insight regarding active microbial populations along the time frame of CM exposure. Live-dead cell staining techniques would clarify whether CT-related toxicity causes cell inactivation or death. To be certain that DCM and CS<sub>2</sub> do not contribute inhibition or toxicity to OHRB, batch tests with direct addition of both should be performed. This was not a concern in the current project since the majority of inhibition occurred at early time before these compounds reached their maximum, or in some cases, were detected at all.

Section 5 Vitamin B12 amendment experiments should be repeated to confirm reproducibility and be expanded to incorporate CM and B12 real-time measurements with an ECD and spectrophotometer, respectively. Additional experiments with B12 concentration ranges could identify the optimal supply for CE rate enhancement under CT-exposure. Further cobamide investigations should include the amendment of lower ligand bases such as DMB, which can be used in *D. mccartyi* corrinoid remodeling<sup>80,86</sup>.

Because recovery experiments were largely inconclusive regarding the reversibility of CT and CF toxicity, future work should aim to better characterize this potential. Sparging CT and CF from reactors at exposure times near to the time at which the majority of inhibition is observed and during times of high CT and CF concentrations would help inform these studies. Additional TCE additions after sparging at increasing lengths of time from sparging may provide more convincing rate increase data and thus a more comprehensive picture of recovery potential. In the case of no recovery,

bioaugmentation may be implemented and optimized to inform remediation decisions. Use of a slow-release substrate such as propionate may also allow for more consistent H<sub>2</sub> supply to the OHRB.

Finally, advances in modeling approaches should involve expanding the Multi-Fit Monod model to incorporate inhibition and toxicity of CT and CF. Initial efforts might add a time dependent expression for biomass, X, to describe its decrease coupled with CT transformation. This type of approach is similar to the concept of transformation capacity, modeled for cometabolically active methanotrophic cells by Alvarez-Cohen and McCarty<sup>125</sup>. Instead of transformation capacity, however, changes in X would be related to the toxicity of CT through an empirically determined constant such as “toxicity capacity” of CT, with units of OHRB biomass per CT mass.

## BIBLIOGRAPHY

- (1) Adrian, L.; Löffler, F. E. Organohalide-respiring bacteria—an introduction. In *Organohalide-Respiring Bacteria*; Springer, Berlin, Heidelberg, 2016; pp 3–6.
- (2) Lee, M.; Marquis, C.; Judger, B.-E.; Manefield, M. Anaerobic microorganisms and bioremediation of organohalide pollution. *Microbiol. Aust.* **2015**, *36* (3), 125–128.
- (3) Vogel, T. M.; Criddle, C. S.; McCarty, P. L. Transformations of halogenated aliphatic compounds. *Crit. Rev. Environ. Sci. Technol.* **1987**, *21* (8), 722–736.
- (4) US EPA, O. Superfund: National Priorities List (NPL) <https://www.epa.gov/superfund/superfund-national-priorities-list-npl> (accessed Sep 3, 2017).
- (5) Löffler, F. E.; Yan, J.; Ritalahti, K. M.; Adrian, L.; Edwards, E. A.; Konstantinidis, K. T.; Müller, J. A.; Fullerton, H.; Zinder, S. H.; Spormann, A. M. *Dehalococcoides mccartyi* gen. nov., sp. nov., obligately organohalide-respiring anaerobic bacteria relevant to halogen cycling and bioremediation, belong to a novel bacterial class, *Dehalococcoidia* classis nov., order *Dehalococcoidales* ord. nov. and family *Dehalococcoidaceae* fam. nov., within the phylum *Chloroflexi*. *Int. J. Syst. Evol. Microbiol.* **2013**, *63* (2), 625–635.
- (6) Stroo, H. F.; Ward, C. H. *In situ remediation of chlorinated solvent plumes*; Stroo, H. F., Ward, C. H., Eds.; SERDP/ESTCP Environmental Remediation Technology; Springer New York: New York, NY, 2010.
- (7) Azizian, M. F.; Semprini, L. Simultaneous anaerobic transformation of carbon tetrachloride to carbon dioxide and tetrachloroethene to ethene in a continuous flow column. *J. Contam. Hydrol.* **2017**, *203*, 93–103.
- (8) Chiu, P.-C.; Reinhard, M. Transformation of carbon tetrachloride by reduced vitamin B12 in aqueous cysteine solution. *Environ. Sci. Technol.* **1996**, *30* (6), 1882–1889.
- (9) Criddle, C. S.; McCarty, P. L. Electrolytic model system for reductive dehalogenation in aqueous environments. *Env. Sci Technol* **1991**, *25* (5), 973–978.
- (10) Hashsham, S. A.; Freedman, D. L. Enhanced biotransformation of carbon tetrachloride by *Acetobacterium woodii* upon addition of hydroxocobalamin and fructose. *Appl. Environ. Microbiol.* **1999**, *65* (10), 4537–4542.
- (11) Hashsham, S. A.; Scholze, R.; Feedman, D. L. Cobalamin-enhanced anaerobic biotransformation of carbon tetrachloride. *Environ. Sci. Technol.* **1995**, *29* (11), 2856–2863.
- (12) McCormick, M. L.; Adriaens, P. Carbon tetrachloride transformation on the surface of nanoscale biogenic magnetite particles. *Environ. Sci. Technol.* **2004**, *38* (4), 1045–1053.
- (13) Workman, D. J.; Woods, S. L.; Gorby, Y. A.; Fredrickson, J. K.; Truex, M. J. Microbial reduction of vitamin B12 by *Shewanella alga* strain BrY with subsequent transformation of carbon tetrachloride. *Environ. Sci. Technol.* **1997**, *31* (8), 2292–2297.

- (14) ATSDR. ATSDR- toxicological profile: chloroform  
<https://www.atsdr.cdc.gov/ToxProfiles/TP.asp?id=53&tid=16> (accessed Sep 4, 2017).
- (15) ATSDR. ATSDR - toxicological profile: vinyl chloride  
<https://www.atsdr.cdc.gov/toxprofiles/TP.asp?id=282&tid=51> (accessed Mar 3, 2017).
- (16) Adamson, D. T.; Parkin, G. F. Impact of mixtures of chlorinated aliphatic hydrocarbons on a high-rate, tetrachloroethene-dechlorinating enrichment culture. *Environ. Sci. Technol.* **2000**, *34* (10), 1959–1965.
- (17) Bagley, D. M.; Lalonde, M.; Kaseros, V.; Stasiuk, K. E.; Sleep, B. E. Acclimation of anaerobic systems to biodegrade tetrachloroethene in the presence of carbon tetrachloride and chloroform. *Water Res.* **2000**, *34* (1), 171–178.
- (18) Wei, K.; Grostern, A.; Chan, W. W. M.; Richardson, R. E.; Edwards, E. A. Electron acceptor interactions between organohalide-respiring bacteria: Cross-feeding, competition, and inhibition. In *Organohalide-respiring bacteria*; Adrian, L., Löffler, F. E., Eds.; Springer Berlin Heidelberg: Berlin, Heidelberg, 2016; pp 283–308.
- (19) Gupta, M.; Gupta, A.; Suidan, M. T.; Sayles, G. D. Biotransformation rates of chloroform under anaerobic conditions—II. Sulfate reduction. *Water Res.* **1996**, *30* (6), 1387–1394.
- (20) Koenig, J. C.; Groissmeier, K. D.; Manefield, M. J. Tolerance of anaerobic bacteria to chlorinated solvents. *Microbes Environ.* **2014**, *29* (1), 23–30.
- (21) Scholten, J. C. M.; Conrad, R.; Stams, A. J. M. Effect of 2-bromo-ethane sulfonate, molybdate and chloroform on acetate consumption by methanogenic and sulfate-reducing populations in freshwater sediment. *FEMS Microbiol. Ecol.* **2000**, *32* (1), 35–42.
- (22) Ghambeer, R. K.; Wood, H. G.; Schulman, M.; Ljungdahl, L. Total synthesis of acetate from CO<sub>2</sub>. *Arch. Biochem. Biophys.* **1971**, *143* (2), 471–484.
- (23) Justicia-Leon, S. D.; Ritalahti, K. M.; Mack, E. E.; Löffler, F. E. Dichloromethane fermentation by a *Dehalobacter* sp. in an enrichment culture derived from pristine river sediment. *Appl. Environ. Microbiol.* **2012**, *78* (4), 1288–1291.
- (24) Kaseros, V. B.; Sleep, B. E.; Bagley, D. M. Column studies of biodegradation of mixtures of tetrachloroethene and carbon tetrachloride. *Water Res.* **2000**, *34* (17), 4161–4168.
- (25) Koenig, J. C.; Lee, M. J.; Manefield, M. Successful microcosm demonstration of a strategy for biodegradation of a mixture of carbon tetrachloride and perchloroethene harnessing sulfate reducing and dehalorespiring bacteria. *J. Hazard. Mater.* **2012**, *219–220*, 169–175.
- (26) Vickstrom, K. E.; Azizian, M. F.; Semprini, L. Transformation of carbon tetrachloride and chloroform by trichloroethene respiring anaerobic mixed cultures and supernatant. *Chemosphere* **2017**, *182*, 65–75.
- (27) Yu, Z.; Smith, G. B. Inhibition of methanogenesis by C1- and C2-polychlorinated aliphatic hydrocarbons. *Environ. Toxicol. Chem.* **2000**, *19* (9), 2212–2217.

- (28) USGS. USGS: Groundwater Use in the United States <https://water.usgs.gov/watuse/wugw.html> (accessed Mar 3, 2017).
- (29) Doherty, R. E. A history of the production and use of carbon tetrachloride, tetrachloroethylene, trichloroethylene and 1,1,1-trichloroethane in the United States: Part 1--historical background; carbon tetrachloride and tetrachloroethylene. *Environ. Forensics* **2000**, *1* (2), 69–81.
- (30) Doherty, R. E. A history of the production and use of carbon tetrachloride, tetrachloroethylene, trichloroethylene and 1,1,1-trichloroethane in the United States: Part 2--trichloroethylene and 1,1,1-trichloroethane. *Environ. Forensics* **2000**, *1* (2), 83–93.
- (31) McCulloch, A. Chloroform in the environment: occurrence, sources, sinks and effects. *Chemosphere* **2003**, *50* (10), 1291–1308.
- (32) Adriaens, P.; Alvarez, P. J. J.; Bastiaans, L.; Diels, L.; Major, D.; Filip, Z.; Springael, D. Biodegradation and bioremediation. In *Innovative approaches to the on-site assessment and remediation of contaminated sites*; NATO Science Series; Springer, Dordrecht, 2002; pp 67–113.
- (33) Bradley, P. M. History and ecology of chloroethene biodegradation: A review. *Bioremediation J.* **2003**, *7* (2), 81–109.
- (34) National Research Council. *Alternatives for managing the nation's complex contaminated groundwater sites*; National Academies Press: Washington, D.C., 2013.
- (35) US EPA, O. Engineered approaches to *in situ* bioremediation of chlorinated solvents: fundamentals and field applications <https://www.epa.gov/remedytech/engineered-approaches-situ-bioremediation-chlorinated-solvents-fundamentals-and-field> (accessed Mar 20, 2017).
- (36) Westrick, J. J.; Mello, J. W.; Thomas, R. F. The groundwater supply survey. *J. Am. Water Works Assoc.* **1984**, *76* (5), 52–59.
- (37) National Research Council. *Groundwater and soil cleanup: Improving management of persistent contaminants.*; National Academies Press: Washington, 1999.
- (38) Government Accountability Office. *DOD uses and develops a range of remediation technologies to clean up military sites*; Groundwater Contamination; Highlights 05-666; 2005.
- (39) US EPA, O. Superfund enforcement: 35 years of protecting communities and the environment <https://www.epa.gov/enforcement/superfund-enforcement-35-years-protecting-communities-and-environment> (accessed Sep 6, 2017).
- (40) Pankow, J. F.; Cherry, J. A. *Dense chlorinated solvents and other DNAPLs in groundwater: history, behavior, and remediation*; Waterloo Press, 1996.
- (41) Ward, C. H.; Hughes, J. B.; Pope, G. A.; Delshad, M.; Dwaranath, V.; Spain, J.; Nishino, S.; Fruchter, J. S.; Vermeul, V. R.; Williams, M. D.; et al. In-situ treatment technologies. In *Innovative approaches to the on-site assessment and remediation of contaminated sites*; NATO Science Series; Springer, Dordrecht, 2002; pp 183–216.

- (42) McCarty, P. L.; Reinhard, M. Biological and chemical transformations of halogenated aliphatic compounds in aquatic and terrestrial environments. In *Biogeochemistry of Global Change*; Springer, 1993; pp 839–852.
- (43) Koenig, J.; Lee, M.; Manefield, M. Aliphatic organochlorine degradation in subsurface environments. *Rev. Environ. Sci. Biotechnol.* **2015**, *14* (1), 49–71.
- (44) Staudinger, J.; Roberts, P. V. A critical compilation of Henry's law constant temperature dependence relations for organic compounds in dilute aqueous solutions. *Chemosphere* **2001**, *44* (4), 561–576.
- (45) Gossett, J. M. Measurement of Henry's law constants for C1 and C2 chlorinated hydrocarbons. *Environ. Sci. Technol.* **1987**, *21* (2), 202–208.
- (46) Schnoor, J. L. *Environmental modeling: fate and transport of pollutants in water, air, and soil*; J. Wiley, 1996.
- (47) ATSDR. Substance Priority List | ATSDR <https://www.atsdr.cdc.gov/spl/index.html> (accessed Sep 3, 2017).
- (48) US EPA, O. National primary drinking water regulations <https://www.epa.gov/ground-water-and-drinking-water/national-primary-drinking-water-regulations> (accessed Sep 3, 2017).
- (49) ATSDR. ATSDR - toxicological profile: 1,2-dichloroethene <https://www.atsdr.cdc.gov/toxprofiles/TP.asp?id=464&tid=82> (accessed Sep 4, 2017).
- (50) ATSDR. ATSDR- toxicological profile: methylene chloride <https://www.atsdr.cdc.gov/toxprofiles/tp.asp?id=234&tid=42> (accessed Sep 4, 2017).
- (51) ATSDR. ATSDR - toxicological profile: carbon tetrachloride <https://www.atsdr.cdc.gov/ToxProfiles/TP.asp?id=196&tid=35> (accessed Sep 4, 2017).
- (52) ATSDR. ATSDR - toxicological profile: tetrachloroethylene (perc) <https://www.atsdr.cdc.gov/ToxProfiles/TP.asp?id=265&tid=48> (accessed Sep 4, 2017).
- (53) ATSDR. ATSDR- toxicological profile: trichloroethylene (tce) <https://www.atsdr.cdc.gov/toxprofiles/TP.asp?id=173&tid=30> (accessed Mar 3, 2017).
- (54) US EPA, O. How EPA regulates drinking water contaminants <https://www.epa.gov/dwregdev/how-epa-regulates-drinking-water-contaminants> (accessed Sep 4, 2017).
- (55) Stroo, H. F. Remedial technology selection for chlorinated solvent plumes. In *In situ remediation of chlorinated solvent plumes*; SERDP/ESTCP Environmental Remediation Technology; Springer, New York, NY, 2010; pp 281–307.
- (56) EPA. Introduction to *in situ* bioremediation of groundwater. **2013**.
- (57) Freedman, D. L.; Gossett, J. M. Biological reductive dechlorination of tetrachloroethylene and trichloroethylene to ethylene under methanogenic conditions. *Appl. Environ. Microbiol.* **1989**, *55* (9), 2144–2151.
- (58) Fincker, M.; Spormann, A. M. Biochemistry of catabolic reductive dehalogenation. *Annu. Rev. Biochem.* **2017**, *86* (1).

- (59) Lee, M. D.; Odom, J. M.; Jr, R. J. B. New perspectives on microbial dehalogenation of chlorinated solvents: Insights from the field. *Annu. Rev. Microbiol.* **1998**, *52* (1), 423–452.
- (60) McCarty, P. L.; Ellis, D. E. Natural attenuation. In *Innovative approaches to the on-site assessment and remediation of contaminated sites*; NATO Science Series; Springer, Dordrecht, 2002; pp 141–181.
- (61) Tiehm, A.; Schmidt, K. R. Sequential anaerobic/aerobic biodegradation of chloroethenes—aspects of field application. *Curr. Opin. Biotechnol.* **2011**, *22* (3), 415–421.
- (62) Atashgahi, S.; Lu, Y.; Smidt, H. Overview of known organohalide-respiring bacteria—Phylogenetic diversity and environmental distribution. In *Organohalide-respiring bacteria*; Springer, Berlin, Heidelberg, 2016; pp 63–105.
- (63) Maillard, J.; Holliger, C. The genus *Dehalobacter*. In *Organohalide-respiring bacteria*; Springer, Berlin, Heidelberg, 2016; pp 153–171.
- (64) Futagami, T.; Furukawa, K. The genus *Desulfitobacterium*. In *Organohalide-respiring bacteria*; Springer, Berlin, Heidelberg, 2016; pp 173–207.
- (65) Goris, T.; Diekert, G. The genus *Sulfurospirillum*. In *Organohalide-respiring bacteria*; Springer, Berlin, Heidelberg, 2016; pp 209–234.
- (66) Sanford, R. A.; Chowdhary, J.; Löffler, F. E. Organohalide-respiring *Deltaproteobacteria*. In *Organohalide-respiring bacteria*; Springer, Berlin, Heidelberg, 2016; pp 235–258.
- (67) Zinder, S. H. The genus *Dehalococcoides*. In *Organohalide-respiring bacteria*; Springer, Berlin, Heidelberg, 2016; pp 107–136.
- (68) McCarty, P. L. Discovery of organohalide-respiring processes and the bacteria involved. In *Organohalide-respiring bacteria*; Springer, Berlin, Heidelberg, 2016; pp 51–62.
- (69) DiStefano, T. D.; Gossett, J. M.; Zinder, S. H. Reductive dechlorination of high concentrations of tetrachloroethene to ethene by an anaerobic enrichment culture in the absence of methanogenesis. *Appl. Environ. Microbiol.* **1991**, *57* (8), 2287–2292.
- (70) Maymó-Gatell, X.; Chien, Y.; Gossett, J. M.; Zinder, S. H. Isolation of a bacterium that reductively dechlorinates tetrachloroethene to ethene. *Science* **1997**, *276* (5318), 1568–1571.
- (71) Cupples, A. M.; Spormann, A. M.; McCarty, P. L. Growth of a *Dehalococcoides*-like microorganism on vinyl chloride and cis-dichloroethene as electron acceptors as determined by competitive PCR. *Appl. Environ. Microbiol.* **2003**, *69* (2), 953–959.
- (72) He, J.; Ritalahti, K. M.; Yang, K.-L.; Koenigsberg, S. S.; Löffler, F. E. Detoxification of vinyl chloride to ethene coupled to growth of an anaerobic bacterium. *Nature* **2003**, *424* (6944), 62–65.
- (73) Mayer-Blackwell, K.; Azizian, M. F.; Green, J. K.; Spormann, A. M.; Semprini, L. Survival of vinyl chloride respiring *Dehalococcoides mccartyi* under long-term electron donor limitation. *Environ. Sci. Technol.* **2017**.
- (74) Seth, E. C.; Taga, M. E. Nutrient cross-feeding in the microbial world. *Front. Microbiol.* **2014**, *5*.

- (75) Richardson, R. E. Organohalide-respiring bacteria as members of microbial communities: Catabolic food webs and biochemical interactions. In *Organohalide-respiring bacteria*; Springer, Berlin, Heidelberg, 2016; pp 309–341.
- (76) Banerjee, R.; Ragsdale, and S. W. The many faces of vitamin B12: Catalysis by cobalamin-dependent enzymes. *Annu. Rev. Biochem.* **2003**, *72* (1), 209–247.
- (77) Yan, J.; Im, J.; Yang, Y.; Löffler, F. E. Guided cobalamin biosynthesis supports *Dehalococcoides mccartyi* reductive dechlorination activity. *Phil Trans R Soc B* **2013**, *368* (1616), 20120320.
- (78) Moore, T. C.; Escalante-Semerena, J. C. Corrinoid metabolism in dehalogenating pure cultures and microbial communities. In *Organohalide-respiring bacteria*; Springer, Berlin, Heidelberg, 2016; pp 455–484.
- (79) Wagner, D. D.; Hug, L. A.; Hatt, J. K.; Spitzmiller, M. R.; Padilla-Crespo, E.; Ritalahti, K. M.; Edwards, E. A.; Konstantinidis, K. T.; Löffler, F. E. Genomic determinants of organohalide-respiration in *Geobacter lovleyi*, an unusual member of the *Geobacteraceae*. *BMC Genomics* **2012**, *13*, 200.
- (80) Yan, J.; Ritalahti, K. M.; Wagner, D. D.; Löffler, F. E. Unexpected specificity of interspecies cobamide transfer from *Geobacter* spp. to organohalide-respiring *Dehalococcoides mccartyi* strains. *Appl. Environ. Microbiol.* **2012**, *78* (18), 6630–6636.
- (81) He, J.; Holmes, V. F.; Lee, P. K. H.; Alvarez-Cohen, L. Influence of vitamin B12 and cocultures on the growth of *Dehalococcoides* isolates in defined medium. *Appl. Environ. Microbiol.* **2007**, *73* (9), 2847–2853.
- (82) Stupperich, E.; Eisinger, H. J.; Kräutler, B. Diversity of corrinoids in acetogenic bacteria. *Eur. J. Biochem.* **1988**, *172* (2), 459–464.
- (83) Men, Y.; Lee, P.; Harding, K.; Alvarez-Cohen, L. Characterization of four TCE-dechlorinating microbial enrichments grown with different cobalamin stress and methanogenic conditions. *Appl. Microbiol. Biotechnol.* **2013**, *97* (14), 6439–6450.
- (84) Tanner, R. S.; Wolfe, R. S.; Ljungdahl, L. G. Tetrahydrofolate enzyme levels in *Acetobacterium woodii* and their implication in the synthesis of acetate from CO<sub>2</sub>. *J. Bacteriol.* **1978**, *134* (2), 668–670.
- (85) Seshadri, R.; Adrian, L.; Fouts, D. E.; Eisen, J. A.; Phillippy, A. M.; Methe, B. A.; Ward, N. L.; Nelson, W. C.; Deboy, R. T.; Khouri, H. M.; et al. Genome sequence of the PCE-dechlorinating bacterium *Dehalococcoides ethenogenes*. *Science* **2005**, *307* (5706), 105–108.
- (86) Men, Y.; Seth, E. C.; Yi, S.; Crofts, T. S.; Allen, R. H.; Taga, M. E.; Alvarez-Cohen, L. Identification of specific corrinoids reveals corrinoid modification in dechlorinating microbial communities. *Environ. Microbiol.* **2015**, *17* (12), 4873–4884.
- (87) Diekert, G.; Wohlfarth, G. Metabolism of homoacetogens. *Antonie Van Leeuwenhoek* **1994**, *66* (1–3), 209–221.
- (88) Zeikus, J. G.; Kerby, R.; Krzycki, J. A. Single-carbon chemistry of acetogenic and methanogenic bacteria. *Science* **1985**, *227* (4691), 1167–1173.

- (89) Ballapragada, B. S.; Stensel, H. D.; Puhakka, J. A.; Ferguson, J. F. Effect of hydrogen on reductive dechlorination of chlorinated ethenes. *Environ. Sci. Technol.* **1997**, *31* (6), 1728–1734.
- (90) Yang, Y.; McCarty, P. L. Competition for hydrogen within a chlorinated solvent dehalogenating anaerobic mixed culture. *Environ. Sci. Technol.* **1998**, *32* (22), 3591–3597.
- (91) Aulenta, F.; Majone, M.; Tandoi, V. Enhanced anaerobic bioremediation of chlorinated solvents: Environmental factors influencing microbial activity and their relevance under field conditions. *J. Chem. Technol. Biotechnol.* **2006**, *81* (9), 1463–1474.
- (92) Chiu, P.-C.; Reinhard, M. Metallocoenzyme-mediated reductive transformation of carbon tetrachloride in titanium(III) citrate aqueous solution. *Environ. Sci. Technol.* **1995**, *29* (3), 595–603.
- (93) Lewis, T. A.; Morra, M. J.; Brown, P. D. Comparative product analysis of carbon tetrachloride dehalogenation catalyzed by cobalt corrins in the presence of thiol or titanium(III) reducing agents. *Environ. Sci. Technol.* **1996**, *30* (1), 292–300.
- (94) Tanaka, K. Abiotic degradation of tetrachloromethane in anaerobic culture media. *J. Ferment. Bioeng.* **1997**, *83* (1), 118–120.
- (95) Criddle, C. S.; DeWitt, J. T.; Grbić-Galić, D.; McCarty, P. L. Transformation of carbon tetrachloride by *Pseudomonas* sp. strain KC under denitrification conditions. *Appl. Environ. Microbiol.* **1990**, *56* (11), 3240–3246.
- (96) Lewis, T. A.; Crawford, R. L. Transformation of carbon tetrachloride via sulfur and oxygen substitution by *Pseudomonas* sp. strain KC. *J. Bacteriol.* **1995**, *177* (8), 2204–2208.
- (97) Egli, C.; Tschan, T.; Scholtz, R.; Cook, A. M.; Leisinger, T. Transformation of tetrachloromethane to dichloromethane and carbon dioxide by *Acetobacterium woodii*. *Appl. Environ. Microbiol.* **1988**, *54* (11), 2819–2824.
- (98) Bouwer, E. J.; McCarty, P. L. Transformations of 1- and 2-carbon halogenated aliphatic organic compounds under methanogenic conditions. *Appl. Environ. Microbiol.* **1983**, *45* (4), 1286–1294.
- (99) McCormick, M. L.; Bouwer, E. J.; Adriaens, P. Carbon tetrachloride transformation in a model iron-reducing culture: Relative kinetics of biotic and abiotic reactions. *Environ. Sci. Technol.* **2002**, *36* (3), 403–410.
- (100) Best, J. H. de; Salminen, E.; Doddema, H. J.; Janssen, D. B.; Harder, W. Transformation of carbon tetrachloride under sulfate reducing conditions. *Biodegradation* **1997**, *8* (6), 429–436.
- (101) Egli, C.; Scholtz, R.; Cook, A. M.; Leisinger, T. Anaerobic dechlorination of tetrachloromethane and 1,2-dichloroethane to degradable products by pure cultures of *Desulfobacterium* sp. and *Methanobacterium* sp. *FEMS Microbiol. Lett.* **1987**, *43* (3), 257–261.
- (102) Shan, H.; Kurtz Jr., H. D.; Freedman, D. L. Evaluation of strategies for anaerobic bioremediation of high concentrations of halomethanes. *Water Res.* **2010**, *44* (5), 1317–1328.
- (103) Marshall, I. P. G.; Azizian, M. F.; Semprini, L.; Spormann, A. M. Inferring community dynamics of organohalide-respiring bacteria in chemostats by

- covariance of *rdhA* gene abundance. *FEMS Microbiol. Ecol.* **2014**, *87* (2), 428–440.
- (104) Mayer-Blackwell, K.; Azizian, M. F.; Machak, C.; Vitale, E.; Carpani, G.; de Ferra, F.; Semprini, L.; Spormann, A. M. Nanoliter qPCR platform for highly parallel, quantitative assessment of reductive dehalogenase genes and populations of dehalogenating microorganisms in complex environments. *Environ. Sci. Technol.* **2014**, *48* (16), 9659–9667.
- (105) Yu, S.; Semprini, L. Kinetics and modeling of reductive dechlorination at high PCE and TCE concentrations. *Biotechnol. Bioeng.* **2004**, *88* (4), 451–464.
- (106) Assaf-Anid, N.; Hayes, K. F.; Vogel, T. M. Reduction dechlorination of carbon tetrachloride by cobalamin (II) in the presence of dithiothreitol: mechanistic study, effect of redox potential and pH. *Environ. Sci. Technol.* **1994**, *28* (2), 246–252.
- (107) Kriegman-King, M. R.; Reinhard, M. Transformation of carbon tetrachloride in the presence of sulfide, biotite, and vermiculite. *Environ. Sci. Technol.* **1992**, *26* (11), 2198–2206.
- (108) Rodríguez-Fernández, D.; Torrentó, C.; Guivernau, M.; Viñas, M.; Hunkeler, D.; Soler, A.; Domènech, C.; Rosell, M. Vitamin B12 effects on chlorinated methanes-degrading microcosms: Dual isotope and metabolically active microbial populations assessment. *Sci. Total Environ.*
- (109) Inoue, K.; Kageyama, S.; Miki, K.; Morinaga, T.; Kamagata, Y.; Nakamura, K.; Mikami, E. Vitamin B12 production by *Acetobacterium* sp. and its tetrachloromethane-resistant mutants. *J. Ferment. Bioeng.* **1992**, *73* (1), 76–78.
- (110) Rozzi, A.; Remigi, E. Methods of assessing microbial activity and inhibition under anaerobic conditions: A literature review. *Rev. Environ. Sci. Biotechnol.* **2004**, *3* (2), 93–115.
- (111) Weathers, L. J.; Parkin, G. F. Toxicity of chloroform biotransformation to methanogenic bacteria. *Environ. Sci. Technol.* **2000**, *34* (13), 2764–2767.
- (112) Speece, R. E. *Anaerobic biotechnology for industrial wastewaters*; Archae Press, 1996.
- (113) Chen, J. L.; Ortiz, R.; Steele, T. W. J.; Stuckey, D. C. Toxicants inhibiting anaerobic digestion: A review. *Biotechnol. Adv.* **2014**, *32* (8), 1523–1534.
- (114) Bauchop, T. Inhibition of rumen methanogenesis by methane analogues. *J. Bacteriol.* **1967**, *94* (1), 171–175.
- (115) Rufener, W. H.; Wolin, M. J. Effect of CCl<sub>4</sub> on CH<sub>4</sub> and volatile acid production in continuous cultures of rumen organisms and in a sheep rumen. *Appl. Microbiol.* **1968**, *16* (12), 1955–1956.
- (116) Sykes, R. M.; Kirsch, E. J. Accumulation of methanogenic substrates in CCl<sub>4</sub> inhibited anaerobic sewage sludge digester cultures. *Water Res.* **1972**, *6* (1), 41–55.
- (117) Thiel, P. G. The effect of methane analogues on methanogenesis in anaerobic digestion. *Water Res.* **1969**, *3* (3), 215–223.
- (118) Blum, D. J. W.; Speece, R. E. A database of chemical toxicity to environmental bacteria and its use in interspecies comparisons and correlations. *Res. J. Water Pollut. Control Fed.* **1991**, *63* (3), 198–207.

- (119) Yang, J.; Speece, R. E. The effects of chloroform toxicity on methane fermentation. *Water Res.* **1986**, *20* (10), 1273–1279.
- (120) Gupta, M.; Sharma, D.; Suidan, M. T.; Sayles, G. D. Biotransformation rates of chloroform under anaerobic conditions - I. Methanogenesis. *Water Res.* **1996**, *30* (6), 1377–1385.
- (121) Adamson, D. T.; Parkin, G. F. Impact of mixtures of chlorinated aliphatic hydrocarbons on a high-rate, tetrachloroethene-dechlorinating enrichment culture. *Environ. Sci. Technol.* **2000**, *34* (10), 1959–1965.
- (122) Maymó-Gatell, X.; Nijenhuis, I.; Zinder, S. H. Reductive dechlorination of *cis*-1,2-Dichloroethene and Vinyl Chloride by “*Dehalococcoides ethenogenes*.” *Environ. Sci. Technol.* **2001**, *35* (3), 516–521.
- (123) Duhamel, M.; Wehr, S. D.; Yu, L.; Rizvi, H.; Seepersad, D.; Dworatzek, S.; Cox, E. E.; Edwards, E. A. Comparison of anaerobic dechlorinating enrichment cultures maintained on tetrachloroethene, trichloroethene, *cis*-dichloroethene and vinyl chloride. *Water Res.* **2002**, *36* (17), 4193–4202.
- (124) Wei, K. Substrates and substrate interactions in anaerobic dechlorinating cultures, University of Toronto, 2012.
- (125) Alvarez-Cohen, L.; McCarty, P. L. Product toxicity and cometabolic competitive inhibition modeling of chloroform and trichloroethylene transformation by methanotrophic resting cells. *Appl. Environ. Microbiol.* **1991**, *57* (4), 1031–1037.
- (126) Gupta, M.; Gupta, A.; Suidan, M. T.; Sayles, G. D. Biotransformation rates of chloroform under anaerobic conditions—II. Sulfate reduction. *Water Res.* **1996**, *30* (6), 1387–1394.
- (127) Link, B.; Dürk, H.; Thiel, D.; Frank, H. Binding of trichloromethyl radicals to lipids of the hepatic endoplasmic reticulum during tetrachloromethane metabolism. *Biochem. J.* **1984**, *223* (3), 577–586.
- (128) Weber, L. W. D.; Boll, M.; Stampfl, A. Hepatotoxicity and mechanism of action of haloalkanes: Carbon tetrachloride as a toxicological model. *Crit. Rev. Toxicol.* **2003**, *33* (2), 105.
- (129) Adamson, D. T.; Parkin, G. F. Biotransformation of mixtures of chlorinated aliphatic hydrocarbons by an acetate-grown methanogenic enrichment culture. *Water Res.* **1999**, *33* (6), 1482–1494.
- (130) Chung, J.; Rittmann, B. E. Simultaneous bio-reduction of trichloroethene, trichloroethane, and chloroform using a hydrogen-based membrane biofilm reactor. *Water Sci. Technol.* **2008**, *58* (3), 495–501.
- (131) Azizian, M. F.; Semprini, L. Simultaneous anaerobic transformation of tetrachloroethene and carbon tetrachloride in a continuous flow column. *J. Contam. Hydrol.* **2016**, *190*, 58–68.
- (132) Pon, G.; Hyman, M. R.; Semprini, L. Acetylene inhibition of trichloroethene and vinyl chloride reductive dechlorination. *Environ. Sci. Technol.* **2003**, *37* (14), 3181–3188.
- (133) Yu, S.; Semprini, L. Comparison of trichloroethylene reductive dehalogenation by microbial communities stimulated on silicon-based organic compounds as slow-release anaerobic substrates. *Water Res.* **2002**, *36* (20), 4985–4996.

- (134) Yu, S.; Dolan, M. E.; Semprini, L. Kinetics and inhibition of reductive dechlorination of chlorinated ethylenes by two different mixed cultures. *Environ. Sci. Technol.* **2005**, *39* (1), 195–205.
- (135) Drake, H. L.; Küsel, K.; Matthies, C. Ecological consequences of the phylogenetic and physiological diversities of acetogens. *Antonie Van Leeuwenhoek* **2002**, *81* (1–4), 203–213.
- (136) Gossett, J. M. Measurement of Henry's law constants for C1 and C2 chlorinated hydrocarbons. *Environ. Sci. Technol.* **1987**, *21* (2), 202–208.
- (137) Sander, R. Compilation of Henry's law constants (version 4.0) for water as solvent. *Atmos Chem Phys* **2015**, *15* (8), 4399–4981.
- (138) Berggren, D. R. V.; Marshall, I. P. G.; Azizian, M. F.; Spormann, A. M.; Semprini, L. Effects of sulfate reduction on the bacterial community and kinetic parameters of a dechlorinating culture under chemostat growth conditions. *Environ. Sci. Technol.* **2013**, *47* (4), 1879–1886.
- (139) The Mathworks, Inc. Two-sample t-test - MATLAB ttest2 <https://www.mathworks.com/help/stats/ttest2.html#description> (accessed Oct 30, 2017).
- (140) Ramsey, F.; Schafer, D. *The statistical sleuth: A course in methods of data analysis*; Cengage Learning, 2012.
- (141) Justicia-Leon, S. D.; Higgins, S.; Mack, E. E.; Griffiths, D. R.; Tang, S.; Edwards, E. A.; Löffler, F. E. Bioaugmentation with distinct *dehalobacter* strains achieves chloroform detoxification in microcosms. *Environ. Sci. Technol.* **2014**, *48* (3), 1851–1858.
- (142) Vickstrom, K. E. Transformation of carbon tetrachloride and chloroform by trichloroethene respiring anaerobic mixed cultures and supernatant. **2016**.
- (143) Berggren, D. R. V. Kinetic and molecular effects of sulfate reduction on a dechlorinating culture under chemostat growth conditions. **2011**.
- (144) Cupples, A. M.; Spormann, A. M.; McCarty, P. L. Vinyl chloride and cis-dichloroethene dechlorination kinetics and microorganism growth under substrate limiting conditions. *Environ. Sci. Technol.* **2004**, *38* (4), 1102–1107.
- (145) Benjamin, M. M.; Lawler, D. F. *Water quality engineering: Physical / chemical treatment processes*; John Wiley & Sons, 2013.

## APPENDIX

### 1. Log-linearization of CT and CF transformation data to obtain first order transformation rate constants

Mass data for triplicate reactors was log-linearized and plotted against time to obtain first order rate degradation constants from the slope of the resulting curve. Figures below illustrate this process for Experiments 1 (CT-exposed) and 4 (CF-exposed).

#### Experiment 1

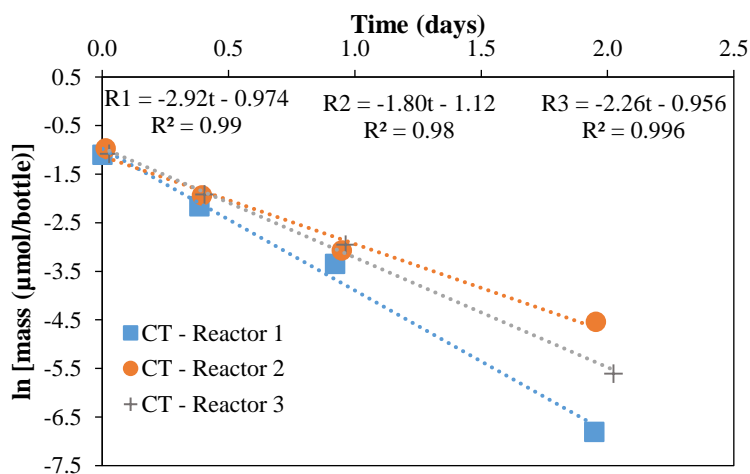


Figure A1. CT mass data long linearization for Experiment 1.

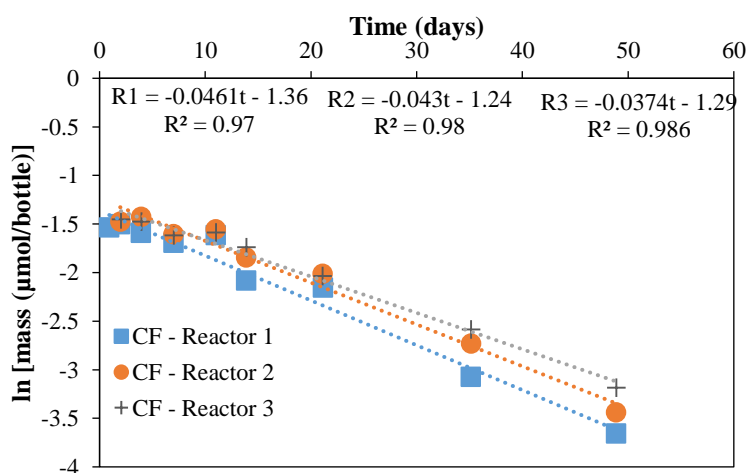


Figure A2. Log linearization of CF mass data from Experiment 1.

Table A1. First Order Transformation Constants for CT and CF in Experiment 1 Reactors.

	CT	CF
Reactor 1	-2.920	-0.046
Reactor 2	-1.807	-0.043
Reactor 3	-2.260	-0.037
Average	-2.329	-0.042
Std. Dev	0.457	0.004

Linear Equation of Best Fit for Averaged Data:

$$\text{CT: } \ln [\text{CT}] = -2.13t - 1.083$$

$$\text{CF: } \ln [\text{CF}] = -0.0421t - 1.29$$

Where [ ] is mass in  $\mu\text{mol}$  and  $t$  is time in days. These are the equations used for mass estimations at unknown time points.

Experiment 4

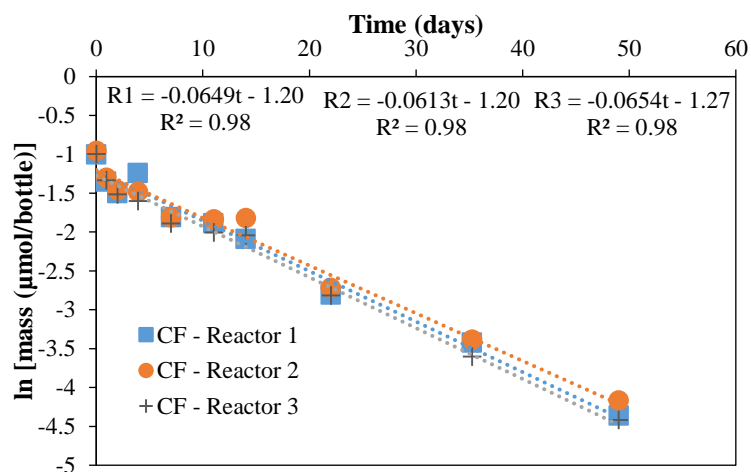


Figure A3. Log-linearization of CF mass data from Experiment 4.

Table A2. First Order Transformation Rate Constants for CF in Experiment 4 Reactors.

	CF
Reactor 1	-0.0649
Reactor 2	-0.0613
Reactor 3	-0.0654
Average	-0.0639
Std. Dev	0.002

Linear Equation of Best Fit for Averaged Data:

$$\text{CF: } \ln[\text{CF}] = -0.0638t - 1.2252$$

## 2. Day 0 CT Exposure – Experiment 3

In addition to data from Experiments 1 and 2, the day 0 CE transformation for Experiment 3 also demonstrated the slowing of VC transformation during the first addition. TCE and cDCE were transformed by 0.1 days, corresponding to the maximum VC mass. After a rapid decline, the VC mass data and model discrepancy begins shortly after 0.2 days, consistent with Experiments 1 and 2. Associated transformation rates are shown in Table A4. Day 1 data is shown in Section 2 of the main text.

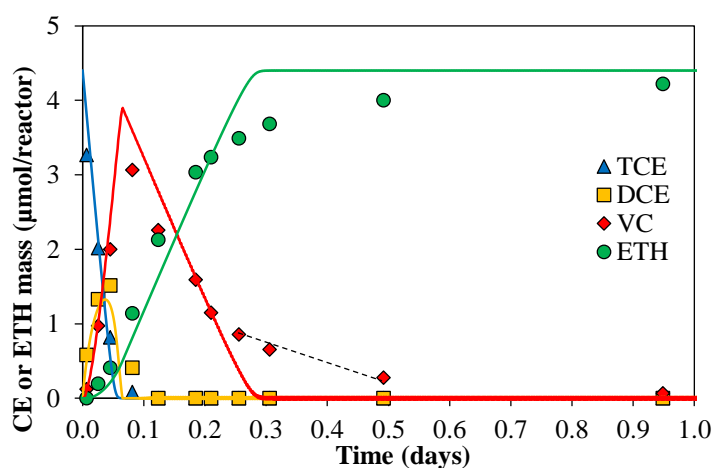


Figure A4. Day 0 CE transformation profile for Experiment 3.

### 3. Comprehensive Transformation Rate Tables for All Experiments

“±” indicates a single sample standard deviation from the mean. Where not shown, only one reactor was evaluated.

Table A3. Control Rates

Rate Type	CONTROL (no CT or CF addition)					
	Day 0				Day 2	Day 14
	10/21/16	1/23/17	3/9/2017**	4/25/2017*	4/25/2017*	3/9/2017**
TCE model	1519 ± 204	1116 ± 41.2	1445 ± 109	1366	1012	826.3 ± 340
TCE linear SOP	1115 ± 200	988.2 ± 118	1175 ± 17.9	1269	925.2	718.5 ± 288
cDCE model	1424 ± 117	947.7 ± 74.9	1500 ± 134	1227	798.1	1062 ± 66.3
cDCE linear SOP	1077 ± 143	647.5 ± 80.2	1193 ± 230	938.0	640.6	651 ± 223
VC model	709.2 ± 217	676.9 ± 51.3	690.7 ± 22.6	713.3	593.7	483.3 ± 101
VC linear SOP	811.3 ± 242	635.1 ± 48.5	705 ± 38.5	716.4	621.2	514.3 ± 180

Table A4. CE Transformation Rates for all 2.3-2.9  $\mu\text{M}$  CT Exposures Tested

Rate Type	EXPERIMENTAL REACTORS, CT EXPOSURE							
	Day 0			Day 1	Day 2	Day 14		
	3/13/17	3/20/17	4/6/17	4/6/17	4/25/17	9/23/16	3/13/17	3/20/17
TCE model	1392 $\pm$ 148	1453 $\pm$ 118	1743 $\pm$ 137	246.0 $\pm$ 32.1	200.8 $\pm$ 21.1	123.1 $\pm$ 12.3	135.6 $\pm$ 20.3	165.8 $\pm$ 36.1
TCE linear SOP	1109 $\pm$ 122	1218 $\pm$ 110	1565 $\pm$ 243	191.8 $\pm$ 41.5	172.6 $\pm$ 18	110.8 $\pm$ 6.51	105.3 $\pm$ 12.4	101.1 $\pm$ 27.3
cDCE model	1406 $\pm$ 217	1503 $\pm$ 207	1733 $\pm$ 323	301.0 $\pm$ 53.5	259.7 $\pm$ 36.1	148.0 $\pm$ 46.5	164.1 $\pm$ 30.0	182.4 $\pm$ 39.8
cDCE linear SOP	885.9 $\pm$ 31.2	932.6 $\pm$ 34.4	1023 $\pm$ 74.4	204.6 $\pm$ 27.7	177.7 $\pm$ 26.5	81.95 $\pm$ 10.4	94.54 $\pm$ 19.6	111.4 $\pm$ 35.7
VC model	420.8 $\pm$ 42.6	406.9 $\pm$ 15.0	409.8 $\pm$ 54.6	30.24 $\pm$ 8.66	23.48 $\pm$ 3.51	11.61 $\pm$ 3.36	10.3 $\pm$ 0.46	12.95 $\pm$ 3.58
VC linear SOP	443.6 $\pm$ 45.3	422.2 $\pm$ 19.0	423.1 $\pm$ 42.5	29.52 $\pm$ 13.7	26.28 $\pm$ 6.40	15.36 $\pm$ 4.84	16.58 $\pm$ 0.43	17.24 $\pm$ 4.99
VC truncated*	76.53 $\pm$ 5.35	68.48 $\pm$ 2.26	41.01 $\pm$ 9.28	24.15 $\pm$ 4.02	20.3 $\pm$ 4.63	N/A	N/A	N/A

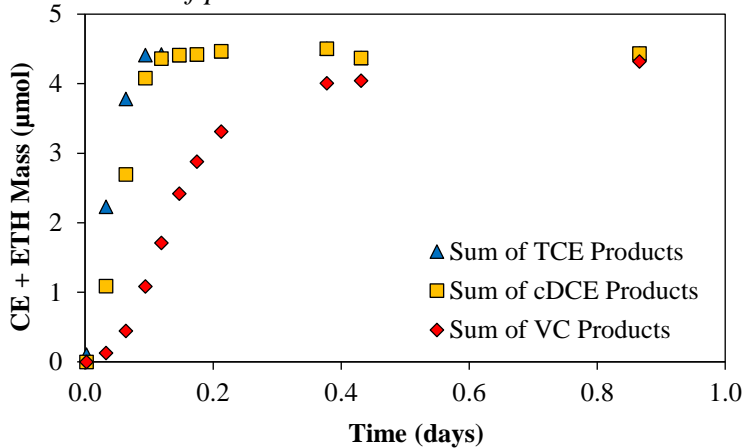
\*Refers to linear observed rates found from the slope of the VC transformation curve.

Table A5. CE Transformation Rates for all 5.8-6  $\mu\text{M}$  CF Exposures Tested

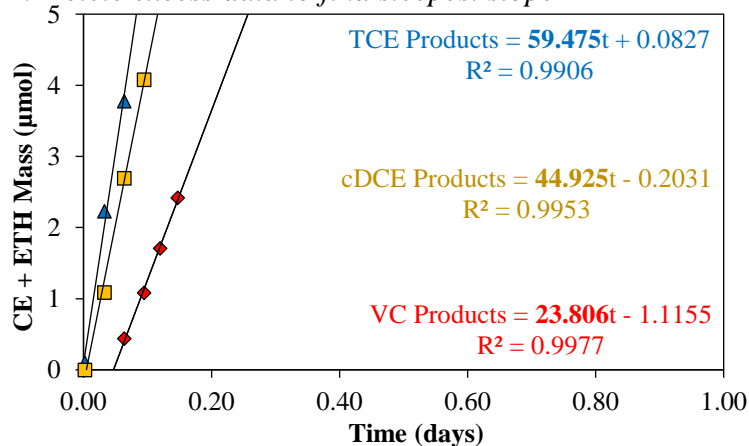
Rate Type	EXPERIMENTAL REACTORS, CF EXPOSURE				
	Day 0			Day 2	Day 14
	1/26/17	3/13/17	4/6/17	4/6/2017	3/13/17
TCE model	1081 $\pm$ 105	1643 $\pm$ 102	1685 $\pm$ 104	500.6 $\pm$ 67.3	357.9 $\pm$ 6.37
TCE linear SOP	896.3 $\pm$ 101	1462 $\pm$ 127	985.3 $\pm$ 68.4	383.4 $\pm$ 31.5	292.1 $\pm$ 24.5
cDCE model	1077 $\pm$ 97.3	1764 $\pm$ 99.5	1685 $\pm$ 398	644.0 $\pm$ 61.5	497.9 $\pm$ 14.0
cDCE linear SOP	710.9 $\pm$ 73.5	1082 $\pm$ 125	1059 $\pm$ 125	464.1 $\pm$ 65.9	288.4 $\pm$ 12.7
VC model	660.4 $\pm$ 97.3	669.2 $\pm$ 66.1	1113 $\pm$ 268	459.7 $\pm$ 93.9	132.2 $\pm$ 28.8
VC linear SOP	595.6 $\pm$ 81.4	665.4 $\pm$ 55.8	723.0 $\pm$ 85.1	513.7 $\pm$ 69.6	274.8 $\pm$ 32.1

4. Process for obtaining the Maximum Observed Rate from Sum of Products with Example Data Set from Experiment 1

A: Plot sum of products data with time



B: Delete excess data to find steepest slope



C: Normalize maximum slopes to batch reactor volume to obtain Observed Maximum Rates from SOP.

	Max Slope ( $\mu\text{mol/day}$ )	Normalize:	Converted Rate ( $\mu\text{mol/L-day}$ )
TCE	59.48	Slope	1190
cDCE	44.93	$\div 50 \text{ mL} \times$	898.5
VC	23.81	(1000 mL/1 L)	476.1

Figure A5. Stepwise process to obtain maximum observed transformation rates.

## 5. Additional CF-Exposed Experiments

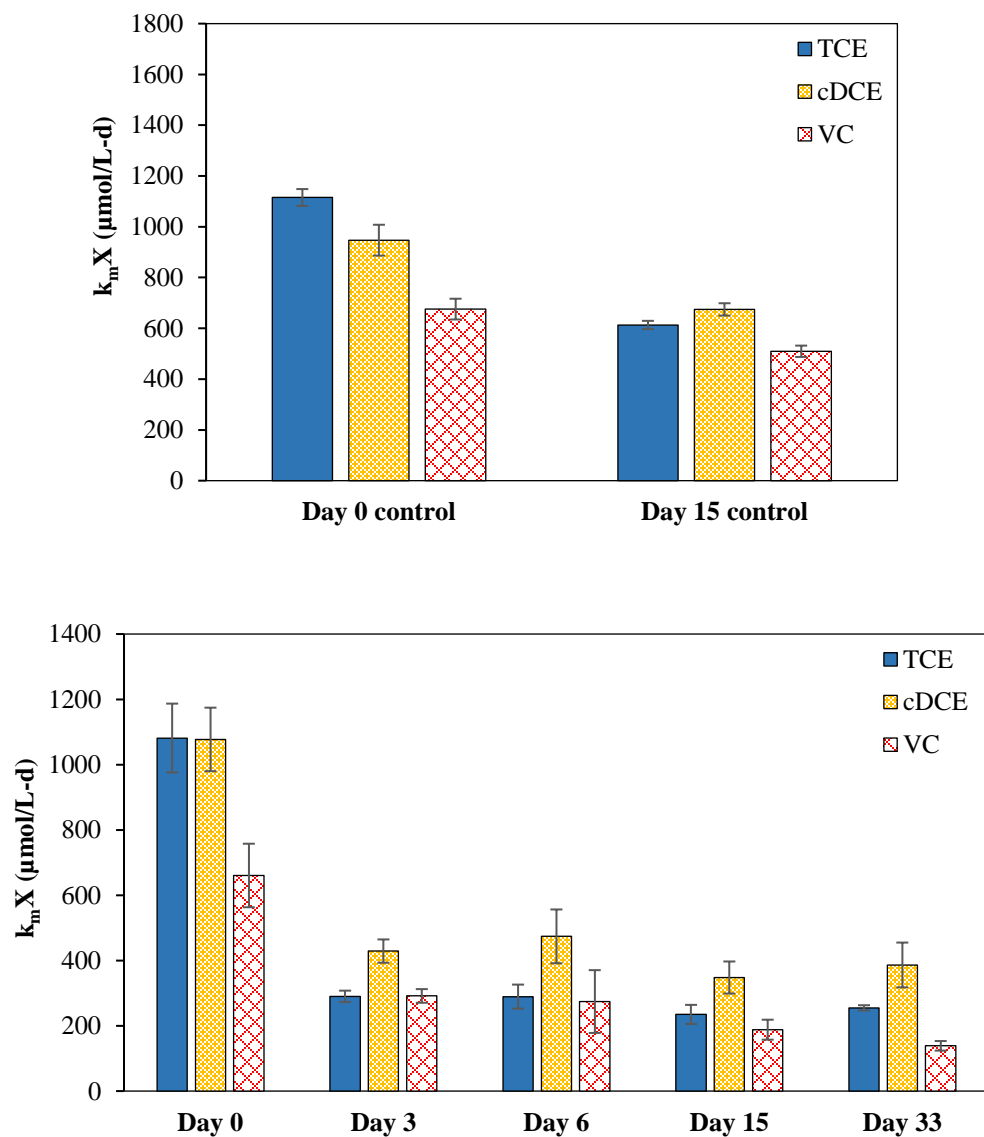


Figure A6. Control (Panel A) and CF-exposed (Panel B) transformation rates from an additional CF exposed experiment with 5 separate TCE additions. Error bars represent one standard deviation.

## 6. CT Rate Analysis for Multiple Delivery Experiment

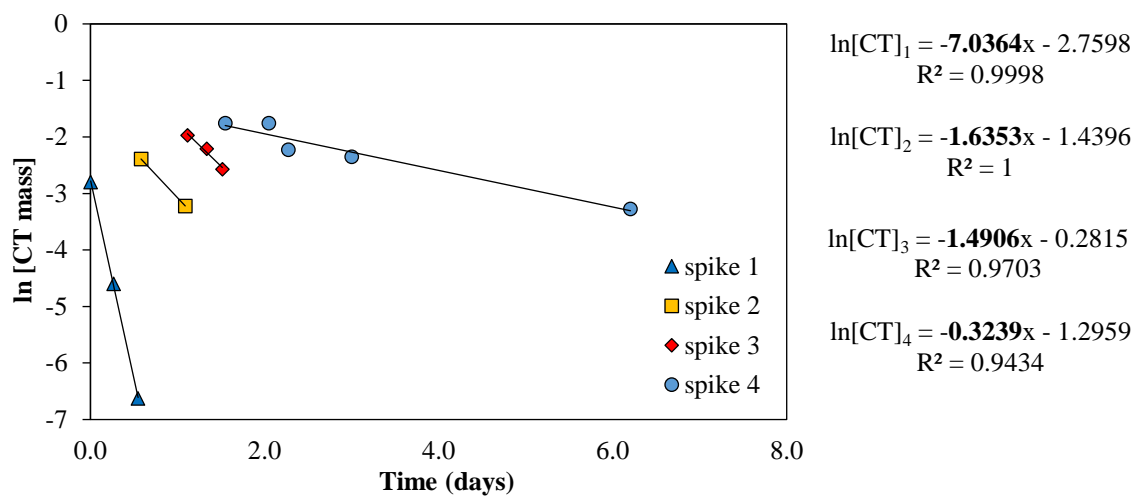


Figure A7. First order CT transformation rate analysis for each addition (“spike”) of a multiple addition delivery experiment. A decrease in slope (shown in bold within regression equations and corresponding to a first order decay constant) indicate a slowing of CT transformation.